Metabolic variation in the toxigenic cyanobacterium *Microcystis aeruginosa*

Marianne Racine
BSc. University of Ottawa, 2014

Thesis submitted to the
Faculty of Graduate and Postdoctoral Studies
in partial fulfillment of the requirements
for the Master degree in Biology
with specialization in
Chemical and Environmental Toxicology

Department of Biology
Faculty of Science
Ottawa-Carleton Institute of Biology
University of Ottawa

© Marianne Racine, Ottawa, Canada, 2018

Abstract

Cyanobacteria are notorious for their potential to produce toxins with human health effects, particularly the hepatotoxic microcystins (MCs), but cyanobacteria also produce other bioactive compounds. A wide variety of oligopeptides including aeruginosins, cyanopeptolins and cyanobactins may be as toxic as MCs. To investigate the production of these compounds, an UPLC QTOF-MS/MS method was developed to compare the metabolomic profiles of various strains of a common bloom-forming and toxigenic species, *Microcystis aeruginosa*, as well as those obtained from lakes with mixed cyanobacterial assemblages. Although many compounds could not be confirmed, MCs were rarely the dominant secondary metabolite in any sample. Since the biological role of MCs remains unknown, I tested the hypothesis that MCs provide protection against oxidative stress as induced through exposure to the herbicide atrazine and UV radiation in pure cultures of toxic vs non-toxic strains. Results were inconclusive and varied between strains suggesting other mechanisms exist to counter oxidative stress.

Résumé

Les cyanobactéries sont reconnues pour leur potentiel toxique qui peut être nocif pour la santé publique. On leur reconnait la production de microcystines (MCs), des cyanotoxines hépatotoxiques, mais elles peuvent aussi produire d'autres composés bioactifs. Les aeruginosines, cyanopeptolines et cyanobactines sont des oligopeptides qui pourraient être aussi dommageables que les microcystines. Pour investiguer la production de ces composés dans la cellule, une méthode utilisant un UPLC-QTOF-MS/MS a été développée pour comparer les profiles métaboliques de plusieurs souches de la même espèce de cyanobactéries, *Microcystis aeruginosa*. Des échantillons environnementaux contenant plusieurs assemblages de cyanobactéries ont aussi été analysés. Malgré le fait que plusieurs composés n'ont pas pu être confirmés, les microcystines étaient rarement les composés secondaires dominants dans les échantillons. Le rôle biologique des microcystines étant toujours inconnu, j'ai testé l'hypothèse d'une protection contre le stress oxydatif induit par une exposition à l'herbicide atrazine, ainsi qu'à la radiation causée par les rayons UV dans des souches toxiques et non-toxiques. Les résultats n'étaient pas concluants et variaient entre les souches, suggérant que d'autres mécanismes sont entrés en jeu pour contrer le stress oxydatif.

Acknowledgments

Over the years, I have received help from many places in every part of my life, and it is this guidance that helped me to keep motivated. First, I need to thank my supervisor, Dr. Frances Pick, for her trust from the beginning and for not giving up on me in rougher times. I really enjoyed my time working with you, and I can now say I am a completely different person from when I first started in your lab, about five years ago; I have grown as a researcher and as a person.

Thank you to my committee, Drs John Arnason and Christopher Boddy from the University of Ottawa and Dr. Myron Smith from Carleton University for being a part of this project. Many thanks to Dr. Ammar Saleem for being available and for answering all the questions I could have asked over the years. A big part of this project could not have been done without you.

I also need to thank Linda Kimpe, Philip Pelletier and my colleagues in CAREG for their time and their patience, and for letting me borrow the equipment I needed for this project and all my other work during my time there. My colleagues in the Pick Lab, Katherine Alambo, Marie-Pierre Varin, Keely Lefebvre, Dr. Rebecca Dalton and Dr. Zofia Taranu, without whom graduate studies would not have been the same. Larissa Reid, Jessica Bérard and Karine Boileau for their assistance with the experiment. More importantly, thank you to Dr. Shinjini Pilon for being the best mentor I could have asked for. Mary Ann Perron, you turned impossible tasks into fun adventures and I cannot thank you enough for your support and friendship!

Et finalement, merci maman et papa pour votre support depuis le premier jour de ma folle aventure universitaire. Vous n'avez jamais cessé de me soutenir dans mes projets et mes rêves, et je n'aurais pas parcouru tout ce chemin sans votre aide. Merci, merci, merci.

This research was done with funding from the NSERC, the NSERC CREATE ABATE (Algal Bloom Assessment Through technology and Education) and the WEAO (Water Environment Association of Ontario).

Table of Content

List of Abbreviations viii
List of Figures ix
List of Tables xii

Chapter I: Introduction

1.1. Harmful cyanobacteria 2
1.2. Bioactive compounds in *Microcystis aeruginosa* 4
1.2.1 Microcystins *4*
1.2.2 Cyanobactins *8*
1.2.3 Cyanopeptolins *9*
1.2.4 Anabaenopeptins *9*
1.2.5 Aeruginosins *10*
1.2.6 Microginins *10*
1.2.7 Microviridins *10*
1.3. Cyanotoxin genes 11
1.4. Biological role of microcystins 13
1.5. Thesis Objectives 15

Chapter II: Metabolome variation between strains of *Microcystis aeruginosa* and environmental samples using advanced mass spectrometry

2.1 Introduction 18
2.2 Material and Methods 20
2.2.1 Culturing techniques *20*
2.2.2 Field sampling *25*
2.2.3 Metabolome analysis *26*
2.3 Results 27
2.3.1 Separation and identification of compounds *27*
2.3.2 Metabolome profile of Microcystis strains and environmental samples *41*
2.4 Discussion 49
2.4.1 Identification of compounds *49*
2.4.2 Metabolome analyses *53*

Chapter III: Variation in metabolite composition and fitness under oxidative stress in the cyanobacterium *Microcystis aeruginosa*

3.1 Introduction 56

3.2 Material and Methods 60

3.2.1 Culturing techniques *60*

3.2.2 UV exposure *60*

3.2.3 Atrazine exposure *61*

3.2.4 Metabolome analysis and compound identification *61*

3.2.5 Growth rates measurements *62*

3.2.6 Chlorophyll a analysis *63*

3.2.7 Statistical analysis *63*

3.3 Results 64

3.3.1 UV exposure *64*

3.3.2 Atrazine exposure *71*

3.4 Discussion 85

Chapter IV: Conclusion **88**

References **92**

Appendix A **107**

Appendix B **115**

List of Abbreviations

a.a. amino acids
APT Anabaenopeptin
ARG Aeruginosins
ASE Accelerated Solvent Extraction
ATZ Atrazine
Chl.a Chlorophyll a
CPT Cyanopeptolin
Da Daltons
FC Flow Cytometry
HABs Harmful Algal Blooms
LD_{50} Lethal dose for 50% of the population
m/z mass to charge ratio
MC Microcystin
mcy microcystin-producing gene cluster
MGN Microginin
MW Molecular Weight
NMR Nuclear Magnetic Resonance spectrometry
NOD Nodularin
NRPS Non-ribosomal peptide synthetase
O.D. Optical Density
OPLS-DA Orthogonal partial least square discriminant analysis
PCA Principal Component Analysis
PKS Polyketides synthetases
PSII Photosystem II
ROS Reactive Oxygen Species
RT Retention Time
S/N Signal to noise ratio
TIC Total Ion Chromatogram
UPLC-QTOF-MS/MS Ultra Performance Liquid Chromatography coupled with a quadrupole time of flight tandem mass spectrometer
WT Wildtype

List of Figures

Figure 1.1. The structure of the non-ribosomally-produced cyclic heptapeptide microcystin-LR (cyclo(-D-Ala-L-Leu-D-MeAsp-L-Arg-Adda-D-Glu-Mdha-).

Figure 1.2. Examples of structures of different classes of oligopeptides found in *Microcystis.*

Figure 2.1. Separation of standards in a positive ion mode.

Figure 2.2. Separation of supplemental standards in a positive ion mode during a subsequent injection.

Figure 2.3. Structure of the oligopeptides a) [Dha^7]-MC-LR, b) [Asp^3]-MC-LR, c) [Leu^1]-MC-LR, d) CPT911.

Figure 2.4. Comparison between high energy spectra from a) the [Dha^7]-MC-LR variant and b) the [Asp^3]-MC-LR variant as detected by tandem mass spectrometry.

Figure 2.5. a) Chromatography of the potent [Leu^1]-MC-LR congener; b) high energy spectrum of [Leu^1]-MC-LR; c) high-energy spectrum of the standard solution of MC-LR.

Figure 2.6. CPT911 detection in *Microcystis aeruginosa* strain CPCC464.

Figure 2.7. Relative amounts of oligopeptides families that were identified in the strains of *Microcystis aeruginosa.*

Figure 2.8. Relative microcystin congener concentrations among toxic strains of *Microcystis aeruginosa.*

Figure 2.9. TIC for the Lac Breton sample.

Figure 2.10. PCA scores from the *Microcystis aeruginosa* cultures and environmental samples.

Figure 2.11. PCA scores for the metabolites profiles for the Microcystis aeruginosa cultures and the environmental samples, excluding the CPCC299 strain.

Figure 2.12. S-plot for metabolome comparison between CPCC300 and CPCC299.

Figure 2.13. S-plot for metabolome comparison between the mutant (mcyB-) and the wildtype cultures of *Microcystis aeruginosa* PCC7806.

Figure 2.14. MC-LR in the mutant strains of PCC7806 (*mcy*B-) and the wildtype (WT).

Figure 3.1. Cellular density (cells/mL) variation in the MC producer *Microcystis aeruginosa* CPCC300 over the 30 min exposure to UV.

Figure 3.2. Cellular density (cells/mL) variation in *Microcystis aeruginosa*.

Figure 3.3. PCA scores for the metabolome of the MC producer *Microcystis aeruginosa* CPCC300 exposed to UV radiation.

Figure 3.4. S-plot of the metabolome profile in the MC producer *Microcystis aeruginosa* CPCC300 before and after 30 minutes of exposure to UV radiation.

Figure 3.5. Microcystins signal intensities in *M. aeruginosa* strains.

Figure 3.6. Cellular density of MC producers strains of *Microcystis aeruginosa* over a period of 48 hours after exposure to atrazine.

Figure 3.7. Rates of decline of the MC producer CPCC300 between 24 and 48 hours post-exposure to atrazine.

Figure 3.8. Growth rates of the MC producer CPCC464 during the first 24 hours following the exposure to atrazine.

Figure 3.9. PCA of the metabolome variation of the MC producer CPCC464 after a 72 hours-exposure to 150 ppb of atrazine.

Figure 3.10. S-plot for the strain CPCC464 after a 72 hours-exposure to atrazine.

Figure 3.11. Unidentified compound 4 signal intensity variation in *M. aeruginosa* CPCC464 for the controls and the beginning and at the end of the experiment and for the 150 ppb exposure to atrazine.

Figure 3.12. Separation and detection of the unidentified compound 4 in *Microcystis aeruginosa* CPCC464.

Figure 3.13. S-plot for the strain CPCC464 exposed to 150 ppb of atrazine.

Figure 3.14. Fragmentation spectrum of compound 5 in in *Microcystis aeruginosa* CPCC464 under high energy collision mode (positive mode)

Figure 3.15. Compound. 5 signal intensity variation in the MC-producing *Microcystis aeruginosa* strain CPCCC464 for the controls (n=3) and under a 150 ppb atrazine exposure for a 72-hours period (n=3).

Figure 3.16. Microcystins concentration in *M. aeruginosa* CPCC464 in the controls and in cultures exposed to 150 ppb of atrazine (n=5) for a period of 72 hours**.**

Figure A.1. Optical density at 750 nm for the strains CPCC300, PCC7806 (WT) and PCC7806mcyB-.

Figure A.2. S/N of the two signals corresponding to the masses and fragmentation of CPT911.

Figure A.3. Unidentified MC 1 separation chromatogram at RT 3.19 min.

Figure A.4. Unidentified MC 2 separation chromatogram at RT 2.98 min.

Figure B.1. PCA for the metabolome variation in samples of *M. aeruginosa* PCC7806 (MC-producing) exposed to UV and visible light.

Figure B.2. S-plot for the metabolome variation in samples of *M. aeruginosa* strain PCC7806 WT (MC-producing) exposed to 30 min of UV radiation.

Figure B.3. PCA for the metabolome variation in samples of *M. aeruginosa* PCC7806*mcy*B- (mutant for *mcy*) exposed to UV and visible light, visible light only and controls at 0 min.

Figure B.4. S-plot for the metabolome variation in *M. aeruginosa* PCC7806*mcy*B- (mutant for *mcy*) exposed to 30 minutes of UV radiation.

Figure B.5. Chl.a (mg/L) in PCC7806 (MC producer) and PCC7806mcyB- (mutant for mcy) over the 30 minutes experiment for UV exposure.

Figure B.6. Total microcystins signal intensity in the MC producer *Microcystis aeruginosa* PCC7806 (WT) in relation to the cellular density (cells/mL) in cultures before and after UV treatments.

Figure B.7. Total microcystins signal intensity in the MC producer *Microcystis aeruginosa* CPCC300 in relation to the cellular density (cells/mL) in cultures before and after UV treatments.

Figure B.8. Separation of unidentified compound 4 in the M-producing *Microcystis aeruginosa* strain CPCC464 at RT 0.45 min.

Figure B.9. Compound 4 signal intensity in *M. aeruginosa* strain CPCC300 for the controls and the 150 ppb treatment to atrazine at the beginning and at the end of the experiment.

Figure B.10. Compound 4 signal intensity in *M. aeruginosa* strain CPCC300, PCC7806 (WT) and PCC7806*mcy*B- for the controls and treatments before and after 30 minutes exposure to UV radiation.

Figure B.11. Separation of compound 5 in *Microcystis aeruginosa* CPCC464 at RT 0.64 min.

Figure B.12. Microcystins concentration *in M. aeruginosa* CPCC300 at T=0 min of atrazine exposure and after 72 hours of exposure.

Figure B.13. Atrazine concentrations in CPCC300 at the beginning and the end of the experiment after 72 hours.

List of Tables

Table 1.1. LD_{50} values of the most abundant microcystin variants, after intraperitoneal (ip.) injection in mice and rats, in order of increasing toxicity.

Table 2.1. *Microcystis aeruginosa* strain characteristics.

Table 2.2. Compounds tentatively identified in *Microcystis aeruginosa* strains and environmental samples classified by oligopeptides families.

Table 2.3. Possible microcystin variants for the three unidentified compounds from *M. aeruginosa* strains CPCC464 and CPCC299 presented in Table 2.2.

Table A.1. Major fragments of MC-LR detected in the standard solution at a RT of 2.84 min.

Table A.2. Major fragments of CPT911 detected in the samples at RT 2.13 and 2.25 min.

Table A.3. Compounds that have previously been observed in the strains of interest in this study, but for which no corresponding signal was found.

Chapter I: Introduction

1.1. Harmful cyanobacteria

Cyanobacteria, previously called "blue-green algae," are present in the vast majority of aquatic environments, including lakes, running waters, marine coastal areas and drinking water reservoirs. Their concentrations are usually low and do not raise any concerns. However, excessive growth and accumulation of cyanobacterial colonies can lead to surface blooms in water bodies that have adverse outcomes (>20 000 cells/mL) (WHO 2003). The eutrophication process that has been occurring during the past few decades in lakes around the world has lead to a rise in cyanobacterial blooms (Taranu *et al.* 2015), as excess nutrient loading leads directly to bloom formation and can affect the overall ecosystem. Global warming and anthropogenic activities (farming, construction, roads) might be acting synergistically and accelerating algal blooms (Pick 2016). As the phenomenon is on the rise in freshwater and marine coastal areas, many environmental and health problems ensue. One of them is a decrease in dissolved oxygen concentrations in the water, inducing death of aquatic life (Chorus & Bartram 1999; Rastogi *et al.* 2015). Another is the production of cyanotoxins.

While many species and populations of cyanobacteria are non-toxic, cyanobacterial and phytoplanktonic blooms have the potential to produce a vast range of toxins, including hepatotoxins, neurotoxins, and endotoxins. Between 25 and 75% of tested cyanobacterial blooms have been reported as toxic (Zurawell *et al.* 2005). Mortality events due to the presence of one of these toxins have been reported in domestic animals and diverse wildlife populations around the world, including giraffes, deers, flamingos and fishes (Krienitz *et al.* 2003; Miller *et al.* 2010; Cook *et al.* 2015; Wood 2016). The presence of toxin cannot be predicted from the species composition and water samples have to be chemically tested in order to determine the potential

toxicity. Therefore, it is hard to limit human contact with these cyanotoxins and harmful algal blooms (HABs) present a significant public health concern through recreational and drinking water exposures.

Efficient water treatment is difficult to achieve when intake raw water contains high densities of toxic cells. Conventional techniques are useful to reduce the water toxicity when the cyanobacterial cells remain intact. However, once the toxins are released in the water, filtration systems, sedimentation, or even chemical processes may not be sufficient to reduce concentrations below the water quality guidelines (Falconer 2005). In 1996, 60 patients died of acute neurotoxicity and subacute hepatotoxicity in Caruaru, Brazil, after hemodialysis treatments using cyanobacteria-contaminated water (Pouria *et al.* 1998). During the summer of 2014, the city of Toledo, Ohio, experienced a problematic situation with its drinking water, drawn from Lake Erie. Water treatment facilities could not obtain a good water quality because of the *Microcystis* bloom that has been increasing in size in the western basin of Lake Erie during the past twenty years or so (Stumpf *et al.* 2012). The resulting ban on drinking water lasted for a few days for half a million people (Stumpf *et al*. 2012; Brooks *et al.* 2016). This degree of bloom severity has not yet been observed on the Canadian side of Lake Erie, but the risk of cyanobacterial blooms in the lower Great Lakes and inland lakes appears to be rising due to ongoing eutrophication, foodweb changes and possibly because of the increasing temperatures related to climate change (van der Waal 2010; Brooks *et al*. 2016; Pick 2016).

1.2. Bioactive compounds in *Microcystis aeruginosa*

Microcystins (MCs) are amongst the most studied cyanobacterial metabolites and they are the most commonly encountered freshwater cyanotoxins (Zurawell *et al.* 2005). Cyanobacteria have the ability to produce several other compounds that can also be toxic, including a variety of oligopeptides often referred to as secondary metabolites or bioactive compounds. Not much is known about these other compounds and their production in different cyanobacteria. Experiments tend to examine a few specific compounds (Briand *et al.* 2016; Beversdorf *et al.* 2017) and not a complete secondary metabolite profile. Microcystin is also classified as an oligopeptide and a link between its production and that of other peptides is possible (Agha & Quesada 2014).

1.2.1 Microcystins

Microcystins are non-ribosomally-produced heptapeptides (Figure 1.1) found in widespread genera such as *Microcystis*, *Dolichospermum* (*Anabaena*), and *Planktothrix* (WHO 2003). Microcystins cause an inhibition of the activity of the protein phosphatases 2A and 1 in vertebrates, leading to an accumulation of phosphorylated proteins in cells. This accumulation can affect different metabolic pathways, including the inhibition of tumor suppressor proteins, potentially leading to cell proliferation, tumor promotion and, eventually, death (Dawson 1998; Chorus & Bartram 1999; Gupta *et al.* 2003; Merel *et al.* 2013). Despite having many ecological effects, the biological role of microcystin within cyanobacteria is still unknown. In toxic strains, concentrations of microcystins can reach those of chlorophyll a (chl *a*) (Hollister & Kreakie 2016), the primary pigment involved in photosynthesis in cyanobacteria, algae and higher plants. Microcystins could play a significant functional role in the cell.

To date, 246 different microcystins congeners have been identified, with molecular weights varying between 880 and 1200 Da (Spoof & Catherine 2017). Amino acid variation in positions one and three of the microcystin molecule (Figure 1.1) is responsible for the most significant differences between congeners as well as the naming (Table 1.1). It will affect the degree of toxicity in vertebrates, as shown by LD_{50} values between and 50 µg/kg (MC-LA) and 800 µg/kg (MC-RR) in mice after intraperitoneal injection (Table 1.1) (Sivonen & Jones 1999). Microcystins are thus potentially more lethal to vertebrates than several highly potent poisons, such as sarin (Lazar *et al.* 2016). Increasing toxic effects are observed when hydrophobic amino acids (e.g. methylated amino acids) are present in the molecule, which can facilitate MC penetration into the tissues (Zurawell *et al.* 2005). However, it is the Adda moiety of the molecule (3-amino-9-methoxy-10-phenyl-2,6,8-trimethyldeca-4,6-dienoic acid) that seems to be at the origin of the toxicity. The inhibition of microcystin toxicity has been observed to occur after the cleavage of this particular part or a change in its stereochemistry (Zurawell *et al.* 2005).

Many studies suggest cyanotoxins may bioaccumulate in aquatic animals, especially in shrimps, fishes, turtles and frogs in both inland waters and oceans (Chen *et al.* 2016). Consumption of contaminated organisms has been shown to be toxic in past events, as shown by the death of sea otters in California in 2007, after microcystin-contaminated shellfish consumption (Miller *et al.* 2010). More recently, the bioaccumulation of microcystins in male and female zebrafish gonads was linked to reduced spawning activities, abnormal cell division in testis and destruction of ovarian tissues (Chen *et al.* 2016), at environmentally relevant concentrations (5- 50 µg/L).

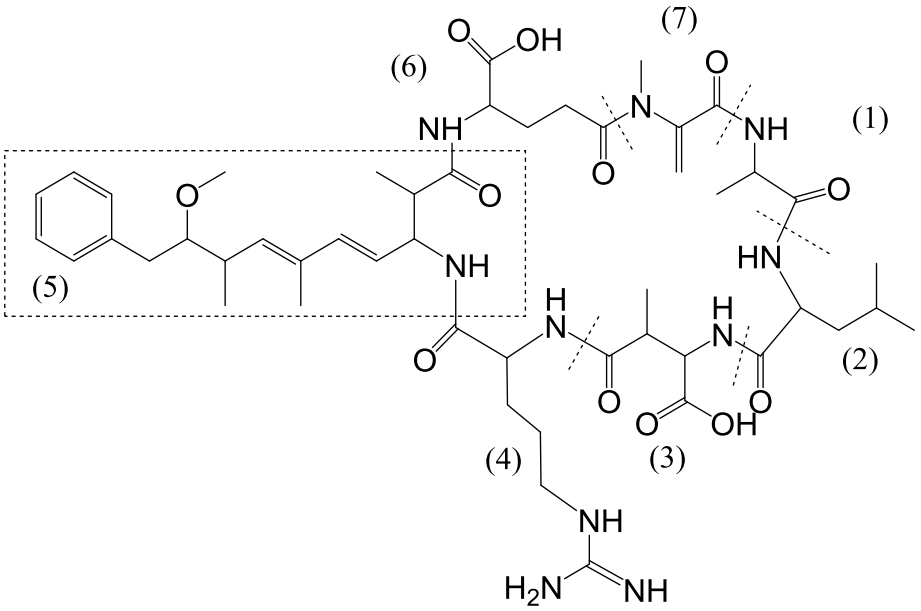

Figure 1.1. The structure of the non-ribosomally-produced cyclic heptapeptide microcystin-LR (cyclo(-D-Ala-L-Leu-D-MeAsp-L-Arg-Adda-D-Glu-Mdha-). MC congeners have amino acid variations at positions 1 (D-alanine) and 4 (L-arginine), while minor variations can occur at positions 2 (L-leucine), 3 (D-erytro-β-methylaspartic acid), 6 (D-glutamic acid) and 7 (N-methyldehydroalanine). The Adda moiety (3-amino-9-methoxy-10-phenyl-2,6,8-trimethyldeca-4,6-dienoic acid) at position 5 is thought to be at the origin of the toxicity of the molecule. Structure shown is as registered in the CAS database (The American Chemical Society ACS 2017).

Table 1.1. LD_{50} values of the most abundant microcystin variants, after intraperitoneal (ip.) injection in mice and rats, in order of increasing toxicity.

Compound	MW (Da)	Molecular Formula	LD_{50} (µg/kg)	Reference
(6Z)-Adda-MC-LR	995.5561	$C_{49}H_{75}N_{10}O_{12}$	>1200[1]	Zurawell *et al.* 2005; Spoof & Catherine 2017
MC-RR	1038.5731	$C_{49}H_{76}N_{13}O_{12}$	300-800	Sivonen & Jones 1999; Spoof & Catherine 2017
[Asp^3]-MC-RR	1024.5574	$C_{48}H_{74}N_{13}O_{12}$	250-360	van der Waal 2010; Spoof & Catherine 2017
MC-AR	953.5091	$C_{46}H_{69}N_{10}O_{12}$	250	Sivonen & Jones 1999; Spoof & Catherine 2017
MC-FR	1029.5404	$C_{52}H_{73}N_{10}O_{12}$	250	Sivonen & Jones 1999; Spoof & Catherine 2017
[Asp^3]-MC-LR	981.5404	$C_{48}H_{73}N_{10}O_{12}$	160-300	van der Waal 2010; Spoof & Catherine 2017
MC-WR	1068.5513	$C_{54}H_{74}N_{11}O_{12}$	150-200	Sivonen & Jones 1999; Spoof & Catherine 2017
MC-LY	1002.5182	$C_{52}H_{72}N_7O_{13}$	90	Sivonen & Jones 1999; Spoof & Catherine 2017
MC-YR	1045.5353	$C_{52}H_{73}N_{10}O_{13}$	70	Sivonen & Jones 1999; Spoof & Catherine 2017
MC-YM	1020.4747	$C_{51}H_{70}N_7O_{13}S$	56	Sivonen & Jones 1999; Spoof & Catherine 2017
MC-LR	995.5561	$C_{49}H_{75}N_{10}O_{12}$	50-60	Sivonen & Jones 1999; Spoof & Catherine 2017
MC-LA	910.4921	$C_{46}H_{68}N_7O1_2$	50	Sivonen & Jones 1999; Spoof & Catherine 2017

[1] *Values over 1200 µg/kg are considered non-toxic* (Zurawell *et al.* 2005).

1.2.2 Cyanobactins

With more than a hundred variants identified to date (Sivonen *et al.* 2010), cyanobactins are the second largest class of compounds in cyanobacteria in terms of different variants, after microcystins. They are also cyclic peptides, but are characterized by the presence of heterocyclized amino acids, or isoprenoid derivatives. Among these variants, tenuecyclamides, trichamides, lyngbyactins, microcyclamides, aerucyclamides, aeruginosamides, and anacyclamides can have different configurations and are found in various genera (*Microcystis*, *Anabaena*, *Lyngbya*, *Nostoc*, *Trichodesmium*, etc.) (Welker *et al.* 2004; Leikoski *et al.* 2009; Sivonen *et al.* 2010;). Variants are characterized by the numbers of thiazoles and oxazoles groupments, as well as the proteogenic amino acids present in the molecule and the length of the peptide (varying between 6 and 20 amino acids). A ribosomal biosynthetic pathway has been characterised in cyanobacteria for these compounds, but their production could be associated with other heterotrophic bacteria (Sivonen *et al*. 2010). Despite being produced in the same pathway, the variations in their structures leads to different biological activities and toxicity. Aerucyclamides and aeruginosamides are described in more details below.

The cyanobactins aerucyclamides (Figure 1.2b) have been identified in some *Microcystis aeruginosa* strains, and shown to be toxic to freshwater crustaceans, as well as showing potential antiparasite and antimalarial activities (Portmann *et al.* 2008a; Sivonen *et al.* 2010). Often found in higher trophic levels, aerucyclamides tend to bioaccumulate (Portmann *et al.* 2008a). The complete amino acid sequence for the aerucyclamide A variant is cyclo-(-Gly-Tzl-Ile-Tzn-Ile-MeOzn-), where Tzl is a thiazole, Tzn a thiazoline and MeOzn is a methyloxazoline (Portmann

et al. 2008b). Their importance in cyanobacteria and in the environment are still unknown (Portmann *et al.* 2008b).

1.2.3 Cyanopeptolins

Cyanopeptolins (CPT) are cyclic peptides produced non-ribosomally, just like microcystins. More than 82 variants have been described to date (Welker & Von Döhren 2006), as variation occurs at almost every amino acid present, except for the Ahp residue that characterizes the peptide (3-amino-6-hydroxy-2-piperidone) and the threonine (Welker & Von Döhren 2006) (Figure 1.2a). However, little is known of their production, regulation and uptake by vertebrates (Faltermann *et al.* 2014). They have been considered non-toxic for a long time (Beversdorf *et al.* 2017), but it was recently shown that some variants are toxic to zebrafish (Faltermann *et al.* 2014) and zooplankton (Pereira & Giani 2014). Among cyanopeptolins are found scyptolins, micropeptin, anabaenopeptilides, aeruginopeptins, and aeruginopeptolins (Welker & Von Döhren 2006).

1.2.4 Anabaenopeptins

Anabaenopeptins (APT) are protease inhibitors (Beversdorf *et al.* 2017) and, like microcystins, also inhibit protein phosphatase (Sano *et al.* 2001). First described in *Anabaena*, they are also found in some *Microcystis* strains. Again, many variants have been identified (>32) (Welker & Von Döhren 2006).

1.2.5 Aeruginosins

Aeruginosins (ARG) are also protease inhibitors produced non-ribosomally in *Microcystis aeruginosa*, *M. viridis* and *Planktohrix (Oscillatoria) agardhii* (Ishida *et al.* 1999) They are characterized by the presence of two uncommon residues, Hpla ((4-hydroxy)phenyllactic acid) and Choi (2-carboxy-6-hydroxyoctahydroindole), at positions (1) and (3), respectively (Figure 1.2d). They include microcins and spumigins, which brings the number of identified variants to 27 (Welker & Von Döhren 2006), but there is potential for a greater number as considerable variation is observed among the residues (Ishida et al. 2009a). They have an anti-inflammatory activity potential (Scherer et al. 2016).

1.2.6 Microginins

Microginins (MGN) are linear peptides (Figure 1.2c) known to be toxic to zooplankton and mammals because of their serine and threonine inhibition potential (Bagchi *et al*. 2008). Some of the 38 variants (Welker & Von Döhren 2006; Bagchi *et al.* 2008) have been investigated for their pharmaceutical potential as they could be used to treat high blood pressure (Okino *et al.* 1993). Their structure includes a derivative of decanoic acid that characterizes the class (see Figure 1.2c) (Bagchi *et al.* 2008).

1.2.7 Microviridins

Ribosomally produced in *Microcystis* spp. and *Planktothrix agardhii,* only 10 variants have been found to date (Welker & Von Döhren 2006). They are among the largest oligopeptides produced in cyanobacteria (Figure 1.2f), with 13 to 14 amino acids (1600-1900 Da) (Ishitsuka *et*

al. 1990; Ziemert *et al.* 2010; Weiz *et al.* 2014). A microviridin was the first tricyclic secondary metabolite observed in cyanobacteria (Ishitsuka *et al.* 1990).

1.3. Cyanotoxin genes

With respect to microcystins, the *mcy* gene cluster encodes the non-ribosomal peptide synthetases (NRPS) complex for their biosynthesis. It was first described by Nishizawa *et al.* (1999) and Tillett *et al.* (2000) including the NRPS, polyketides synthetases (PKS), tailoring enzymes, and ABC transporters. The latter's role has not been identified yet, and the hypothesis of an extracellular messenger is still being investigated (Schatz *et al.* 2005).

The *mcy* gene cluster is thought to be constitutive: when present, it is always expressed. However, the levels of expression may be influenced by different factors (Zurawell *et al.* 2005). Incomplete genes or mutations could prevent the formation of a complete molecule. There is typically a strong correlation between the presence of microcystin in environmental samples and the presence of the gene, although the relationship is variable depending on the species or strain of species. The regulation of the *mcy* gene complex is not yet well understood, but could be related to light and UV intensity, temperature and pH (Neilan *et al.* 2013; Leblanc-Renaud *et al.* 2011) and no primary role for microcystins (growth, reproduction) has been identified to date. Therefore, microcystins are still considered secondary metabolites.

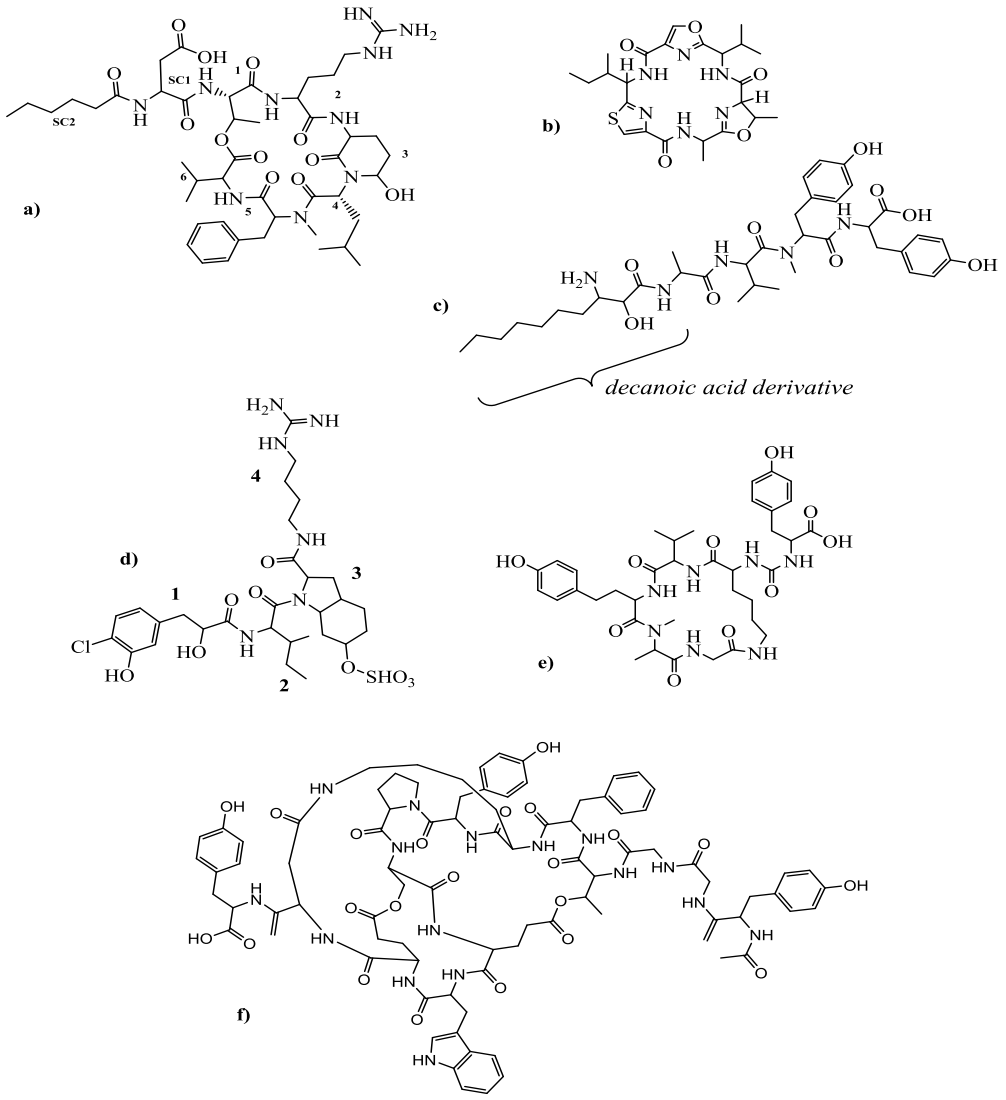

Figure 1.2. Examples of structures of different classes of oligopeptides found in *Microcystis*: **a)** Cyanopeptolin A, where the residue (3), Ahp (3-amino-6-hydroxy-2-piperidone), and the amino acid (1), threonine, are conserved among variants; **b)** the cyanobactin aerucyclamide C; **c)** the linear peptide microginin 690, **d)** aeruginosin 98A, where Hpla (4-hydroxy)phenyllactic acid is situates at (1) and Choi (2-carboxy-6-hydroxyoctahydroindole) at positions (3); **e)** anabaenopeptin general structure; and **f)** microviridin A. Structures shown are as registered by the CAS (The American Chemical Society ACS 2017).

The insertion of a chloramphenicol resistance gene in the middle of the *mcyB* gene of the *M. aeruginosa* strain PCC7806 by Dittmann *et al.* (1997) lead to a mutant, non-toxic strain, due to the inactivation of the peptide synthetase responsible for microcystin synthesis. The *mcyB* gene is thought to be partly responsible for the differentiation of the congeners, by incorporation of different amino acids in position (2) (Figure 1.1) (Kaebernick & Neilan 2001; Bittencourt-Oliveira 2003; Rastogi *et al.* 2014), since *mcyB* is involved in the peptide bond formation between leucyl and glutamyl residues. The resulting mutant does not produce any form of microcystins, but can still produce other secondary metabolites and proteins (Martin *et al.* 1993). The Adda moiety is coded by a combination of the *mcy*D, E, G and J gene clusters (Kaebernick & Neilan 2001). Even though microcystin production is slightly different because of its Adda moiety (Welker & Von Döhren 2006), NRPS/PKS complexes among the oligopeptides presented above are similar.

1.4. Biological role of microcystins

On a fundamental level, the biological role of microcystins remains unclear. Additional knowledge on this subject is essential in order to understand the production of cyanotoxins and in turn contribute to the control of toxic blooms. A few hypotheses have been proposed for the biological role of microcystin, such as a defense against zooplankton feeding (Rohrlack *et al.* 1999; Jang *et al.* 2003; Lürling & Oosterhout 2013), an extracellular messenger (Schatz *et al.* 2007), iron chelator (Utkilen & Gjolme 1995; Orr & Jones 1998) or some light-related processes (Kaebernick *et al.* 2000; Wiedner *et al.* 2003; Young *et al.* 2005; Young *et al.* 2008). There has not been sufficient evidence to support these hypotheses (Rohrlack *et al.* 1999; Zilliges *et al.* 2011; Kaplan *et al.* 2012) perhaps because of the differences in techniques and strains used. It is

clear that different environmental factors contribute to the variation in toxin expression (Wiedner *et al.* 2003; Schatz *et al.* 2007). Some experiments have shown a toxicity increase under higher light intensities (Utkilen & Gjolme 1995; Kaebernick *et al*. 2000; Tonk *et al.* 2005) but it is not always clear if this is simply related to changes in growth rates. Methods and conditions employed differ from one experiment to another, as well as between cyanobacterial strains. It is also difficult to compare experiments and results as different microcystin congeners may be involved (Kaplan *et al.* 2012).

A study by Zilliges *et al.* (2011) suggested microcystins could play a role in protection against oxidative stress. This last hypothesis is new in the field and needs more investigation. Whether caused by UV radiation, high light exposure or pesticides, oxidative stress implies the formation of reactive oxygen species (ROS) in cyanobacterial cells (Blot *et al.* 2011; Chen *et al.* 2012a; Deblois *et al.* 2013). ROS are normally formed during the electron transfer process in photosystem II (PSII), but could be harmful to the cell when produced in excess, further limiting cellular growth (Jursinic *et al.* 1991; Jacoby *et al*. 2000; Ross *et al.* 2006; Blot *et al.* 2011; Tao *et al.* 2013; Paerl & Otten 2013; Ha *et al.* 2014).

To date, research on this hypothesis has lead to intriguing results. Immunogold assays performed in cyanobacteria cells demonstrated a higher microcystin content near the thylakoids of the cells, where photosynthesis and oxidative stress occur (Young *et al.* 2005; Young *et al.* 2008). However, many studies do not support this hypothesis.

Recently, Wang *et al*. (2016) performed a study where *M. aeruginosa* (strain TY001) was exposed to various concentrations of the plant extract pyrogallol, a polyphenol. Antioxidants enzymes were upregulated by the extract following a dose-response model, starting at concentrations as low as 1 mg/L, which could be a direct response to oxidative stress. A Quantitative PCR performed on the *mcyD* and *mcyB* genes also showed an upregulation, but only under an exposure of 10 mg/L, which environmentally is quite unrealistic. Microcystins were increasing during this experiment, but only under the highest pyrogallol concentrations, 15 mg/L. The lack of response at other concentrations makes it difficult to link to the oxidative stress induced in the cells.

1.5. Thesis Objectives

In this thesis, I examined as a first objective the similarities and differences in the overall metabolome profile of strains of *Microcystis aeruginosa* (CPCC299, CPCC464, CPCC300, PCC7806 and its mutant for microcystin, PCC7806*mcyB*-) and environmental samples (Chapter 2). This required the development of a UPLC-QTOF-MS/MS method. While past experiments have tended to study specific compounds, only a few have considered more global metabolic profiles (e.g. Welker *et al.* 2006). In 2004, Guyot *et al.* demonstrated than more than 90% of cyanobacterial metabolites still had not been found. In 2014, about 100 microcystin variants had been characterized (Niedermeyer *et al.* 2014). Now with more than 240 variants identified (Spoof & Catherine 2017) for microcystins only, we can only imagine the number of oligopeptides still remaining to be discovered.

In the third chapter of this thesis, I tested the hypothesis that the biological function of microcystins is to counter oxidative stress. My approach included the use of a mutant strain (PCC7806*mcyB*-) for the microcystin gene of the common cyanobacteria, *Microcystis aeruginosa*, and its wild type (PCC7806), as well as various strains of this same species varying in their capacity to produce microcystins (CPCC300, CPCC464). The use of a mutant allows for the comparison of strains with no other molecular or physiological difference than the presence of microcystin. *M. aeruginosa.* PCC7806 and its mutant have been used many times since Dittman *et al*. (1997) made the latter available, and the strain has been shown to be non-toxic, but still producing all other secondary metabolites (Martin *et al.* 1993; Tillett *et al.* 2000). This is confirmed in Chapter 2.

A few experiments have been done in the past to evaluate the combined effects of two oxidative stress factors (Blot *et al.* 2011; Briand *et al*. 2012; Deblois *et al.* 2013; Wang *et al.* 2013) on different cyanobacterial species and strains by measuring PSII activity. Others measured enzymatic activities inside the cells after a high light intensity exposure (Zilliges *et al.* 2011) or UV radiation (Wu *et al.* 2005; Jiang & Qiu 2005; Rath & Adhikary 2007; Jiang & Qiu 2011; Tao *et al.* 2013; Yang *et al.* 2014). In every case, no comparison was made between different *Microcystis* strains, which might have different oxidative stress responses.

Chapter II

Metabolome variation between strains of *Microcystis aeruginosa* and environmental samples using advanced mass spectrometry

2.1 Introduction

Cyanobacteria are phototrophic bacteria found in freshwaters, marine coastal areas and drinking water reservoirs around the world. Visible accumulations of cyanobacterial biomass in the form of surface blooms have been increasing over the past few decades (Falconer 2005; Michalak *et al.* 2013), as well as the public awareness of the phenomenon. Many cyanobacterial blooms that have been tested have been shown to be toxic (Rastogi *et al.* 2015), mostly because of the presence of the hepatotoxic microcystins (MC). The increasing presence of blooms in surface waters has been associated with nutrient loading from various sources including agriculture (Michalak *et al.* 2013), with pesticide use (Harris & Smith 2016), and possibly also with global warming (van der Waal 2010). However, whether blooms are becoming more toxic is less clear.

Microcystins are the most studied bioactive compounds in cyanobacteria because of their toxicity, high occurrence and widespread distribution in inland and coastal waters. Other oligopeptides produced by cyanobacteria are, however, not as well known (Guyot *et al.* 2004) despite the increasing number of structures (>600) that have been elucidated to date (Welker & Von Döhren 2006; Spoof & Catherine 2017). These other peptides could also be bioactive or even toxic to vertebrates, since many are produced through the same general pathway as the microcystins (Rouhiainen *et al.* 2004) and present similar structures (Welker & Von Döhren 2006) (Chapter 1). Besides the public and environmental health needs for more research on these compounds, cyanobacterial oligopeptides have potential applications in the pharmaceutical, food and energy industries (Rastogi & Sinha 2009). A few recent studies have examined these other compounds specifically (Ishida *et al*. 1999; Ishida *et al.* 2009a; Leikoski *et al.* 2009) or in

combination with microcystin analyses (Briand *et al.* 2016), but the diversity and variation among species are still largely unknown (Welker *et al.* 2004; Welker & Von Döhren 2006). With respect to the microcystins, the variation in congeners within one of the most widely distributed bloom-forming species, *Microcystis aeruginosa*, suggests that the variation in other oligopeptides may be equally important across strains of the same species. Along with variation in microcystins the overall variation in oligopeptides may explain different toxicological outcomes, including bioaccumulation and tumour promotion, among cyanobacterial species and complex environmental samples (Anglada *et al*. 2016).

Chromatography techniques coupled with mass spectrometry analyses have been used in microcystin identification (Puddick *et al.* 2015). These techniques can be coupled with nuclear magnetic resonance (NMR) spectroscopy analyses when no standards are available for comparison (Niedermeyer *et al.* 2014). Even though efficient techniques have been developed over the years for microcystin detection and identification (e.g. Roy-Lachapelle *et al.* 2014; Fayad *et al*. 2015), efficient total metabolome analyses on cyanobacteria are lacking. To my knowledge, UPLC-QTOF mass spectrometry has not been used as yet to conduct studies on cyanobacteria and their response to changing environmental conditions. No library of compounds is available to couple the spectral results (Schwarz *et al.* 2013). For a complete metabolomics analysis, the use of a UPLC-QTOF-MS/MS as an advanced analytical instrument facilitates the identification of new molecules in several ways. First, the UPLC permits a better separation of the compounds in the column than other conventional instruments such as HPLC. Lower detection limits and increased sensitivity of the QTOF-MS/MS are also among the advantages of using this approach. It offers more possibilities in compound analysis for

cyanobacterial studies, as it permits the separation, identification and quantification of a vast range of both known and unknown compounds faster than other techniques, and with a more accurate mass acquisition.

The following study provides a preliminary insight into the cyanobacterial metabolome and improves the number of identified compounds that can be detected. The objectives were:

a) to develop a new method for cyanobacterial extract analysis with advanced mass spectrometry, using an UPLC-QTOF MS/MS;

b) to assess the diversity of the metabolome present across different strains of the same cyanobacterial species, *Microcystis aeruginosa*, and across environmental samples from surface waters in Ontario and Québec.

2.2 Material and methods

2.2.1 Culturing techniques

Strains CPCC300, CPCC464 and CPCC299 of *Microcystis aeruginosa* were purchased from the Canadian Phycological Culture Collection (CPCC - University of Waterloo, Ontario, Canada). Strains PCC7806 and PCC7806*mcy*B- of this same species were purchased from the Pasteur Culture Collection (PCC - Institut Pasteur, Paris, France). All cultures were grown in BG11 medium (Andersen 2005) diluted from a concentrated stock solution provided by the CPCC. A supplement of 10 µM of $NaHCO_3$ was added to the media for PCC cultures, to optimize their growth conditions (as suggested by the PCC). All cultures were kept in a growth chamber (Conviron) under white light (50 µM $m^{-2} \cdot s^{-1}$), with a light and dark cycle of 12 hours and a temperature of 20°C. Prior to all experiments, strains were kept in semi-continuous culture

to maintain a constant growth rate (hence physiological state) as monitored by optical density at 750 nm (Carry 100 Bio Spectrophotometer, Varian, Winnipeg, Manitoba) (see Figure A.1, Appendix A). Strain characteristics are presented in Table 2.1.

Table 2.1. *Microcystis aeruginosa* strain characteristics. Strain origins are presented as recorded by the respective culture collection. Maximum growth rates were calculated from optical density (750 nm), under growth conditions described in section 2.2.1.

Strain	Origin	Max growth rates (d^{-1})	Daily dilution (%)	MC producer
CPCC300	Deposited by E. Prepas/A. Lam. Isolated by A. Lam from Pretzlaff Pond, Alberta, Canada, Aug. 1990.	0.600	10	Yes
CPCC464	Deposited by D. Parker. Isolated by E.A.D. Allen/P. Gorham from Trampling Lake, SK, Canada, Aug. 1980.	0.048	20	Yes
CPCC299	Deposited by E. Prepas/A.Lam. Isolated by A. Lam from Pretzlaff Pond, Alberta, Canada, Aug. 1990	0.024	N/A	Yes
PCC7806	Deposited by F.I. Kappers. Isolated from Braakman Reservoir, Netherlands, 1984.	0.024	15	Yes
PCC7806*mcyB*-	Deposited by E. Dittman, 1997. Genetically modified from PCC7806.	0.072	15	No

2.2.2 Field sampling

Plankton samples containing cyanobacteria were collected from four sites across Ontario and Québec, when surface blooms were reported. Surface water samples were collected in pre-rinsed plastic bottles and kept at 4°C until processed within, at most, 24 hours.

The Rideau Canal flows through Ottawa, Ontario and connects the Rideau Lakes and Rideau River with the Ottawa River. Sampling occurred near the University of Ottawa campus (45°42' N, 75°68'W) on September 7, 2016, after the observation of a cyanobacteria bloom that lasted a few days. Sampling was also conducted in the Smiths Falls portion of the Rideau River (44°89' N, 76°01'W).

Jack Lake (44°68' N, 78°05' W) is situated North of Peterborough, Ontario, in the Kawartha region of lakes. Sampling occurred on September 5th, 2016. Past studies indicated the presence of cyanobacteria colonies that could have the potential of being toxic (*Gloeotrichia echinulata*), but surface blooms are not typical of this mesotrophic lake.

Lac Breton (45°87' N, 74°23'W) is a small headwater lake situated in the municipality of Saint-Sauveur, Québec. Cyanobacterial blooms have been observed for a two-year period, from 2012 to 2013 (MDDELCC, 2016) and *Microcystis aeruginosa* is the main bloom-forming species observed in the water body.

2.2.3 Metabolome analysis

Sub-samples of cultures (20 mL) were filtered on pre-dried (60°C for 4 hours) and pre-weighed (Mettler Toledo Balance, Switzerland, ± 1 mg) glass fiber filters (GF/C, Whatman, ~ 1.2 µm) and frozen at -20°C until further analysis. Samples were dried at 60°C for 4 hours and the mass taken. Re-hydration and freeze-thaw cycles were used to increase cell lysis as the original extraction protocol suggested (Aranda-Rodriguez *et al.* 2005). The particulate samples were used to extract metabolites with accelerated solvent extraction, ASE, (Dionex, ThermoScientific, Oakville, Ontario), following the method described for microcystins by Aranda-Rodriguez *et al.* (2005). The filters were placed in 11 ml stainless steel cells lined with cellulose filters and packed with HydroMatrix (Varian) before being extracted twice by a 75% methanol solution under high pressure (2000 psi) and high temperature (80°C) for 5 minutes. The 20 mL-extract was evaporated to dryness under nitrogen pressure and heat at 60°C using a TurboVap LV (Zymark Corp.) and resuspended in 2 mL of 100% methanol (LC-MS grade). The solution was evaporated to dryness a second time under nitrogen pressure, resuspended in 50% methanol (LC-MS grade) for a final volume of 1 mL. The solution was filtered on polycarbonate filters (0.2 µm) and kept in a 1.5 mL amber glass vial at -80°C until ready to process.

To confirm and quantify possible oligopeptides found in the cultures and environmental samples, commercially available standards of microcystins (9 variants) and nodularin were analyzed. The oligopeptide nodularin has been used in previous studies as an internal standard to estimate the recovery of microcystins during extraction (Aranda-Rodriguez *et al.* 2005; Ortelli *et al.* 2008; Fayad *et al.* 2015). It has not been found to date in freshwater cyanobacteria or freshwater environmental samples and appears restricted to the marine environment.

Nodularin standard (CAS 118399-22-7) and microcystin standards for LR (CAS 101043-37-2) and LA (CAS 96180-79-9) variants were bought from Cayman Chemicals. MC-LF (CAS 154037-70-4), MC-LW (CAS 157622-02-1), MC-LY (CAS 123304-10-9), MC-RR (CAS 111755-37-4), MC-WR (CAS 138234-58-9), MC-YR (CAS 101064-48-6) and [Asp^3]-LR variants were bought from Enzo Life Sciences (Farmingdale, New York, USA). Microcystin standard for the variant [Dha^7]-LR (CRM-dmMCLR, Lot 20061116) was provided by Dr. S. Sauvé, Département de Chimie, Université de Montréal. All standards have a purity over 95%, and 10 ppm solutions in methanol were prepared as identification references.

An UPLC system (Waters AcquityTM) was used for separation of the compounds, using a Acquity UPLC BEH C18 column (2.1 mm × 50 mm, i.d. 1.7 μm, Waters Corp., Milford, USA). Mobile phase A was an acetonitrile and 0.1% formic acid solution (LC-MS grade), and phase B was a water and 0.1% formic acid solution (LC-MS grade). The solvent gradient went from 5% to 95% A in five minutes, under a constant temperature of 50°C. The flow rate in the column was 0.8 mL per minute. The injection volume was 0.2 μL.

A quadrupole time of flight (QTOF) tandem mass spectrometer (MS/MS) was used for compound analysis (Xevo-G2, Waters Corp.) in positive and negative ions mode (6V collision energy). The following optimized parameters were used: scan time 0.1 seconds; sample cone voltage, capillary 1.2 kV for positive ionization and 2.5 kV for negative ionization extraction cone 4.0; 35 V; source temperature, 150 °C; desolvation temperature, 500 °C; desolvation gas flow, 1200 L/h; cone gas flow, 20 L/h. MS data were collected in the full scan mode from *m/z* 50-1500 Da. All the data were acquired in continuous mode without mass correction using an independent reference lock mass, Leucine encephalin, in the positive ion mode ([M+H] = 556.27 Da at 2 ng/μL under a flow rate of 5 μL/min).

Spectral analysis was done with MassLynx V4.1 SCN918 and MarkerLynx software (Waters Corp.). Peaks were detected between 0.3 and six minutes of retention time (RT). The intensity of each compound was normalized against the total ion count and the dry weight of the sample to account for the possible variation in biomass extracted. To be considered present, the mass spectrum of a compound had to present three isotopic peaks (Silverstein *et al.* 2007), which lead to a selection of a signal to noise ratio (S/N) above two in the samples.

In order to investigate the differences in metabolites between strains of *Microcystis* in cultures and from environmental samples, MarkerLynx software (Waters Corp.) was used for principal component analysis (PCA) and two-classes orthogonal partial least-squares discriminant analysis (OPLS-DA) was conducted followed by S-plot generation. The METLIN database (Scripps Center for Metabolomics: https://metlin.scripps.edu) was used for a tentative identification of bioactive compounds (±5 ppm *m/z*). Tentative identification was also done by examining the fragmentation products expected for the molecule using ChemDraw (PerkinsElmer Informatics) or as seen in available standards of similar compounds. To search for unidentified microcystins in the samples, the total ion chromatograms (TIC) were scanned for the Adda moiety molecular weight (structure available in Table A.1), as it is specific to this group of compounds. When the signal was above the S/N ratio, the mass spectra were analyzed to find other possible fragments, and a plausible pseudo molecular ion [M+H].

2.3 Results

2.3.1 Separation and identification of compounds

A good separation of compounds was observed as demonstrated by chromatograms of standard mixtures (Figure 2.1). Retention times (RTs) were different for all microcystin congeners despite their similar structures and chemical properties. The only exception can be observed in Figure 2.2, where a subsequent injection of two variants of desmethylated MC-LR ([Dha^7] and [Asp^3] variants) along with MC-LR demonstrated RTs close to each other, making them more difficult to differentiate. [Dha^7]-MC-LR (Figure 2.3a) had a slightly higher RT (2.88 min) than MC-LR and [Asp^3]-MC-LR (Figure 2.3b) (2.87 min).

Variants could also be differentiated by examining the fragmentation under a high energy collision mode (Figure 2.4). For example, in the strains CPCC299 and CPCC464, a [M+H]= 1037.60 Da was detected at RT 3.07 min, which could correspond to the microcystin congener [Leu^1]-MC-LR (Figure 2.3c) (Park *et al.* 2001; Spoof & Catherine 2017). Under a high-energy collision mode, fragmentation (Figure 2.5b) was similar to that of MC-LR (Figure 2.5c), the most important fragment being the Adda moiety at *m/z* = 135.08 Da. The presence of this fragment and the similar spectra provided additional evidence in the identification of this molecule as a microcystin congener. An example of fragmentation of MC-LR and the corresponding signals in positive ionization mode is presented in Table A.1 (Appendix A).

Another example of the use of fragmentation under high energy was the identification of a type of cyanopeptolin in *Microcystis aeruginosa* CPCC299 and CPCC464. For this compound, two other major peaks were observed at RT 2.13 and 2.25 min (Figure 2.6a), both presenting the same signals corresponding to the cyanopeptolin variant CPT911 (Figure 2.3d). Masses

corresponding to fragments of the molecule were found in both signals (Table A.2, Appendix A). The two peaks could be explained by the presence of an isomer in the analyzed mixture. The higher signal intensity of the first peak (CPT911A) might reflect the dominance of this isomer. Both signals were however well above the S/N threshold ratio as demonstrated in Figure A.2 (Appendix A).

The instrument detected 2168 different signals across all samples, each signal corresponding to a specific fragment in a different retention time, between 0.43 and five minutes. The average signal number per sample was 628, with a maximum of 934 in CPCC464, and a minimum of 392 in CPCC300. PCC7806 (WT) had slightly more signals (514) than the mutant (489). All compounds tentatively identified using the method described in this study are presented in Table 2.2. In this table, three unidentified compounds had major fragments signals in common with the microcystin standards used in the study, including the fragment for the Adda moiety at *m/z*=135.09 Da (complete spectra in Appendix A, Figures A.3 and A.4). They are presented as unidentified microcystin, as a further investigation as standard comparison or NMR analysis would be required to confirm their identity. A list of known microcystins that could be represented by those signals is presented in Table 2.3. These three unidentified compounds were considered as microcystins for the rest of this study. A list of compounds that were previously found in the strains of interest as reported in the scientific literature, but not found in this study, is presented in Table A.3.

Relative amounts of oligopeptides in the strains are presented in Figure 2.7. The environmental samples are not presented in Figure 2.7, as only one compound, an aeruginosin, was identified in all the lakes samples (Table 2.2). The wildtype strain PCC7806, was the only culture studied with four different oligopeptides families: microcystins, aeruginosins,

aerucyclamides and cyanopeptolins, while all the others had different combinations of the four families. In PCC7806 (WT) and CPCC299, microcystins represented 53% and 49% of the detected compounds respectively, while aeruginosin was the dominant family of oligopeptides found in CPCC464 (54%), and aerucyclamides in CPCC300 (63%) and PCC7806*mcy*B- (57%) (Figure 2.7). A breakdown of the different microcystins congeners was also performed (Figure 2.8). MC-LR was the dominant variant found in CPCC300 and PCC7806 (54% and 53% respectively), while four different signals for microcystins were found in CPCC299. A total of 34% of microcystins found in CPCC464 corresponded to the signal for an unidentified microcystin variant (Compound 2).

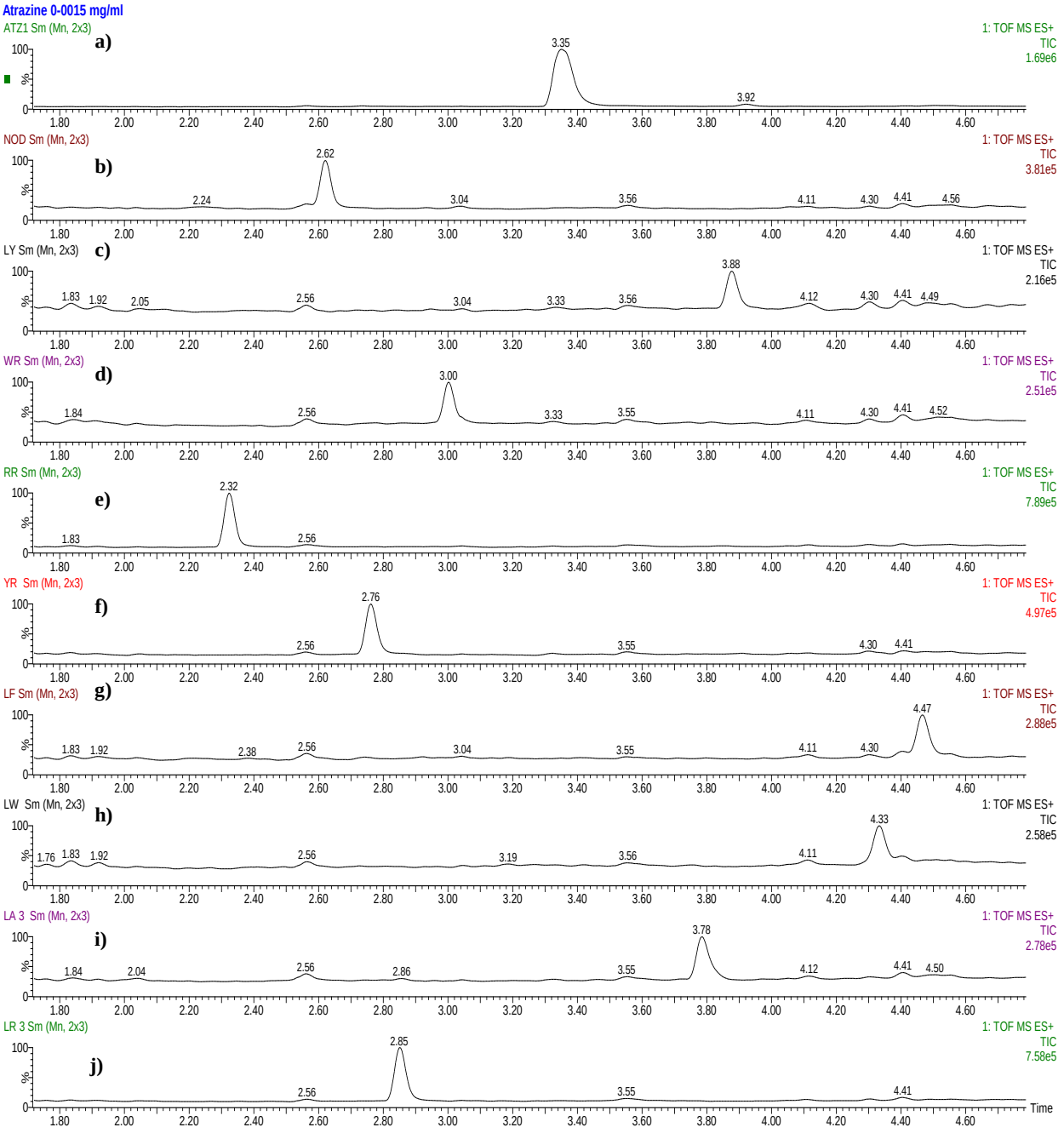

Figure 2.1. Separation of standards in a positive ionization mode. **a)** ATZ (3.35 min); **b)** NOD (2.62 min); **c)** MC-LY (3.88 min); **d)** MC-WR (3.00 min); **e)** MC-RR (2.32 min); **f)** MC-YR (2.76 min); **g)** MC-LF (4.47 min); **h)** MC-LW (4.33 min); **i)** MC-LA (3.78 min); **j)** MC-LR (2.85 min).

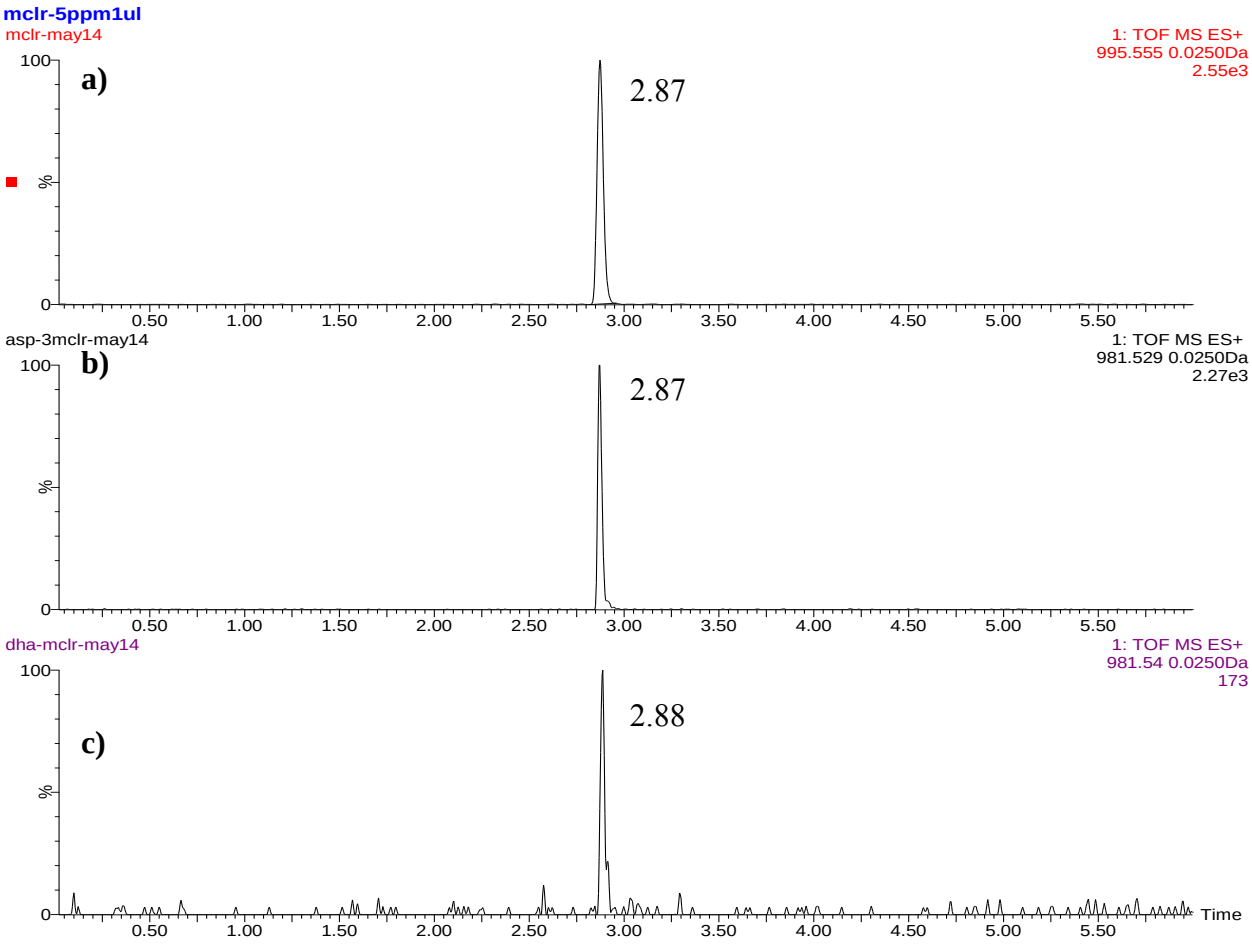

Figure 2.2. Separation of supplemental standards in a positive ionization mode during a subsequent injection. The MC-LR variant was used as a control for minor changes in RT. **a)** MC-LR (2.87 min); **b)** [Asp^3]-MC-LR (2.88 min); **c)** [Dha^7]-MC-LR (2.87 min).

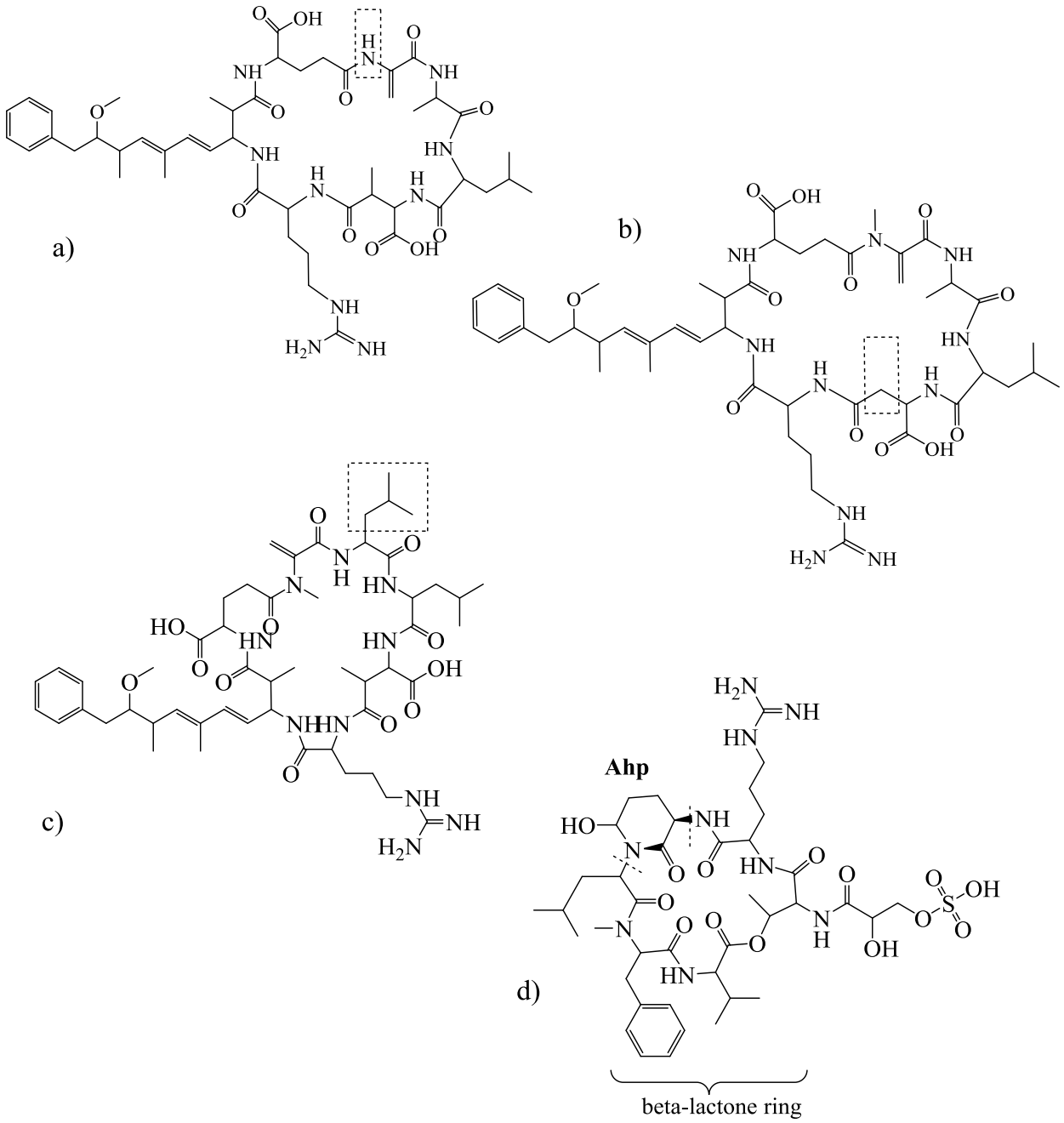

Figure 2.3. Structures of the oligopeptides **a)** [Dha^{7}]-MC-LR; **b)** [Asp^{3}]-MC-LR; **c)** [Leu^{1}]-MC-LR; **d)** CPT911. The cyanopeptolins characteristics are easily recognizable by the presence of a β-lactone ring and the residue Ahp (3-amino-6-hydroxy-2-piperidone). Moiety differentiation between a) to c) are enclosed in dashed boxes in their respective structures.

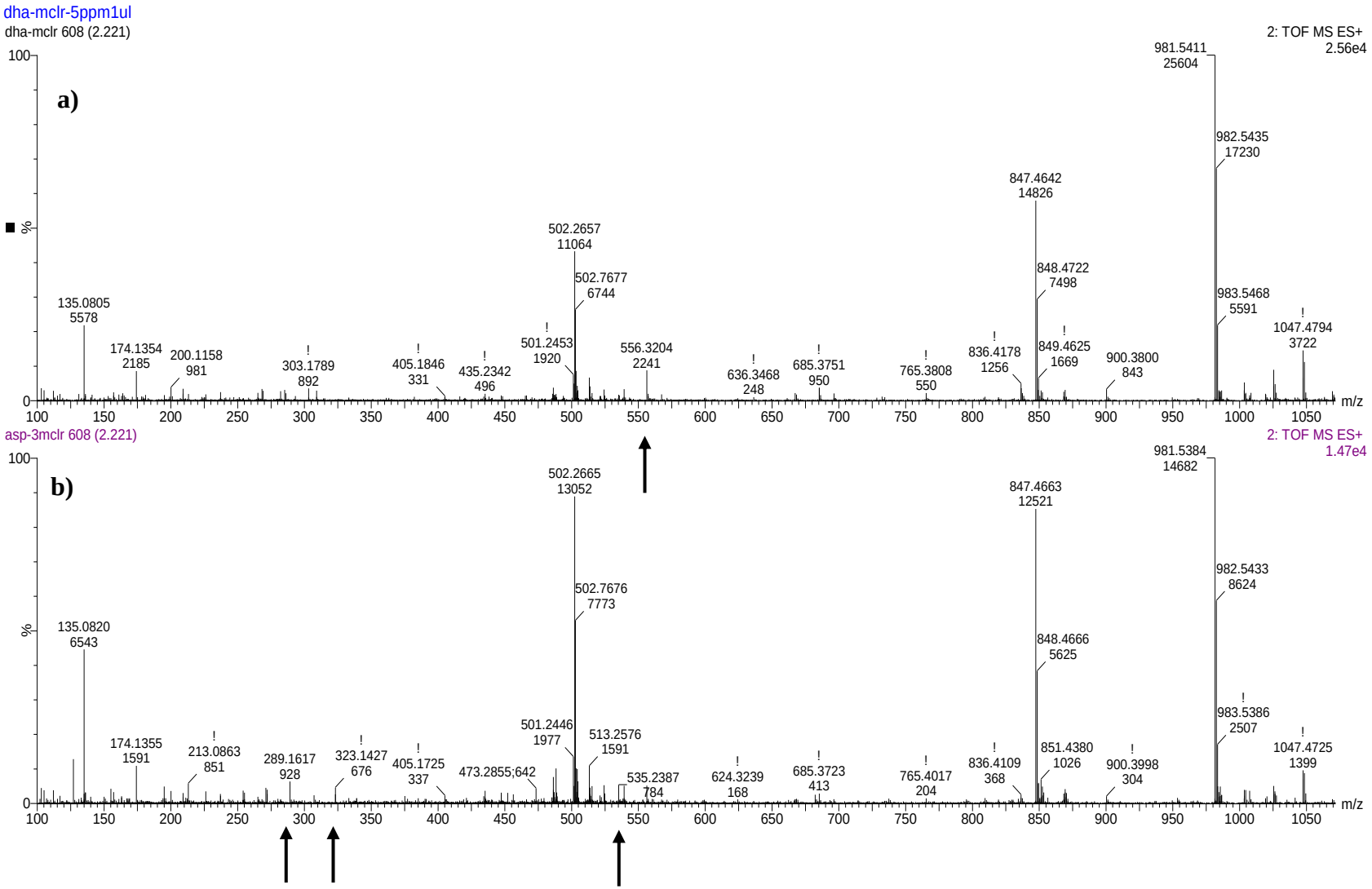

Figure 2.4. Comparison between high energy spectra from **a)** the [Dha^{7}]-MC-LR variant and; **b)** the [Asp^{3}]-MC-LR variant as detected by tandem mass spectrometry. Both variants have the same mass, and a similar RT (2.88 and 2.87 min respectively). Differentiation between the two can only be made by examining the smaller fragments indicated by the arrows.

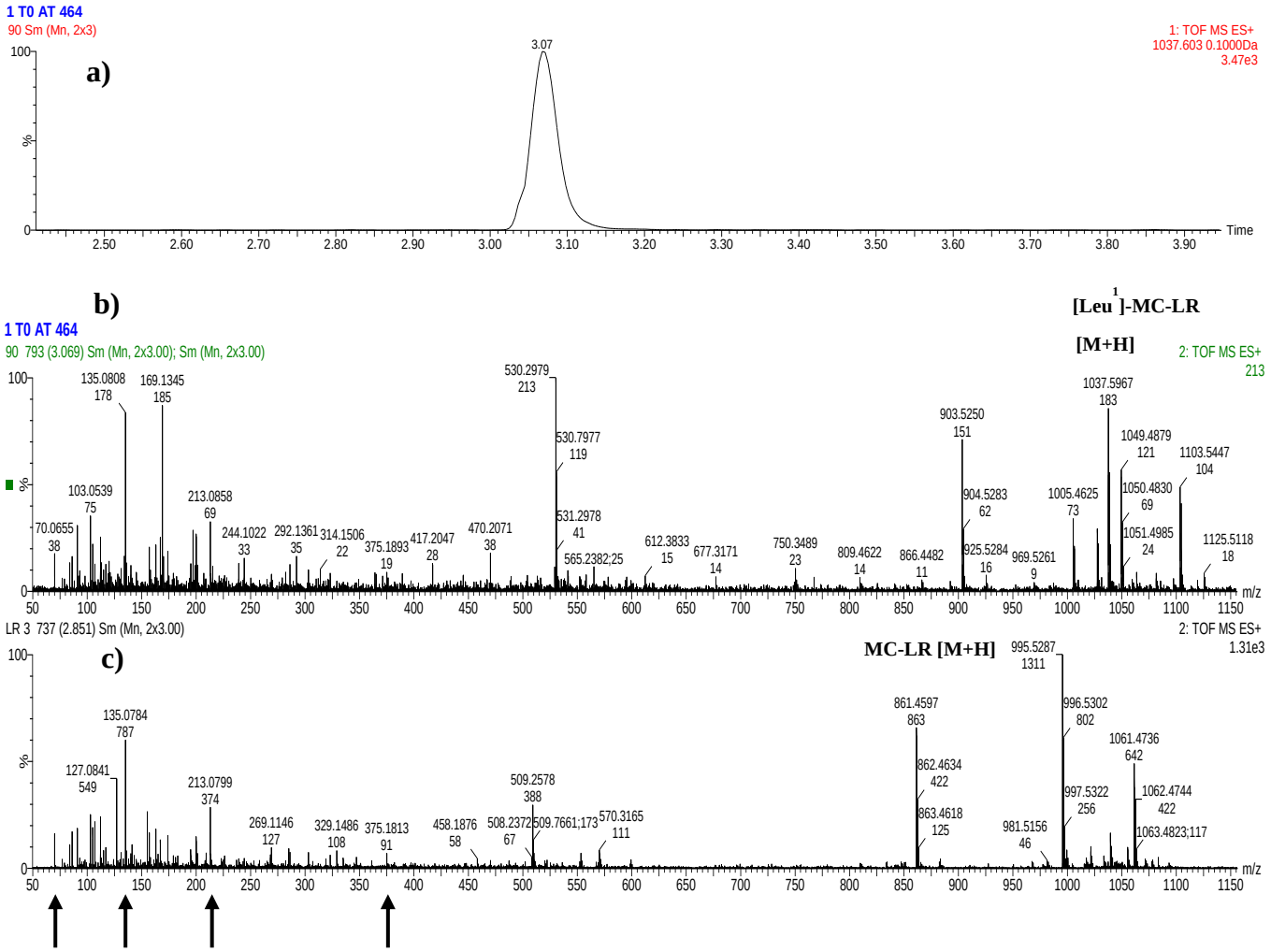

Figure 2.5. a) Chromatography of the potent [Leu[1]]-MC-LR congener; **b)** high energy spectrum of [Leu[1]]-MC-LR; **c)** high-energy spectrum of the standard solution of MC-LR. The arrows point the common fragments between the two molecules.

a)

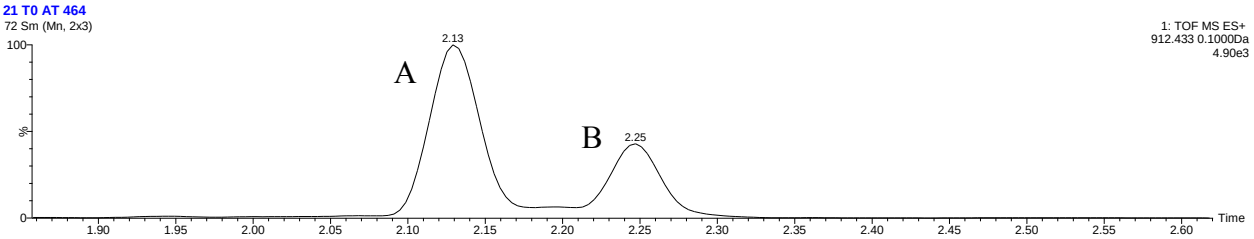

b)

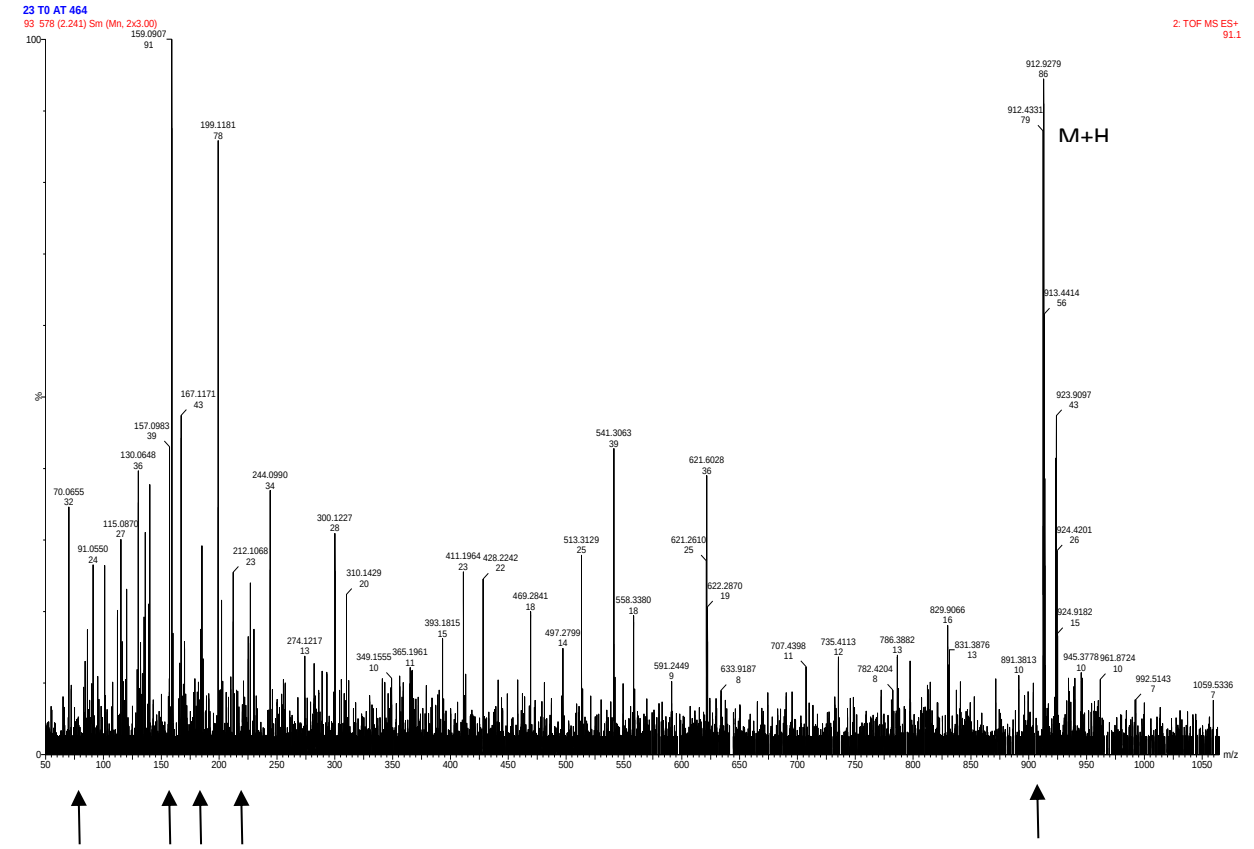

Figure 2.6. CPT911 detection in *Microcystis aeruginosa* strain CPCC464; **a)** Separation of two isomers, CPT911A at RT 2.13 min and CPT911B at RT 2.25 min; **b)** High energy spectra for CPT911B. Signals corresponding to identified fragments are indicated by an arrow. The pseudo molecule [M+H] represents the signal of the mass of the whole molecule under positive mode ionization.

Table 2.2. Compounds identified and tentatively identified in *Microcystis aeruginosa* strains and environmental samples classified by oligopeptides families. Standards were not available for most compounds; therefore, identification is based on RT, mass, and fragmentation only. [M+H] is the observed value expressed in Daltons (Da).

Compounds	Formula	[M+H]	RT (min)	CPCC464	CPCC299	CPCC300	PCC7806	PCC7806 *B-*	Rideau Canal	Smiths Falls	Jack Lake	Lac Breton
Microcystins												
[Asp^3]-MC-LR*	$C_{48}H_{72}N_{10}O_{12}$	981.5220	2.84			X	X					
[Leu^1]-MC-LR	$C_{52}H_{80}N_{10}O_{12}$	1037.6033	3.06	X	X							
MC-LR*	$C_{49}H_{74}N_{10}O_{12}$	995.5287	2.84			X	X					
Microcystin *(compound 1)*	*N/A*	1031.4791	3.18		X							
Microcystin *(compound 2)*		1055.5521	2.98	X	X							
Microcystin *(compound 3)*		1009.4915	2.97		X							
Cyanobactins												
Aerucyclamide B	$C_{24}H_{32}N_6O_4S_2$	533.1835	4.59			X	X	X				
Aerucyclamide C	$C_{24}H_{32}N_6O_5S$	517.2213	4.47			X						
Cyanopeptolins												
Cyanopeptolin 911	$C_{39}H_{61}N_9O_{14}$	912.4331	2.13	X	X							
Cyanopeptolin 911 *(isomer)*			2.25	X	X							
Cyanopeptolin 954	$C_{46}H_{63}ClN_8O_{12}$	955.4891	3.62		X							
Cyanopeptolin D	$C_{48}H_{76}N_8O_{12}$	957.5405	3.13			X	X	X				
Aeruginopeptin 228B	$C_{52}H_{72}N_8O_{15}$	1049.4680	2.79		X							
Anabaenopeptilide 90B	$C_{45}H_{61}ClN_8O_{14}$	973.4313	3.47	X	X							

The star (*) indicates a compound comfirmed by comparison to the standard.

Table 2.2. ***(continued)*** Compounds identified and tentatively identified in *Microcystis aeruginosa* strains and environmental samples classified by oligopeptides families. Standards were not available for most compounds; therefore, identification is based on RT, mass, and fragmentation only. [M+H] is the observed value expressed in Daltons (Da).

Compounds	Formula	[M+H]	RT (min)	CPCC464	CPCC299	CPCC300	PCC7806	PCC7806 *B-*	Rideau Canal	Smiths Falls	Jack Lake	Lac Breton
Aeruginosins												
Aeruginosin KT608A / KT608B / Microcin SF608	$C_{32}H_{44}N_6O_6$	609.2664	5.53	X								
Aeruginosin KT608A / KT608B / Microcin SF608		609.3372	1.65	X								X
Aeruginosin 98A / DA688	$C_{29}H_{45}ClN_6O_9S$	689.2940	1.46	X	X							
Aeruginosin 98A / DA688		689.2833	1.28				X	X				
Other small peptides												
N-acetylornithine	$C_7H_{14}N_2O_3$	175.1187	0.40	X		X						

Table 2.3. Possible microcystin variants for the three unidentified compounds from *M. aeruginosa* strains CPCC464 and CPCC299 presented in Table 2.2. Corresponding molecular weights are expressed in Daltons (Da). List of MC variants from Spoof & Catherine (2017).

	MC Variants	[M+H]	Molecular Formula
Microcystin *(Compound 1)*	[Asp^3]MC-M(O_2)R *(oxidation artefact)*	1031.4865	$C_{47}H_{71}N_{10}O_{14}S$
	[d-Asp^3, Dha^7]MC-HtyR	1031.5197	$C_{51}H_{71}N_{10}O_{13}$
	[Asp^3, DMAdda^5]MC-HtyR		
	[Asp^3]MC-RY		
	[Dha^7]MC-RY		
	[Asp^3, Dhb^7]MC-RY		
	[d-Asp^3]MC-YR		
	[Dha^7]MC-YR		
	[Asp^3, (E)-Dhb^7]MC-YR		
	[DMAdda^5]MC-YR		
MC *(compound 2)*	[Met^1]MC-LR	1055.5594	$C_{51}H_{79}N_{10}O_{12}S$
	[Leu^1, NMeSer^7]MC-LR	1055.6136	$C_{52}H_{83}N_{10}O_{13}$
Microcystin *(Compound 3)*	[D-Asp^3, ADMAdda^5, Dha^7]MC-HilR	1009.5353	$C_{49}H_{73}N_{10}O_{13}$
	[Gly^1, Asp^3, ADMAdda^5, Dhb^7]MC-LHAr		
	[d-Asp^3, ADMAdda^5]MC-LR		
	[ADMAdda^5, Dha^7]MC-LR		
	[Asp^3, ADMAdda^5, Dhb^7]MC-LR		
	[MeAla^1]MC-LR or [MeLeu^2]MC-LR	1009.5717	$C_{50}H_{77}N_{10}O_{12}$
	MC-HilR		
	MC-Lhar		
	[d-Glu(OCH_3)$_6$]MC-LR		
	[Mdhb^7]MC-LR		
	[Leu^1, Asp^3, DMAdda^5]MC-LR		

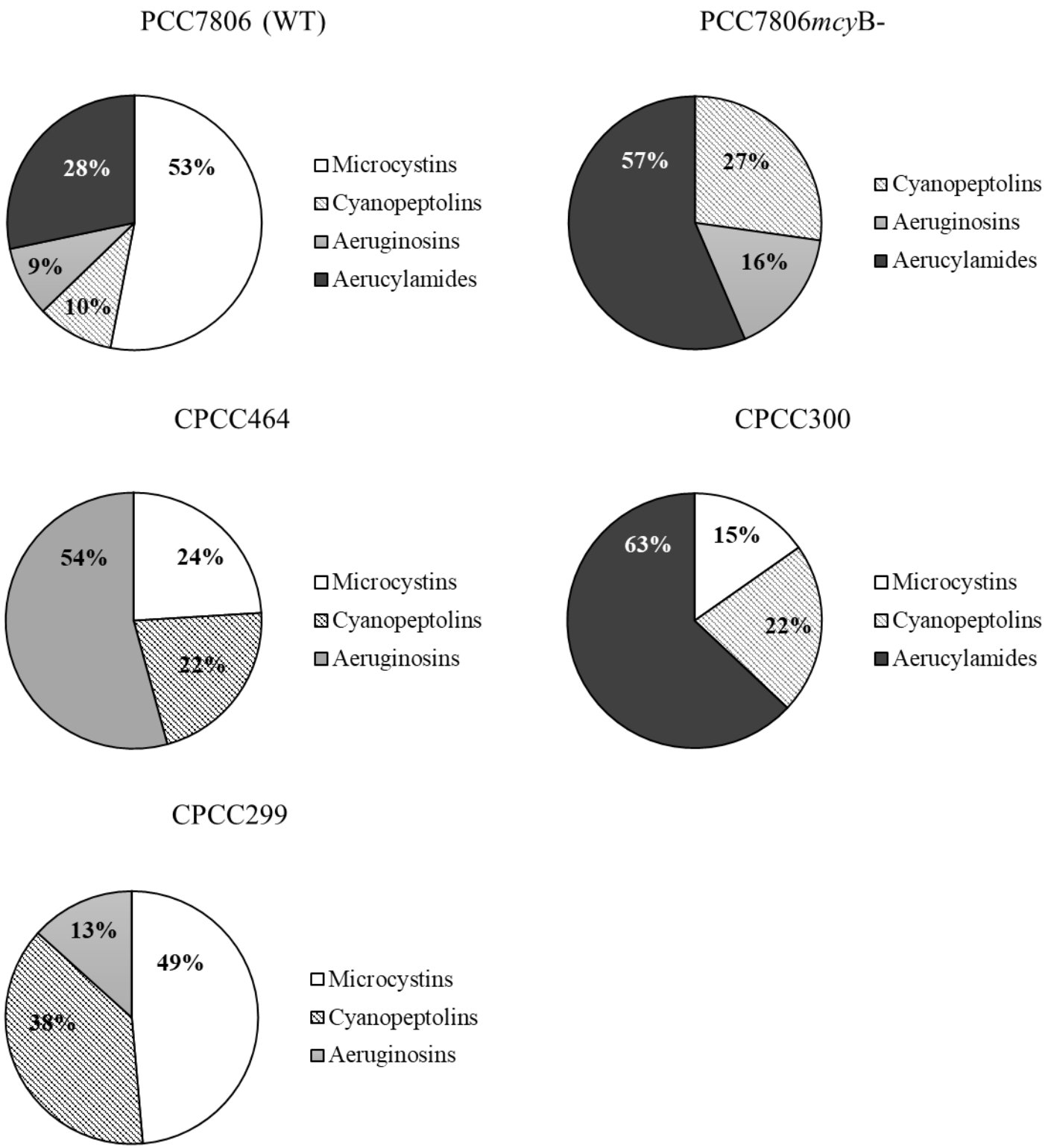

Figure 2.7. Relative amounts of oligopeptides families that were identified in the strains of *Microcystis aeruginosa.* This does not take into consideration the unidentified compounds that could also be part of the families represented here.

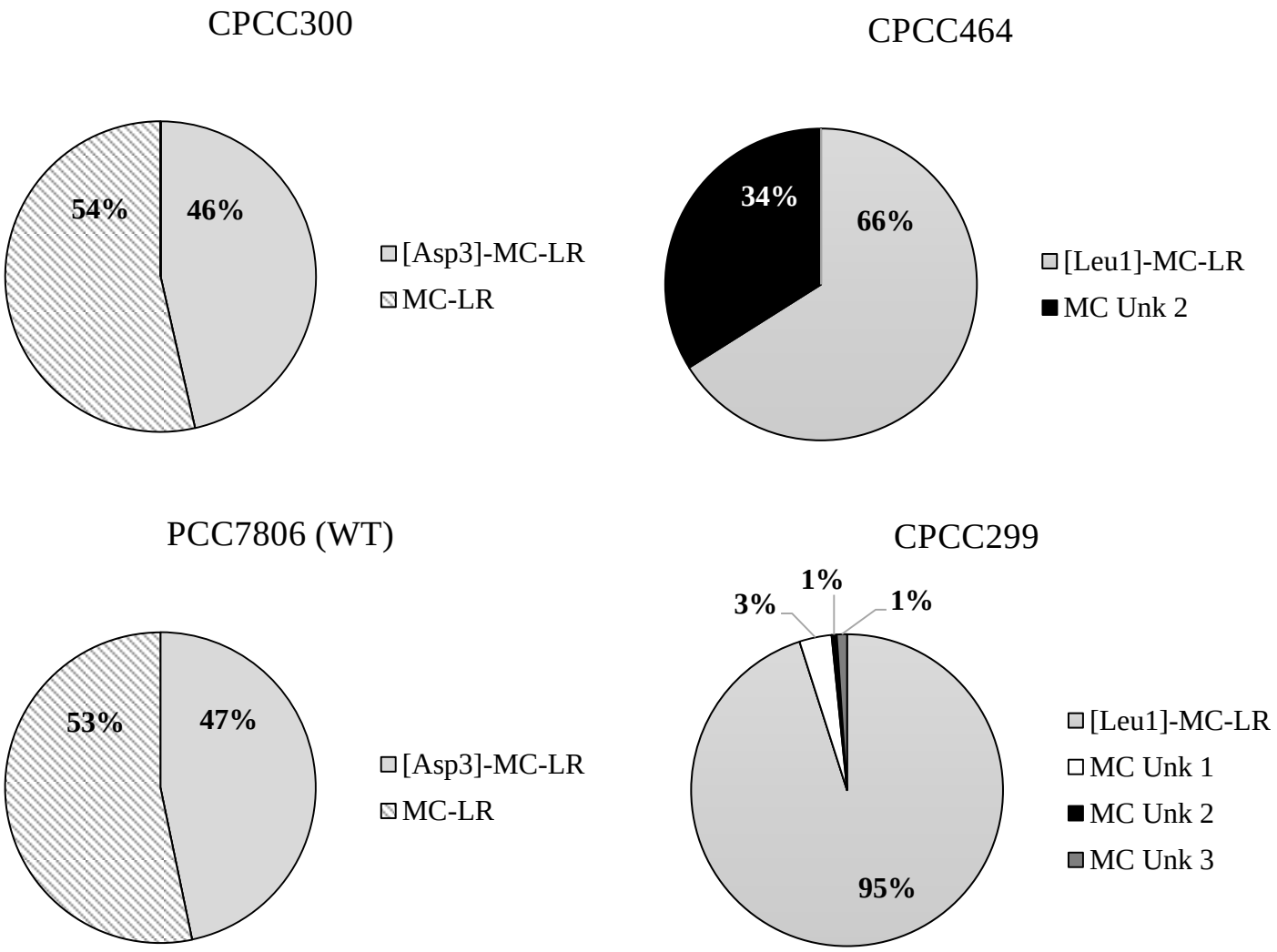

Figure 2.8. Relative microcystin congener concentrations among toxic strains of *Microcystis aeruginosa*. This does not take into consideration unidentified microcystin congeners that could be present in the samples.

2.3.2 Metabolome profile of Microcystis *strains and environmental samples*

The separation and resolution of individual compounds was better in the pure cultures than environmental samples (Figure 2.9a) when compared, for example, to the chromatogram of the MC-producing strain CPCC299 (Figure 2.9b). The considerable number of signals at various RT can be analyzed by examining the combination of metabolites to obtain a profile for each sample through Principal Component Analysis (PCA) even when the compounds are unidentified (Figure 2.10). Hotelling's ellipse for 95% confidence clearly excludes the strain CPCC299 because of its very large separation from all the other samples in the analysis. A new PCA excluding CPCC299 was therefore produced (Figure 2.11). The strains were clearly separated from each other along the first axis (PCA1) which represents metabolite composition and explained 24.17% of the overall variation. The low variation with respect to Principal Component 2 (19.35%) indicated the relative metabolite concentrations between groups was more similar between species or environmental samples. The largest variation observed along Principal Component 2 was found among the CPCC300 replicates. This is likely because the individual cultures were not grown at the same time, in contrast to the CPCC464 cultures, where replicates were grown at the same time.

The S-plot for comparison of CPCC300 and CPCC299 strains (Figure 2.12) showed many differences between the two. The data found at the extremities of the S-plot provide information regarding the compounds found in each culture. Only the data with a high confidence (further from the core on the x-axis) with the highest correlation to the strain (y-axis) can be considered significantly different from the data of the other strain. There was a large number of fragments detected in CPCC299 that were not present in CPCC300, as represented by

the long tail on the top right extremity of the "S" shape. A comparison of the metabolome of PCC7806 (WT) and PCC7806*mcy*B- (mutant) showed only two fragments with a strong correlation to the WT strain (Figure 2.13). The fragments had a mass of 502.2 Da and 509.2 Da at a RT of 2.84 min. These signals correspond to MC-LR (Figure 2.1). The detection of the MC-LR pseudo-molecule is presented for both the WT and the *mcy*B mutant, in five biological replicates (Figure 2.14). MC-LR was completely absent from the PCC7806*mcy*B- strain.

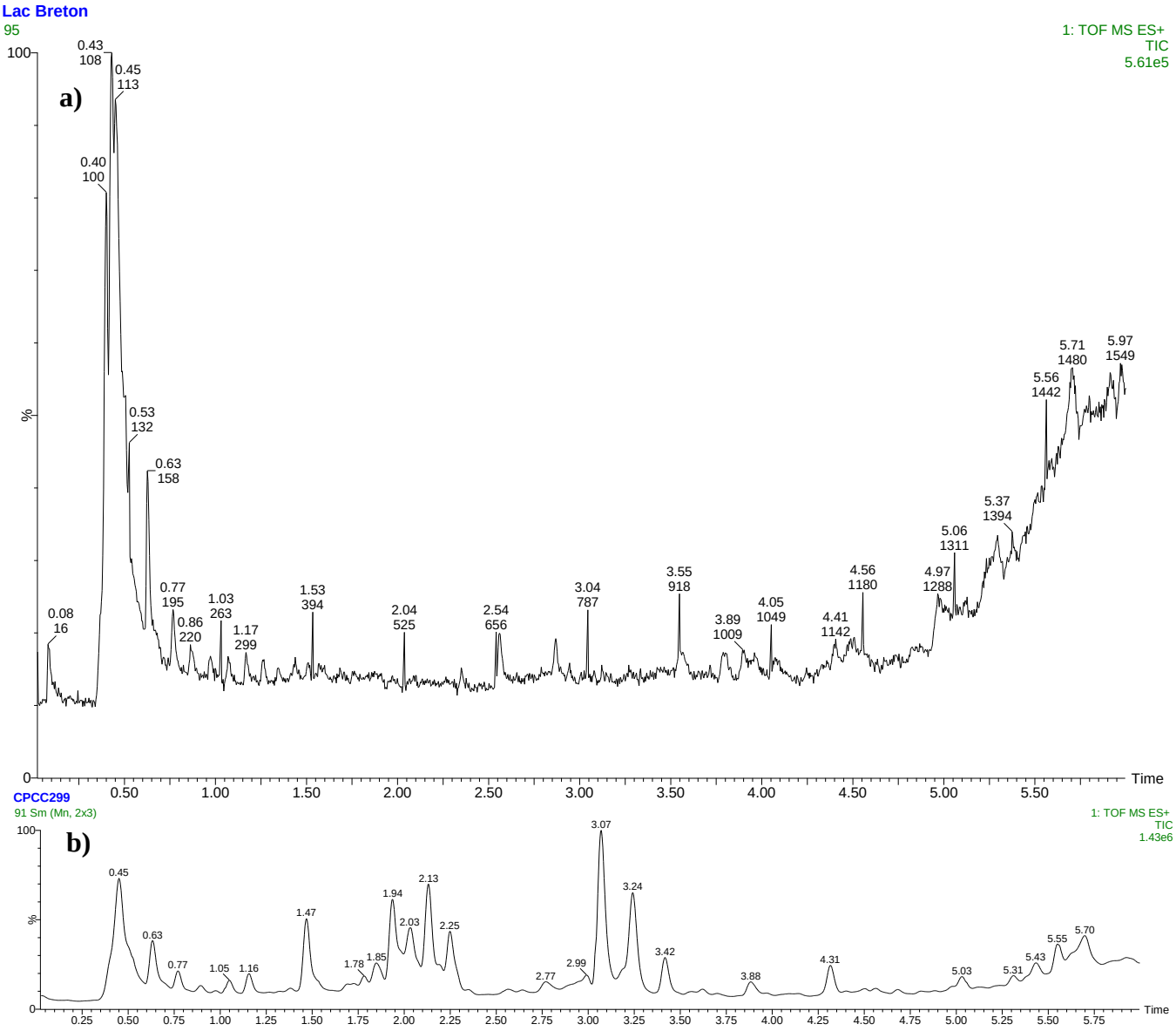

Figure 2.9. a) TIC for the Lac Breton sample. The retention time is present on the x-axis, while the relative intensity of each peak is present on the y-axis. Major signals around 0.43 min are typical of amino acids. Their close molecular weights lead to a low resolution of the separation, as the instrument and conditions were optimized for larger molecules; **b)** TIC for the CPCC299 strain. A strong separation of compounds is visible, despite a smaller count of compounds as presented in the right top corner of each panel.

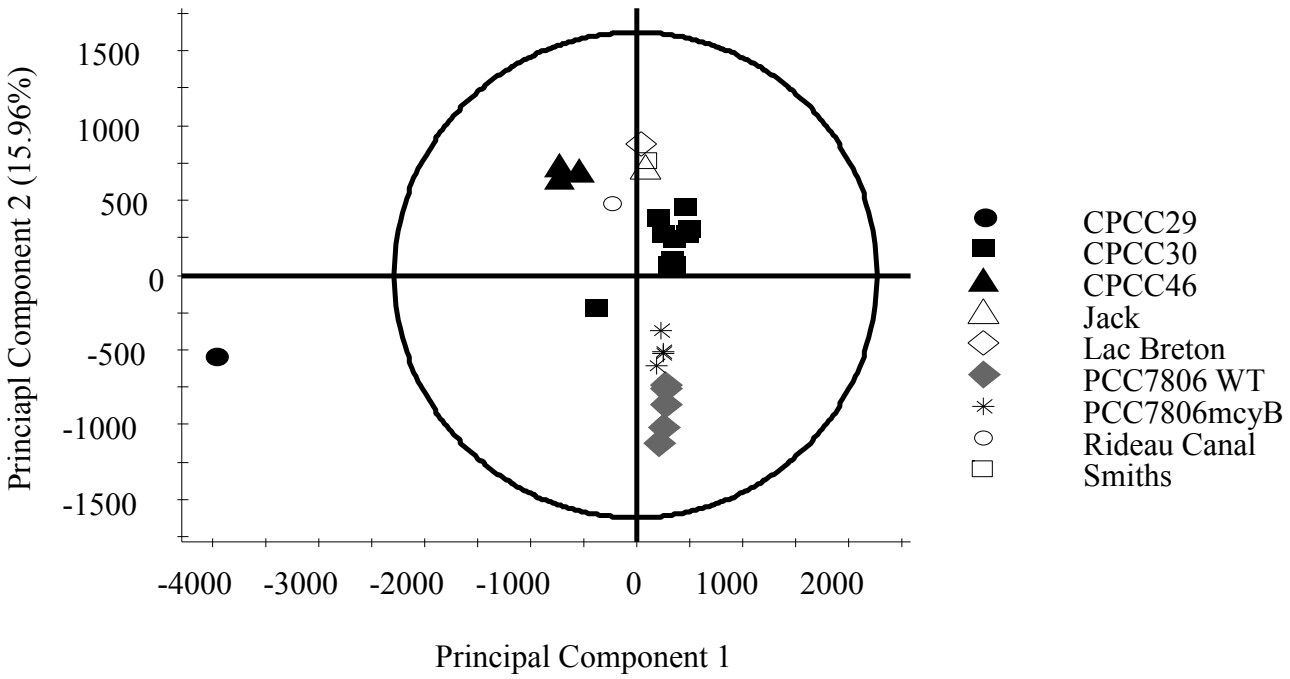

Figure 2.10. PCA scores from *Microcystis aeruginosa* cultures and environmental samples show variation between metabolomes of different samples. Each point represents the combination of metabolites in the sample. Component 1, variation in composition, explains 31.58% of the variation between strains. Component 2, changes in concentration, explains 15.96% of the variation. Hotelling's ellipse for 95% confidence excludes the CPCC299 profile.

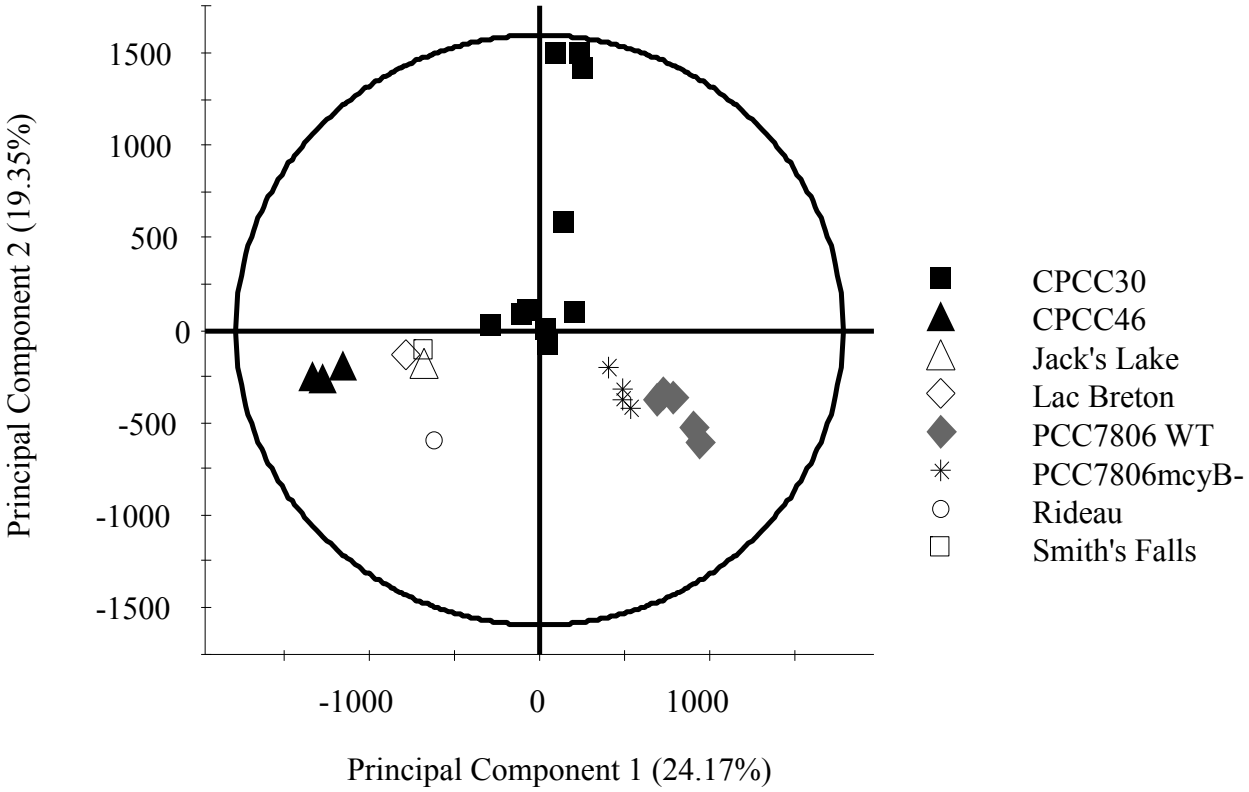

Figure 2.11. PCA scores for the metabolites profiles for the *Microcystis aeruginosa* cultures and the environmental samples, excluding the CPCC299 strain, shows variation between the strans of the same species. Each point represents the combination of metabolites found in one sample. Principal Component 1, variation in composition, explains 24.17% of the variation between strains. Principal Component 2, changes in concentration, explains 19.35% of the variation. Hotelling's ellipse represents the 95% confidence's range.

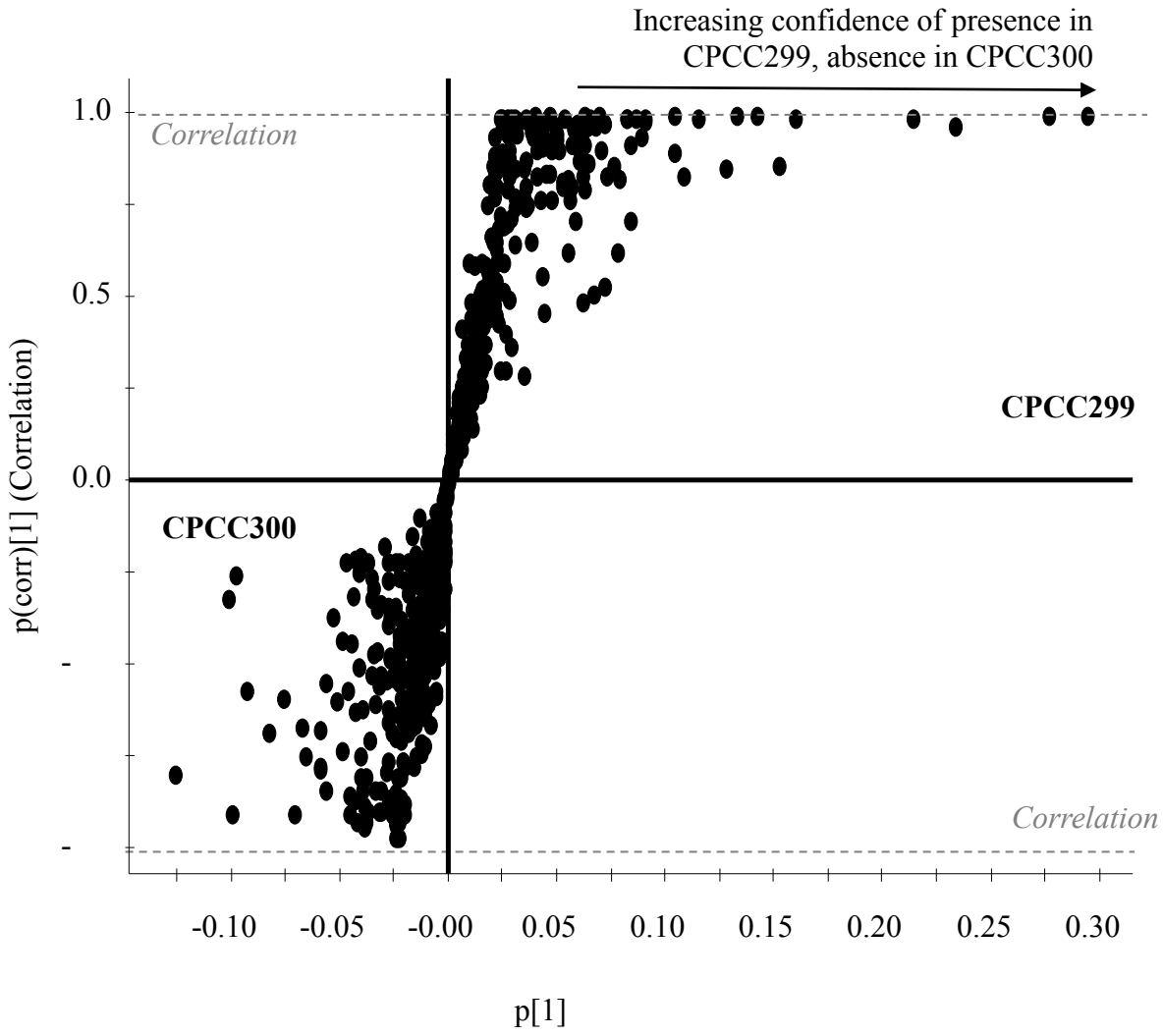

Figure 2.12. S-plot for metabolome comparison between CPCC300 (bottom left) and CPCC299 (top right). Each dot represents a compound fragment. The further at the extremity of the "S" shape, the greater the confidence of variation between the two cultures.

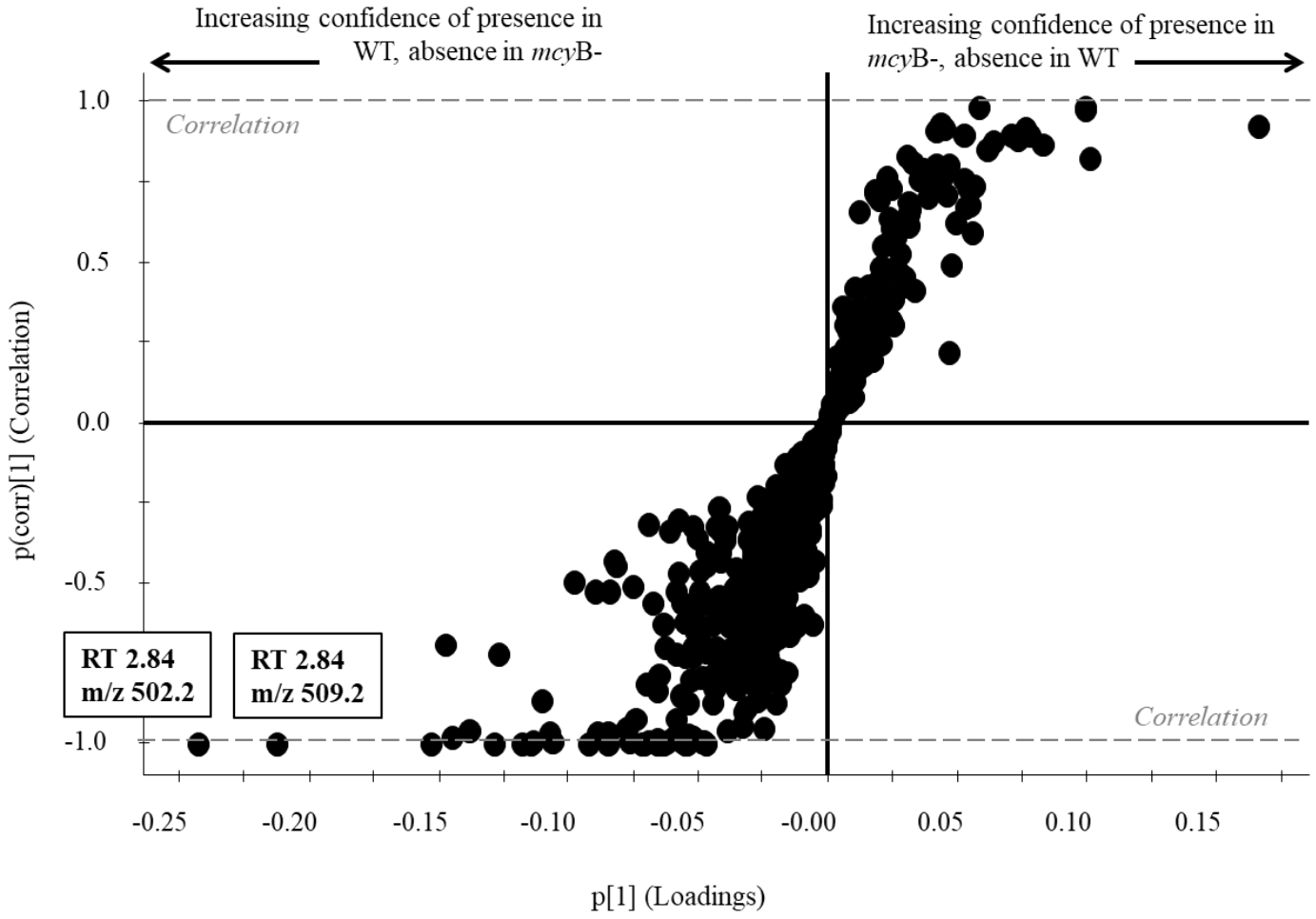

Figure 2.13. S-plot for metabolome comparison between the mutant (*mcy*B-) and the wildtype cultures of *Microcystis aeruginosa* PCC7806. The top right extremity of the S represents the mutant, while the left bottom extremity shows signals found in the wildtype cultures. Each dot represents a compound fragment. The further at the extremity of the "S" shape, the greater the confidence of variation between the two cultures. Signal details were indicated for compounds for which a high correlation and high confidence were found.

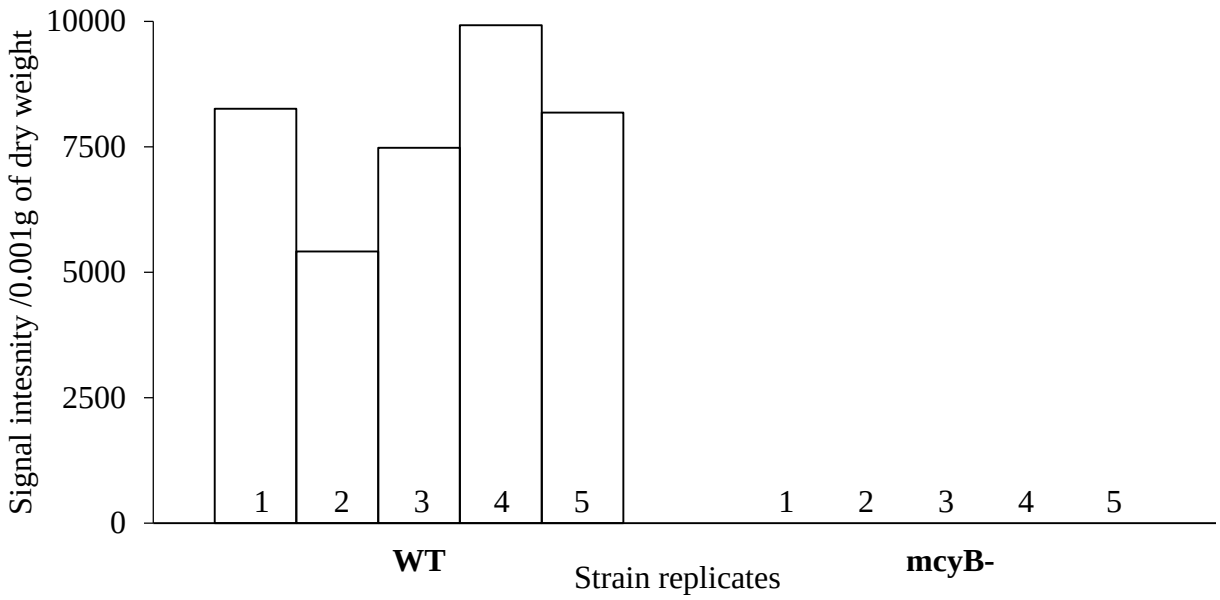

Figure 2.14. MC-LR in the mutant strains of PCC7806 (*mcy*B-) and the wildtype (WT), as detected by the [M+H]= 981.541 Da signal at a RT of 2.84 min corresponding to the standard. Values are expressed per 0.1 g of dry weight. Five biological replicates are presented for each strain.

2.4. Discussion

2.4.1 Identification of compounds

The large number of signals detected in each sample corresponded to as many metabolite fragments at various RTs. Most of these could not be identified (500-900 per sample). This was particularly the case for the environmental samples. Despite the number of signals detected in the lake samples (e.g. Lac Breton, Figure 2.9), only oligopeptides of the aeruginosin family (aeruginosin KT608A, KT608B or microcin SF608) were detected in one environmental sample, while the others did not exhibit signals that could be clearly identified (Table 2.2). Confirmation of this identification was not possible, as an analytical standard should be used in order to compare the retention and the fragmentation; no aeruginosin is currently available as a commercial standard. Environmental samples contain other organic matter (allochthonous and autochthonous) and other planktonic organisms (heterotrophic bacteria, eukaryotic algae, protozoa, etc.) that were collected on the filters as seston at the same time as the phytoplankton. This could explain the high number of signals that did not correspond to any major known cyanobacterial metabolite. It was surprising that few cyanobacterial compounds could be identified, as cyanobacteria were observed and confirmed through microscopy in these environmental samples (data not shown). The monocultures of *Microcystis aeruginosa* also had large numbers of signals but far fewer than the environmental samples.

Many unidentified and possible oligopeptides were found in the MC-producing strains CPCC299, CPCC300, PCC7806 and in the mutant PCC7806*mcyB*-. However, fewer were observed in the CPCC464 strain (Table 2.2 and 2.3). CPCC464 appeared to produce several different and undescribed microcystins as in a previous analysis

(LeBlanc Renaud 2009), and the absence of other peptides in the sample seems unusual, as the instrument should detect a vast range of them. The number of identified molecules in the samples therefore does not reflect all the variety of compounds present in each strain and environmental samples. The relative concentrations of the families (Figures 2.13 and 2.14) could also change with further detection and identification of compounds. With respect to microcystins, several congeners were tentatively identified. These were all MC-LR variants: [Asp^3]-MC-LR, [Leu^1]-MC-LR and MC-LR. This is a small number given that 246 congeners have been identified to date (Spoof & Catherine 2017). The strains CPCC464 and CPCC299 were closer in their metabolome profile than CPCC300 and PCC7806 (Figures 2.7 and 2.8), all microcystin producers. In the wild-type PCC7806, more than half the oligopeptides detected (53%) were microcystins (two variants, MC-LR and [Asp^3]-MC-LR, Figure 2.8). If we exclude this class from the analysis, the relative amounts of the compounds remaining correspond to that of the mutant strains, PCC7806*mcy*B-. The *mcy*B mutation therefore does not affected other peptides, which corresponds to what was shown previously (Martin *et al.* 1993). The mutation was also confirmed by the absence of MC-LR in the samples (Figures 2.3 and 2.4).

Aside from MC-LR and its closely related variants [Asp^3]-MC-LR and [Dha^7]-MC-LR, three unconfirmed variants of microcystins were detected. Those compounds were identified as microcystins because of the presence of the Adda fragment (Table A.1) under the high energy collision mode (*m/z*=135.08 Da), which is found in every MC variant. A few other signals were observed in the spectra, which were similar to those of the MC standards available and could be a product of microcystin fragmentation. Further

investigation of those spectra could lead to a better identification, although a few possibilities were identified by comparing the pseudo-molecule masses in the spectra to the theoretical values of known MC variants. For example, the unidentified compound 2 could be another MC-LR variant (Table 2.3). In the case of CPCC464, one unidentified microcystin (compound 2) represented a large fraction of the total microcystins detected. With only a few analytical standards, it is not possible to confirm the identification of these molecules with mass spectrometry only. Further analyses, based on extraction, separation, and purification of the molecules, would be necessary to pursue the identification of the molecules by NMR.

Despite their presence in the cultures, microcystins were not always the dominants oligopeptides produced by *Microcystis aeruginosa* (Figure 2.7). A few specific compounds known to be produced by cyanobacteria, and more particularly *Microcystis*, were detected, and the vast majority of them can be described as oligopeptides. Aeruginosins, cyanopeptolins and aerucyclamides were three groups with an equal or more important presence in the samples. Aeruginosins are protease inhibitors produced non-ribosomally, with potentially antiviral properties. Cyanopeptolins are produced non-ribosomally and are cyclic peptides like microcystins, but their upregulation and toxicity are not well understood. Finally, aerucyclamides are ribosomally produced and may have antimalarial and antiparasite activities (Chapter 1).

Some other compounds were expected in the cultures but were not found or the signal was below the detection limit. For example, β-cyclocitral, a volatile compound produced in all *Microcystis* species (Jüttner *et al.* 2010), was not detected in any sample. This could be due to its volatile nature that would be easier to isolate and detect with a

GC/MS (Jüttner *et al.* 2010). Moreover, the natural amino acid β-methylamino-L-alanine (BMAA), a neurotoxin, was not detected in cultures nor in environmental samples while its occurrence in freshwater cyanobacteria appears to be widespread (Roy-Lachapelle *et al.* 2015): BMAA was previously discovered in the PCC7806 strain (Cox et al. 2005) also tested in this study. The explanation here most likely lies in the concentration or extraction process. BMAA recovery is optimal with the use of nitrocellulose or nylon filters rather than glass fiber filters, which tend to adsorb BMAA and other polar molecules. BMAA extraction is also usually done in water (Cohen 2012), because of the polarity of the molecule. However, in this study, a 75% methanol solution in water was used to optimize microcystins extraction. Also among expected molecules, Briand *et al*. (2016) detected a new variant of cyanopeptolin, CPT895, with a pseudo-molecule [M+H] of 896 Da in the strain PCC7806. However, no trace of this compound was found in the present study using the same strain. In the present protocol, a 75% methanol solvent was used to extract whereas Briand *et al.* (2016) used dichloromethane and methanol, which is a less polar mixture. Other studies in the literature have used various concentrations of methanol for extractions (Rohrlack *et al.* 2008; Faltermann *et al.* 2014; Pereira & Giani 2014).

Whether the absence of some compounds is due to the extraction solvent or the filter is unknown. To optimize the extraction protocol, cultures should be extracted using various combinations of filters types and solvents as discussed above and compare the TIC and compounds present by UPLC-QTOF MS/MS analysis.

2.4.2 Metabolome analyses

The selected strains of *Microcystis aeruginosa* varied widely in their metabolome, even when grown under the same environmental conditions. The most significant difference was observed in CPCC299. As the first PCA showed (Figure 2.10), its metabolome was very different from all the others. This difference can be seen in Figure 2.12, where many signals (unidentified) appeared absent from CPCC300 in comparison to CPCC299. Among the few compounds that were identified (Table 2.2), a clear majority were indeed present in CPCC299, but absent from CPCC300: an aeruginosin (98A or DA688), [Leu^1]-MC-LR, CPT911, CPT954, aeruginopeptin 228B, anabaenopeptilide 90B, and the three unidentified microcystins.

It is interesting to note all peptides found in the strains CPCC464 and CPCC299 were produced non-ribosomally (Figure 2.7) while CPCC300 and PCC7806 (WT and mutant) had peptides from both the ribosomal and non-ribosomal pathway. The differences observed among the strains could be explained by this variation in the expressed pathways. Therefore, in this experiment, environmental growth conditions such as temperature and light exposure were shown to be less important than underlying genetic differences between strains in determining overall metabolite profiles.

Interestingly, the isolates of *Microcystis aeruginosa* showed more variation within the same species than the environmental samples from Ontario and Québec (Figure 2.10). Besides having more than just cyanobacteria present in the environmental samples, one significant difference was that culture conditions were optimal for growth under high nutrient concentrations. These conditions are not encountered in natural systems, where extreme nutrient deficiency (and/or light limitation under bloom conditions) is more

typical: it is possible that very low nutrient concentrations leads to the convergence of metabolomic profiles. With only one sample from each lake taken at a specific time, it is difficult to provide a conclusion on the specific compounds present and relative concentrations in environmental samples, but this preliminary work provides some information on the metabolites that could be present in natural systems. Since toxicity from algal blooms can be the result of more than one compound, future research should aim at the complete characterization of the cyanobacterial metabolome.

Chapter III

Variation in metabolite composition and fitness under oxidative stress in the cyanobacterium *Microcystis aeruginosa*

3.1 Introduction

Cyanobacteria are known to produce a vast range of small peptides and oligopeptides (Welker & Von Döhren 2006; Welker *et al.* 2006; Rohrlack *et al.* 2008; Ishida *et al.* 2009). Most of these compounds are considered secondary metabolites, as no primary cell function (e.g. reproduction) has been linked to their synthesis to date. The most notorious of these compounds are the microcystins, which are cyclic heptapeptides with a range of hepatotoxicity related to structural variations (Chapter 1). Microcystins can affect the whole ecosystem by changing the zooplankton community and being directly or indirectly toxic to vertebrates. The biological role of microcystins in cyanobacteria has been investigated, but continues to be debated. While they are useful in defense against grazing by zooplankton, this is not likely to be their biological role because the microcystin-producing gene cluster evolved in many cyanobacterial species well before the evolution of zooplankton and vertebrates (Brock *et al.* 1999). Their original purpose in the cell, therefore, has to relate to another process.

One of the current hypotheses being investigated is that microcystins provide protection against oxidative stress (Zilliges *et al.* 2011), the process involving the production of reactive oxygen species (ROS) in cyanobacteria. Oxidative stress can inhibit photosynthesis, degrade DNA and further impair protein synthesis and membrane formation. This can in turn affect growth, reproduction and survival of the cells (Chen et al. 2012b). Environmental factors that can lead to oxidative stress include high light exposure, UV, and certain pesticides. Oxidative stress can also be caused by extreme nutrients concentrations (too high or too low), and high salt concentrations (Kaebernick *et al.* 2000; Kaplan *et al.* 2012). Studies combining more than one factor have been

conducted since the hypothesis was first suggested in 2011 (Zilliges *et al.* 2011), but investigations are ongoing as the hypothesis is not fully supported. Among the supporting evidence, there is some tolerance of herbicides under high light exposure (Deblois *et al.* 2013), while light and nutrients also promoted growth and survival of toxic strains when compared to non-toxic ones (Alfonso & Kirilovsky 2001; Kaplan *et al.* 2012). Among the indirect evidence, immunogold assays have shown that microcystins are located in close proximity to thylakoid membranes (Young *et al*. 2005; Young *et al.* 2008), where ROS would form through photosystem II (PSII) activity (Jursinic *et al.* 1991; Blot *et al.* 2011; Tao *et al.* 2013).

UV radiation has been extensively studied and linked to DNA and protein damage in cyanobacterial cells, with effects observed under short- and long-term exposures (Strid *et al.* 1994; Jiang & Qiu 2005; Latifi *et al.* 2009; Jiang & Qiu 2011; Soule *et al.* 2013). Because UV exposure leads to oxidative stress responses, one might predict that UV exposure would influence microcystin production or favour the dominance of microcystin containing taxa in mixed natural communities. The increasing toxicity of blooms could be related to an increasing UV_B (280-315 nm) radiation at the surface of the Earth (Latifi *et al.* 2009), as a result of ozone layer destruction (Madronich *et al.* 1998). Several studies have been conducted on the effects of UV on microcystin production (Wang *et al.* 2011; Chen *et al.* 2012; Moon *et al.* 2012; Yang *et al.* 2015). However, the results have been quite variable and largely inconclusive (Soule *et al.* 2013). This could be explained by varying UV exposure across different wavelengths and the many different species and strains used across these studies. Both species and strains might be expected to respond differently.

Another agent of oxidative stress found in aquatic environments is the herbicide atrazine (6-chloro-N-ethyl-N'-1-methylethyl-1,3,5-triazine-2,4-diamine). Banned in the European Union, atrazine is still the most widely used herbicide in the United States, and the second most used in Ontario because of its low cost and effectiveness in controlling weeds (Regnault-Roger 2014). It is mostly used in crops, but can also be used in recreational waters and for domestic uses (e.g. lawn care) (Regnault-Roger 2014). Atrazine metabolites are highly soluble in water and their persistence makes them a long-term environmental problem as traces in sediments and groundwater can still be retrieved many years after atrazine application in agricultural watersheds (Graymore *et al.* 2001; Gilliom 2006; Deblois *et al.* 2013). Recently, atrazine has been found in 30% of tested lakes in the United States, even though levels were generally not high enough to raise concern (EPA 2012). Atrazine has been shown to be a strong inducer of oxidative stress (Rutherford & Krieger-Liszkay 2001; Chalifour & Juneau 2011; Chen *et al.* 2012; Deblois *et al.* 2013). By blocking the electron transfer in PSII, atrazine leads to ROS production in the cell. A few studies have examined the effects of atrazine on cyanobacteria (Stratton 1984; Abou-Waly *et al.* 1991; Deblois *et al*. 2013; Liu *et al.* 2014), but few have examined the effect on microcystins production per se.

In general, the production of microcystins in cultures is associated with higher light exposures (Kaebernick *et al.* 2000; Hesse *et al*. 2001; Young *et al.* 2005). Several studies have found a strong relationship between microcystin concentrations, the growth rate and the photosynthesis process in cyanobacteria (e.g. Orr & Jones 1998; Kaebernick *et al.* 2000), such that the production of total microcystins appears to be largely a function of growth rates. However, few studies have determined whether microcystin

variant composition changes with environmental factors and in particular oxidative stress. An early study by Tonk *et al.* (2005) suggested that high light promoted the production of more toxic congeners in the cyanobacterium *Planktothrix*. Since indeed some congeners are more toxic than others, it would be useful to better understand the factors that lead to their production. Aside from microcystin, other oligopeptides could vary as a function of oxidative stress, and affect the overall toxicity of a population by their possible toxicological effects (Chapter 1).

The specific objectives of this chapter are:

a) to assess the impact of various agents of oxidative stress on *Microcystis aeruginosa* fitness by comparing growth rates and related end-points for a wildtype and mutant strain for *mcyB*;

b) to determine if microcystin production and composition are affected by oxidative stress in various strains of *Microcystis aeruginosa*;

c) to identify the effects of oxidative stress on the overall metabolome of various strains of *Microcystis aeruginosa*.

If the hypothesis of a protection against oxidative stress is correct, then toxigenic strains of *M. aeruginosa* should demonstrate a higher growth rate than the non-toxic strains under oxidative stress conditions. Microcystins concentrations should also increase with stress if growth rate is kept constant.

3.2 Material and methods

3.2.1 Culturing techniques

Strains CPCC300 and CPCC464 of *Microcystis aeruginosa* were obtained from the Canadian Phycological Culture Collection (CPCC - University of Waterloo, Ontario, Canada). Strains PCC7806 and PCC7806*mcy*B- of this same species were purchased from the Pasteur Culture Collection (Institut Pasteur, Paris, France). All cultures were grown in BG11 medium (Andersen 2005) diluted from a concentrated form provided by the CPCC. A supplement of 10 µM of $NaHCO_3$ was added to the PCC cultures, to optimize their growth conditions (as suggested by the PCC). All cultures were kept in a growth chamber (Conviron) under white light (50 µM $m^{-2} \cdot s^{-1}$), with a light and dark cycle of 12 hours and a temperature of 20°C. Prior to all experiments, strains were maintained in semi-continuous culture, to keep a constant growth rate monitored with optical density at 750 nm (Carry 100 Bio Spectrophotometer, Varian, Winnipeg, Manitoba) (see Chapter 2 section 2.6.1). Strain characteristics are found in Table 2.1 (Chapter 2).

3.2.2 UV Exposure

Semi-continuous cultures of strains CPCC300, PCC7806 and PCC7806*mcyB*- were grown in batch cultures. Subsamples were taken from the batch for initial measurements before it was separated into ten flasks. Five were exposed to natural light (UV and visible) for 30 minutes, by direct exposure on the rooftop of CAREG (Center for Advanced Research in Environmental Genomics, University of Ottawa, ON). The other five flasks consisted of "controls" exposed to the same conditions in polycarbonate flasks

(non-UV penetrant) to maintain the high light intensity (visible light only, 400-700nm) and similar temperature. During the 30 minutes-exposure, culture temperature increased from 25 to 30°C, with an average of 28°C for the period. UV intensity was measured using a light meter (G&R labs, Model 200, mid UV probe, 300nm). UV exposure on the rooftop ranged from 1.40 to 3.90 mW/cm^2 with an average of 2.44 mW/cm^2.

3.2.3 Atrazine exposure

Semi-continuous cultures of strains CPCC300 and CPCC464 were exposed to atrazine (98%, CAS 1912-24-9, Cayman Chemicals, Ann Arbor, Michigan, USA). Concentrations of 15, 25, 40, 60 and 150 ppb were added to the cultures, and sub-samples taken at times 0 (at the same time as the atrazine addition), 24, 48 and 72 hours. The concentration range was chosen based on environmentally relevant concentrations (up to 20 ppb) and the response reported for cyanobacterial strains in the literature (Fairchild *et al.* 1998; Chalifour & Juneau 2011) to create a stress in the cells. Controls and treatments cultures were kept in normal growth conditions during the whole exposure (as described in section 3.2.1).

3.2.4 Metabolome analysis and compound identification

Sub-samples of cultures were filtered, extracted and analyzed with UPLC QTOF-MS/MS following the protocol described in Chapter 2 for analysis of cyanobacterial secondary metabolites. MarkerLynx software (Waters Corp.) was used for principal component analysis (PCA) and two-classes orthogonal partial least-squares discriminant

analysis (OPLS-DA) followed by S-plot generation to investigate the differences in metabolites between treatments and controls. METLIN database (Scripps center for metabolomics: https://metlin.scripps.edu) was used for a tentative identification of bioactive compounds (±5 ppm *m/z*).

3.2.5 Growth rates measurements

Sub-samples of cultures were preserved in a 1% p-formaldehyde solution and kept at 4°C in the dark until analysis by flow cytometry (FC-500, Beckman Coulter, California, USA) to calculate cell density. Cell counts were compared to yellow-green fluorescent beads (Polyscience Fluoresbite YG microspheres, 1 µm) added to the samples at a final concentration of 15% (about 10^6 beads/mL). Events were detected up to 2 minutes or 100,000 events. Bead fluorescence was detected in FL1 (515-545 nm), and cyanobacterial cells in FL4 (phycocyanin fluorescence, 653-669 nm). Growth rates were calculated using the formula below (Andersen 2005), where N_t represents the cell concentration at the end of the exposure period, and N_0 the cell concentration at the beginning of the experiment. Δ_t represent the time variation over the entire experiment.

$$\text{Growth rate} = \frac{lnNt - lnN0}{\Delta t}$$

Optical density at 750 nm was taken during sub-sampling using a Carry 100Bio (Varian). At 750 nm there is minimal interference from pigments (Andersen 2005). The

slope of the optical density plotted against the time was used to calculate a growth rate and compared to the growth rates obtained with cellular density.

3.2.6 Chlorophyll a analysis

Sub-samples were filtered on glass fiber filters (GF/C, Whatman, 1.2 µm) and kept at -20°C until further analysis. Pigments were extracted following the protocol described by Sartory and Grobbelaar (1984) and absorbances taken at 750, 665 and 649 nm using a Cary 100 Bio (Varian). Chlorophyll a (chl.a) concentrations were calculated using the following formula, where *V* is the volume in mL, *F* the filtration volume in L and *L* the length of the field length in cm (Bergmann & Peters, 1980).

$$[\text{Chl a}]\text{mg/L} = \frac{13.7(\text{A}_{665} - \text{A}_{750}) - 5.76137(\text{A}_{649} - \text{A}_{750})}{\text{FxL}} \text{x V}$$

Chl.a measurements give an approximation for biomass that can be used for the photosynthetic potential of the samples.

3.2.7 Statistical analyses

Student's t-test, one-way, and two-way ANOVA were performed on datasets using R. Unpaired t-test was used to compare data from different treatments (independent values), while paired t-test was used to compare datasets of treatments overtime (dependant). Normality and equal variances were confirmed prior to the analysis.

3.3 Results

3.3.1 UV exposure

All *Microcystis aeruginosa* strains exposed to UV radiation for 30 minutes responded the same way as the controls ($p<0.2$) in term of growth rates. It is however possible to observe a decrease in cellular density for CPCC300 (Figure 3.1) and PCC7806*mcyB*- (Figure 3.2a) during the course of the experiment in both controls and treatments, although significant only in the case of CPCC300. In contrast, the strain PCC7806 (Figure 3.2b, MC producer) showed a small increase in cell density for both controls and treatments during the same exposure.

The metabolome comparison of CPCC300 cultures showed that there was most likely no difference between controls and treatments, as indicated by the PCA scores before and after UV exposure (Figure 3.3). Principal Component 1 on the x-axis (metabolome variation) was responsible for 22.74% of the variation between samples, and Principal Component 2 (metabolite concentrations) was responsible for 18.91% of the variation. There was no clear separation of the UV treatments and controls. The S-plot (Figure 3.4) shows the metabolites present in the CPCC300 strain before and after the exposure, with each point representing a fragment of a molecule at a specific RT. In S-plots, higher reliabilities at the extremities of the "S" shape show correlation between treatments and metablome variation, which was not the case in Figure 3.4. The PCA scores and S-plots for PCC7806 and the mutant PCC7806*mcy*B- are presented in Appendix B (Figures B.1 to B.4). They both followed the same pattern as CPCC300 and presented no clear differences with respect to UV exposure relative to controls.

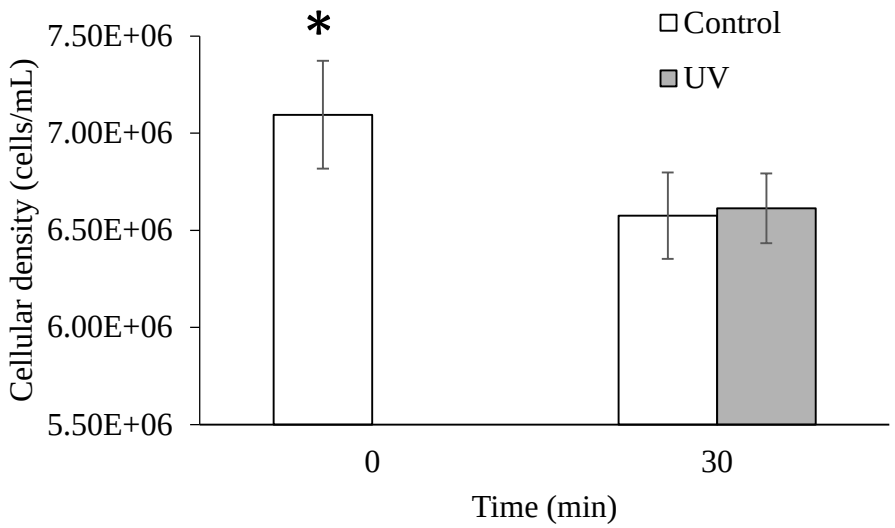

Figure 3.1. Cellular density (cells/mL) variation in the MC-producing *Microcystis aeruginosa* strain CPCC300 before (0 min) and after a 30 min exposure to UV radiation. Error bars represent the standard deviation of the average (n=5). The star indicates a significantly different density based on a paired t-test ($p<0.05$).

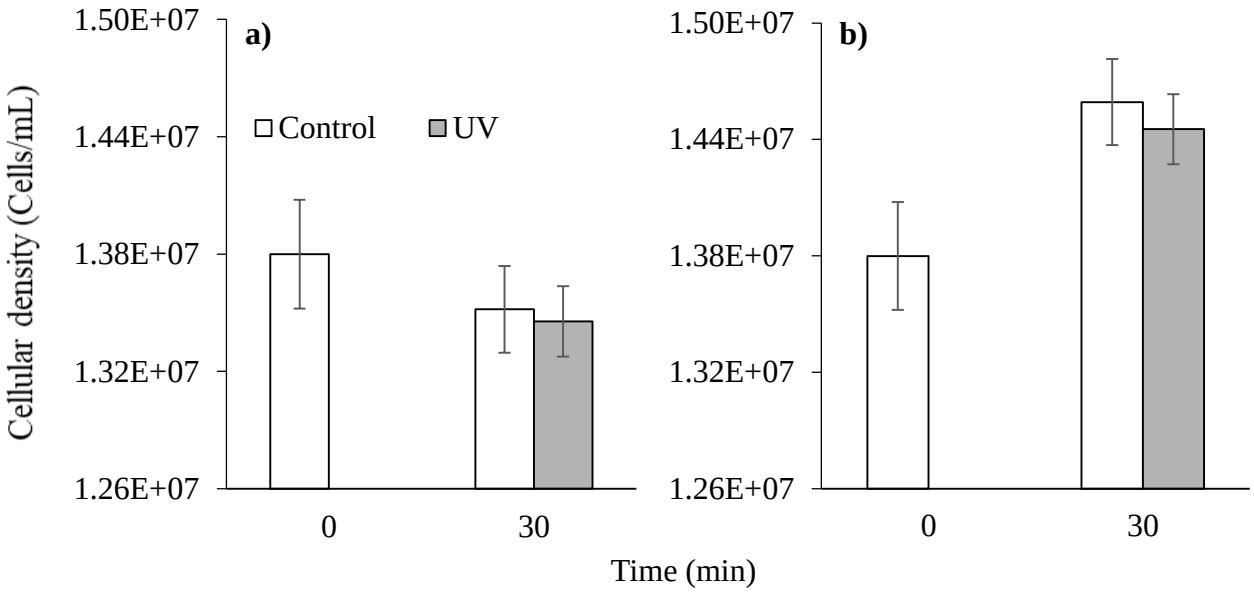

Figure 3.2. Cellular density (cells/mL) variation in *Microcystis aeruginosa* **a)** PCC7806*mcy*B- (mutant for *mcy*); **b)** PCC7806 (MC producer) over the 30 min exposure to UV radiation. Error bars represent the standard deviation for the average (n=5). A paired t-test showed there is no significant differences (p=0.2842).

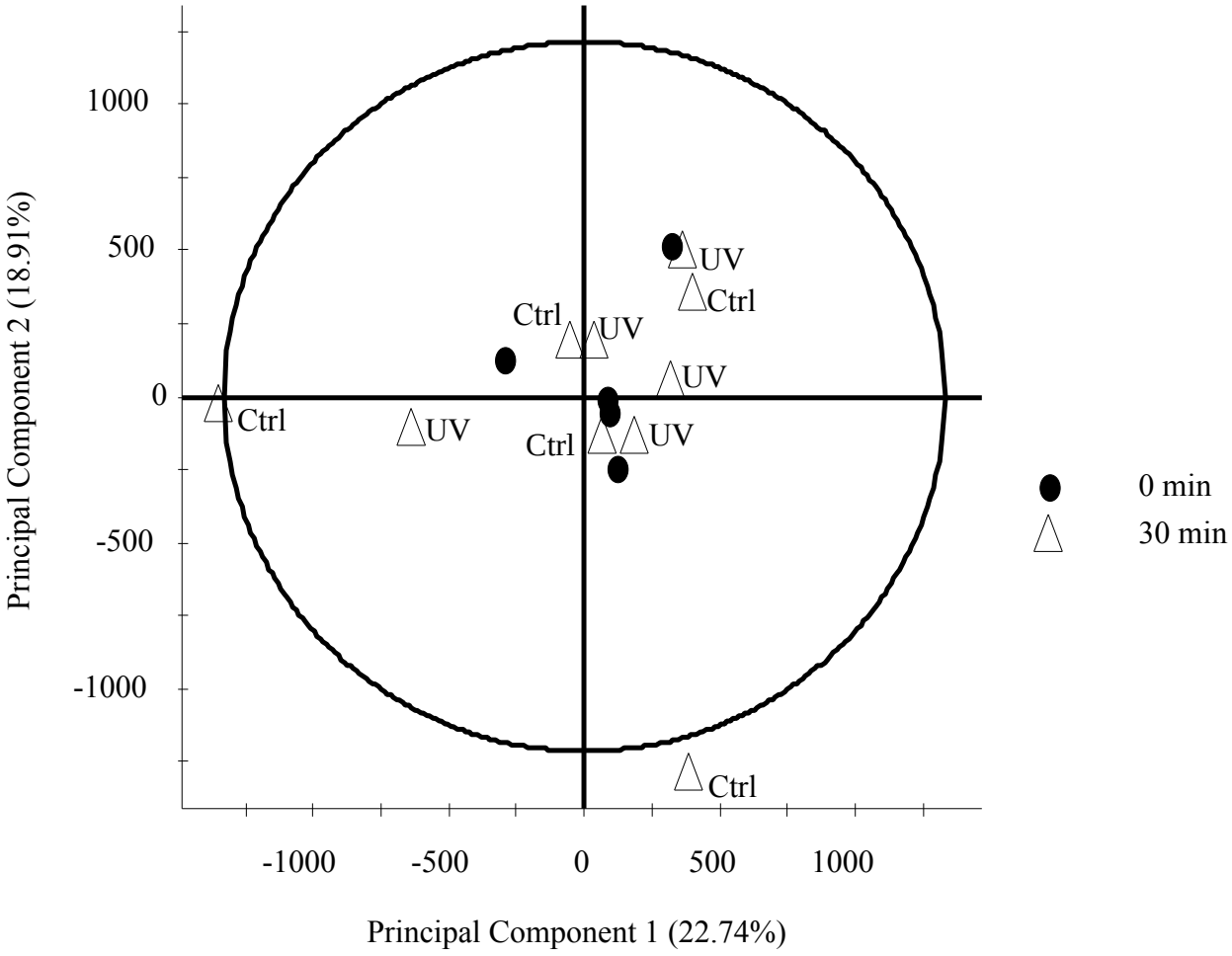

Figure 3.3. PCA scores for the metabolome of the MC-producing *Microcystis aeruginosa* strain CPCC300 exposed to UV radiation. Treatments (UV) and controls (Ctrl) before and after the exposure are shown. Principal Component 1 represents metabolome variation while Principal Component 2 represents changes in metabolite concentration.

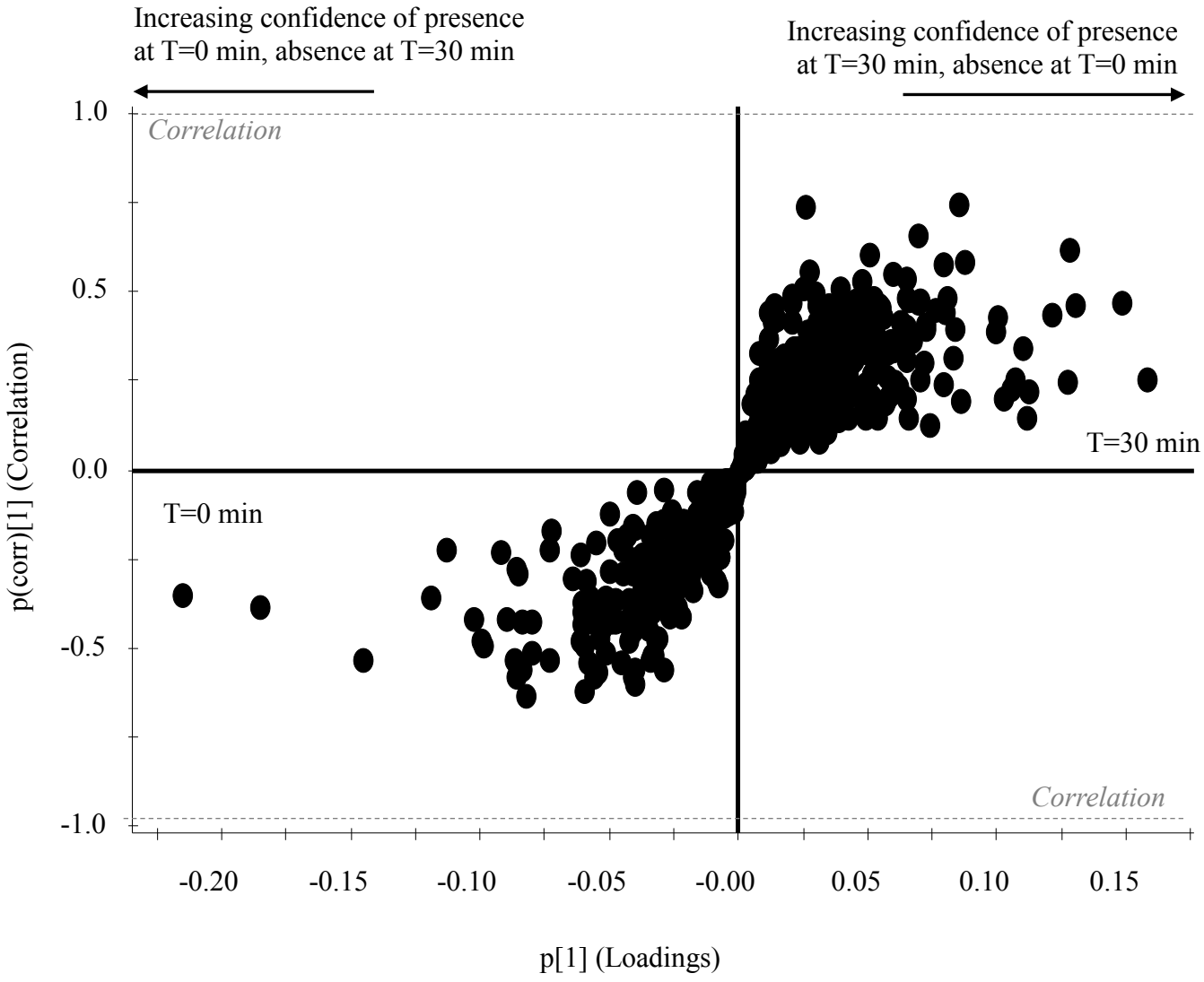

Figure 3.4. S-plot of the metabolome profile in the MC-producing *Microcystis aeruginosa* strain CPCC300 before (n=5) and after 30 minutes (n=5) of exposure to UV radiation. All treatments (UV or visible light only) are plotted together as no differences were previously observed (Figure 3.3). Each point represents a fragment at a specific RT.

The chl.a content in PCC7806 (WT) and the mutant PCC7806*mcy*B- also did not change with exposure to UV radiation (Figure B.5). All treatments and controls had a similar chl.a concentration before and after the experiment, even though some evidence of bleaching in the treatments was visible to the naked eye.

Total microcystin signal intensity was plotted against cellular density in both CPCC300 and PCC7806 (WT) (Figures B.6 and B.7). For all treatments and controls, no change in the correlation was observed under UV exposure. The same observation was made for the specific congeners MC-LR and [Asp^3]-MC-LR in the samples (data not shown). MC-LR and [Asp^3]-MC-LR signal intensities normalized against dry weight of samples indicated an important increase in production of microcystins in the strain CPCC300 following UV exposure (Figure 3.5a). Although no statistical analysis (t-test) was possible due to a low number of replicates, the averages were quite different from each other with no overlap in standard deviations. The average signal in the control was 2,500 (n=2), while the treatment was 3,750 (n=5). No change was observed in PCC7806 (Figure 3.5b). Overall neither strain showed a clear shift in the proportion of the two dominant microcystins (MC-LR and [Asp^3]-MC-LR) in response to UV exposure.

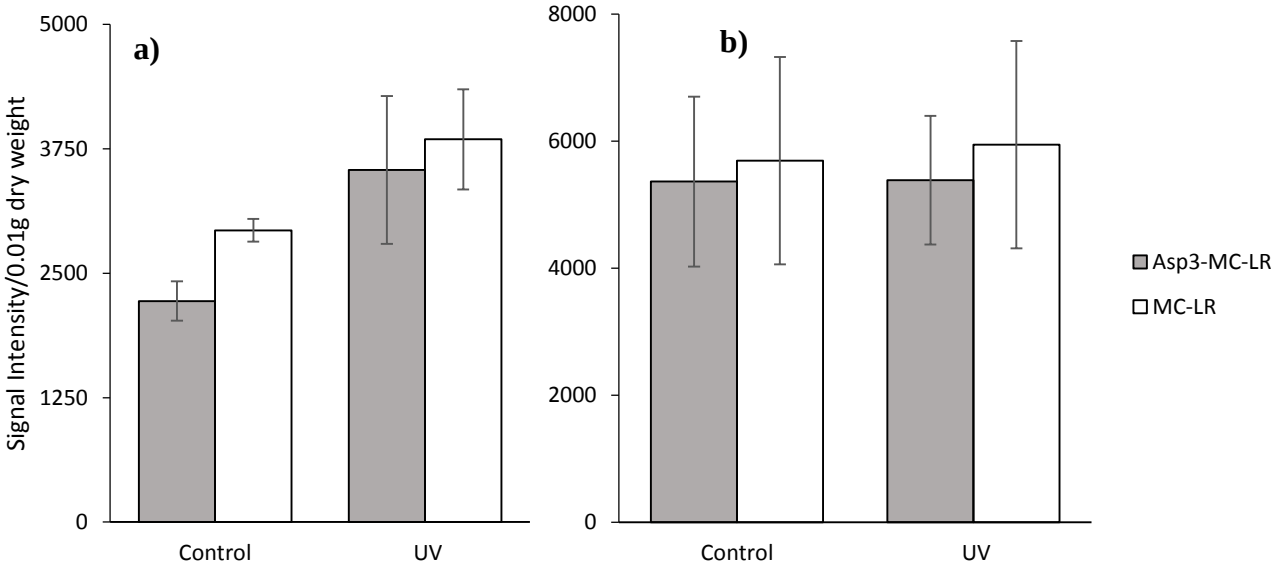

Figure 3.5. Microcystin signal intensities in *Microcystis aeruginosa* strains **a)** CPCC300 after 30 minutes of UV exposure (n=5) and controls (n=2); **b)** PCC7806 (n=5). Error bars represent the standard deviation of the averages. Note the difference in scales. Student's t-test suggested no difference in concentrations in the WT, b) ($p>0.9$).

3.3.2 Atrazine exposure

Cellular densities of two MC-producing *M. aeruginosa* strains exposed to atrazine, CPCC300 and CPCC464, were plotted against time of exposure (Figure 3.6). In CPCC300, cellular density was relatively constant over the first 24 hours of exposure for all atrazine concentrations tested, following the same trend as the controls (Figure 3.6a) There was a significant decrease in the cellular density in the second day after exposure for treatments of 150 ppb of atrazine in comparison to all the other concentrations. The growth rates per hour for this period showed a significant difference at the highest concentration (Figure 3.7) ($p<0.001$). The decrease in growth rates did not follow a dose-response trend over the range of 0 to 150 ppb.

In CPCC464, a different pattern was observed. The cultures exposed to 150 ppb of atrazine increased slightly in cellular density over the first 24 hours (Figure 3.6b), before decreasing to the same level as the other treatments and controls, which remain relatively constant over the entire experiment. The growth rates per hour for the first 24 hours (Figure 3.8) showed a significant difference ($p<0.0001$) between the highest treatment (150 ppb) and the other concentrations.

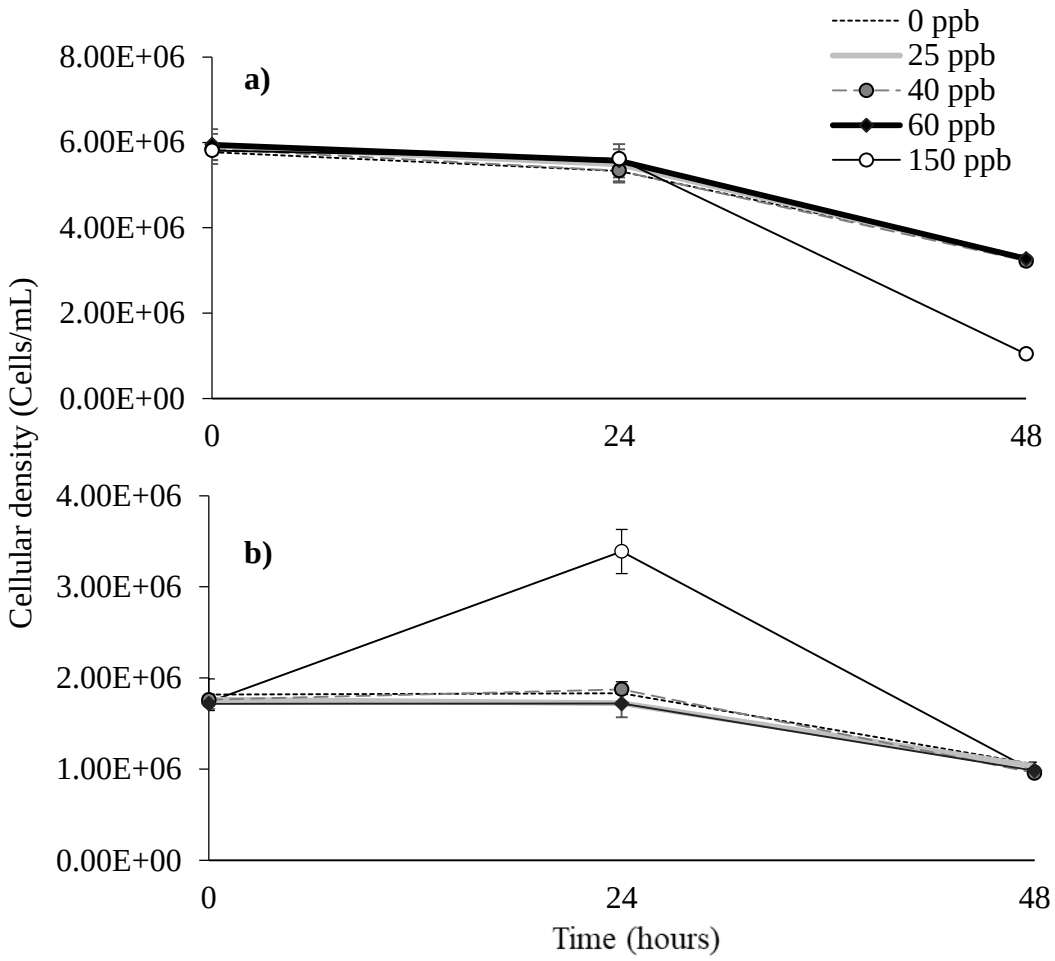

Figure 3.6. Cellular density of the MC-producing *Microcystis aeruginosa* strains **a)** CPCC300 exposed to 0 ppb (n=4), 25 ppb (n=5), 40 ppb (n=5), 60 ppb (n=5) and 150 ppb (n=3) of atrazine; **b)** CPCC464 exposed to 0 ppb (n=3), 25 ppb (n=5), 40 ppb (n=5), 60 ppb (n=5) and 150 ppb (n=4) of atrazine for 48 hours. Error bars represent the standard deviation of the average values. When not visible, error bars were smaller than symbol size. Note the difference in scale.

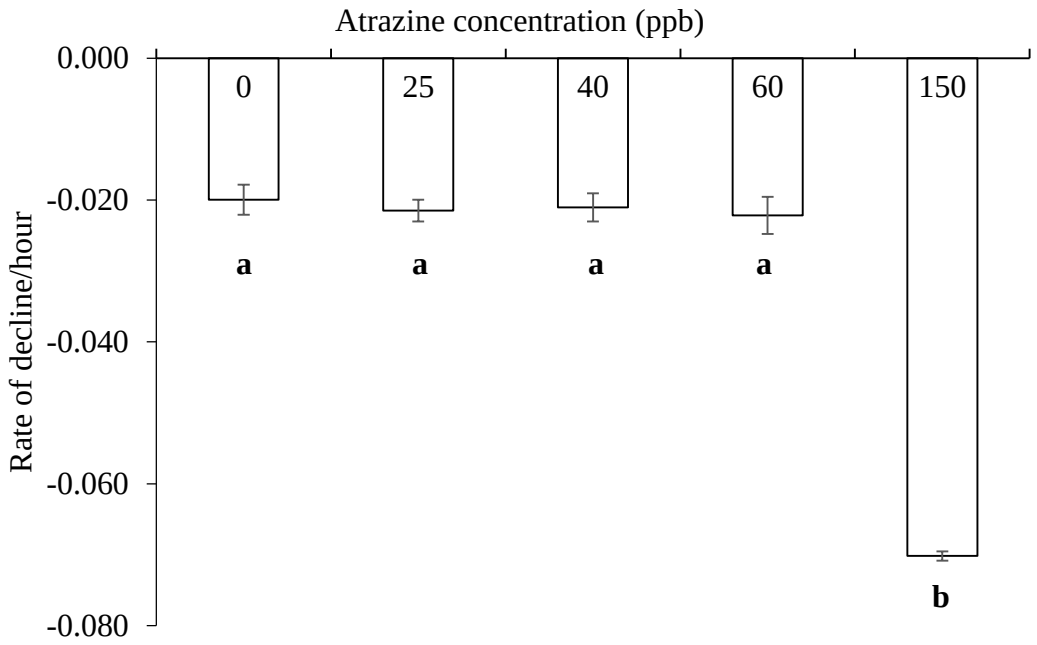

Figure 3.7. Rates of decline of the MC-producing *Microcystis aeruginosa* strain CPCC300 between 24 and 48 hours post-exposure to 0 ppb (n=4), 25 ppb (n=5), 40 ppb (n=5), 60 ppb (n=5) and 150 ppb (n=3) of atrazine. Error bars show the standard deviation of the average values. The different letters represent a significant difference in the data ($p<0.0001$) after a one way ANOVA.

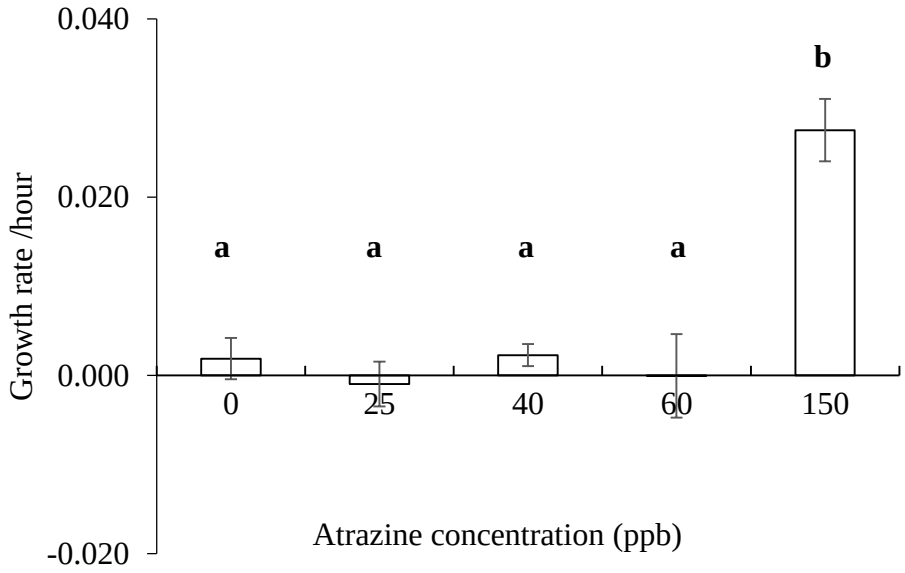

Figure 3.8. Growth rates of the MC-producing *Microcystis aeruginosa* strain CPCC464 during the first 24 hours following the exposure to atrazine, 0 ppb (n=3), 25 ppb (n=5), 40 ppb (n=4), 60 ppb (n=5) and 150 ppb (n=4). Error bars represent the standard deviation of the average values. The different letters show a significant difference among concentrations ($p<0.0001$) after a one way ANOVA.

The PCA of the metabolome in CPCC464 shows data for controls and treatments at 150 ppb of atrazine after 72 hours-exposure (Figure 3.9). Individual controls and treatment cultures overlapped, showing no clear difference between them. Principal Component 1 (metabolome variation) on the x-axis was responsible for 26.72% of the variation among the samples, while Principal Component 2 (metabolite concentrations) was responsible for 20.73% of the variation.

The S-plot of these data however showed small differences by points present in the 150 ppb treatment but absent from the control (Figure 3.10). A signal at RT 3.24 min with *m/z* =216.1007 Da corresponded to the atrazine that was added to the cultures. A signal at RT 5.68 min with a *m/z*=750.5577 Da corresponded to an unidentified compound. This point was however close to the core of the "S" shape, meaning the chances of finding it in the control were also high and it was not further investigated. For the same reasons, points at RT 0.43 min, 0.61 min and 5.95 min were also ignored for further analysis (Figure 3.10). In the control samples, there was a point at RT 0.45 min with *m/z*=365.0870 Da (compound 4) (Figure 3.10). This compound was apparently absent from the 150 ppb treatment. Signal intensities regarding compound 4 were studied in more details (Figure 3.11), based on the separation chromatogram and the detection signals (Figures 3.12 and B.8). The signals indicated that compound 4 concentrations were higher in control cultures than in treatments right after the addition of atrazine (Figure 3.11). The molecule was not successfully identified based on the fragmentation (Figure 3.12). While this same compound (compound 4) was also detected in other strains (CPCC300, PCC7806, PCC7806*mcyB*-), no significant differences in concentrations were found with UV exposure (Figures B.9 and B.10).

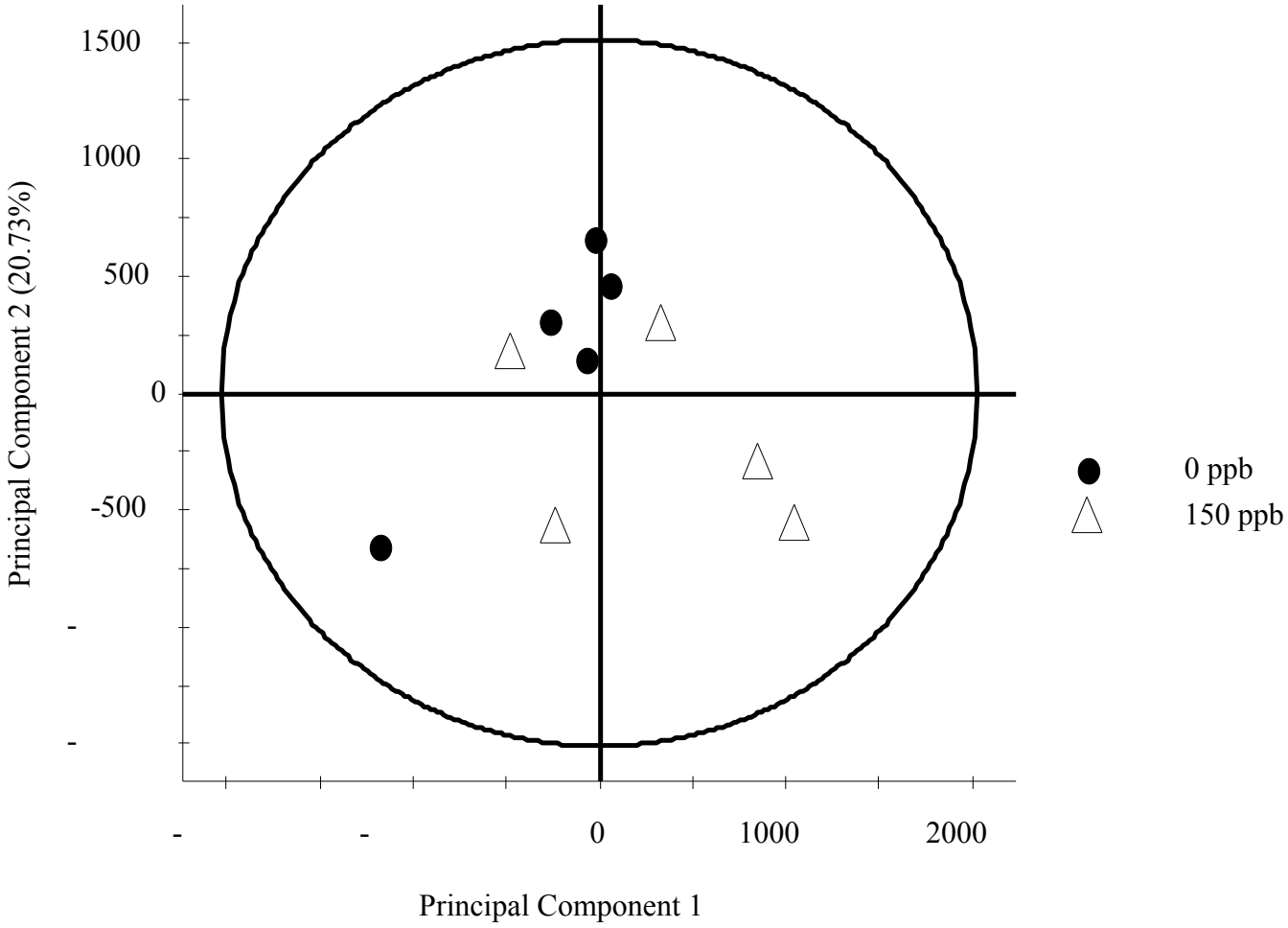

Figure 3.9. PCA of the metabolome variation of the MC producer CPCC464 after a 72 hours-exposure to 150 ppb of atrazine. Principal Component 1 presents metabolome variation among samples, while Principal Component 2 presents changes in metabolite concentrations.

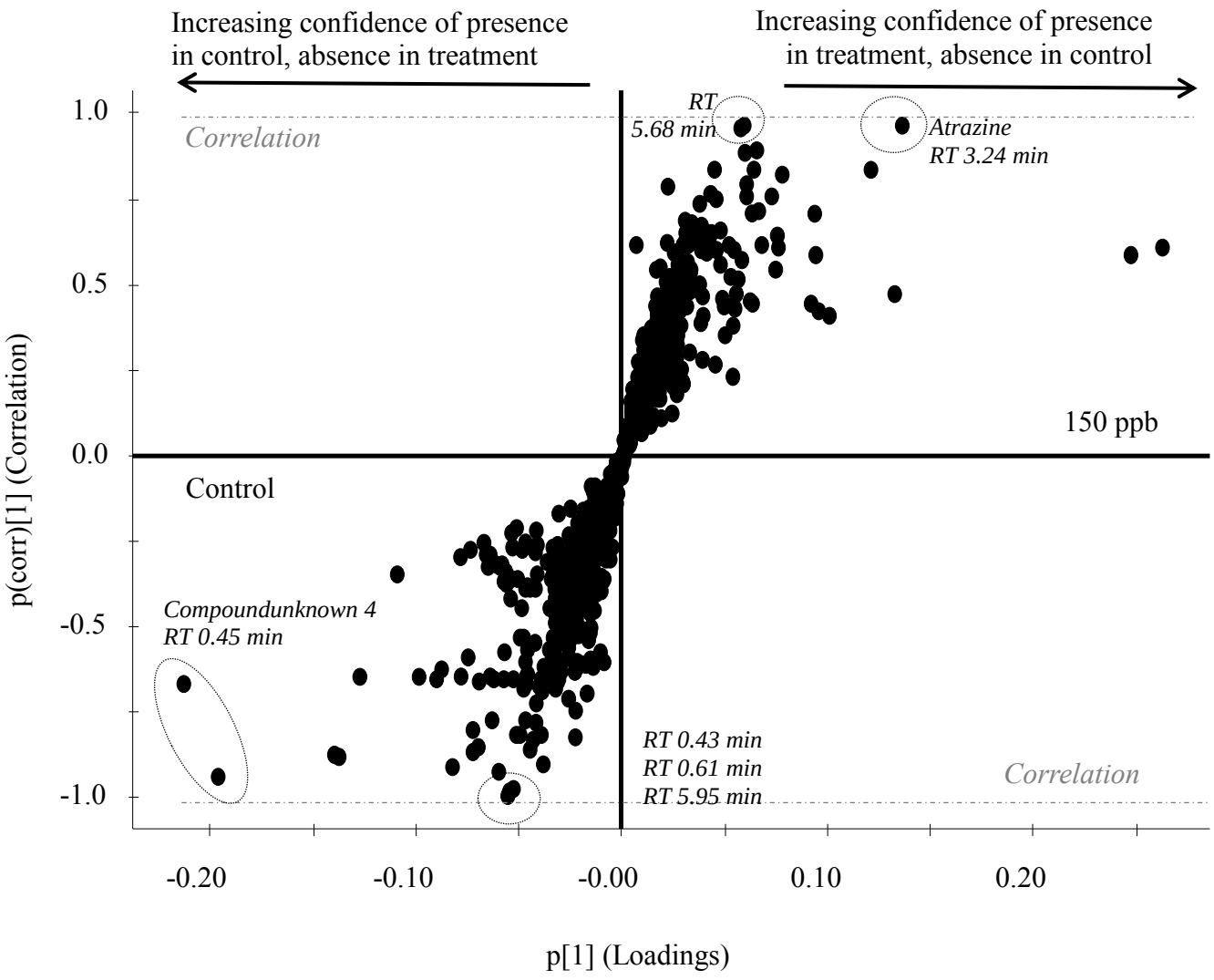

Figure 3.10. S-plot for the strain CPCC464 after a 72 hours-exposure to atrazine. The control signals are present in the bottom left quadrant of the graph, while the cultures exposed to 150 ppb of atrazine are in the top right quadrant.

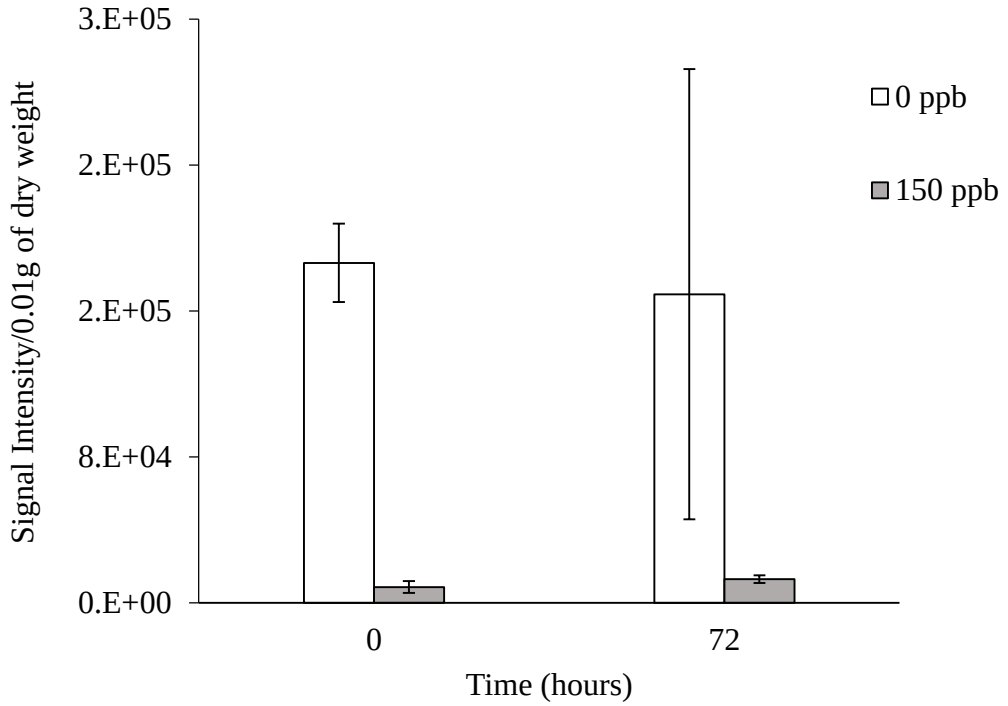

Figure 3.11. Unidentified compound4 signal intensity variation in *M. aeruginosa* CPCC464 for the controls (n=3) and the 150 ppb treatment (n=2) to atrazine at the beginning (n=3) and at the end of the experiment.

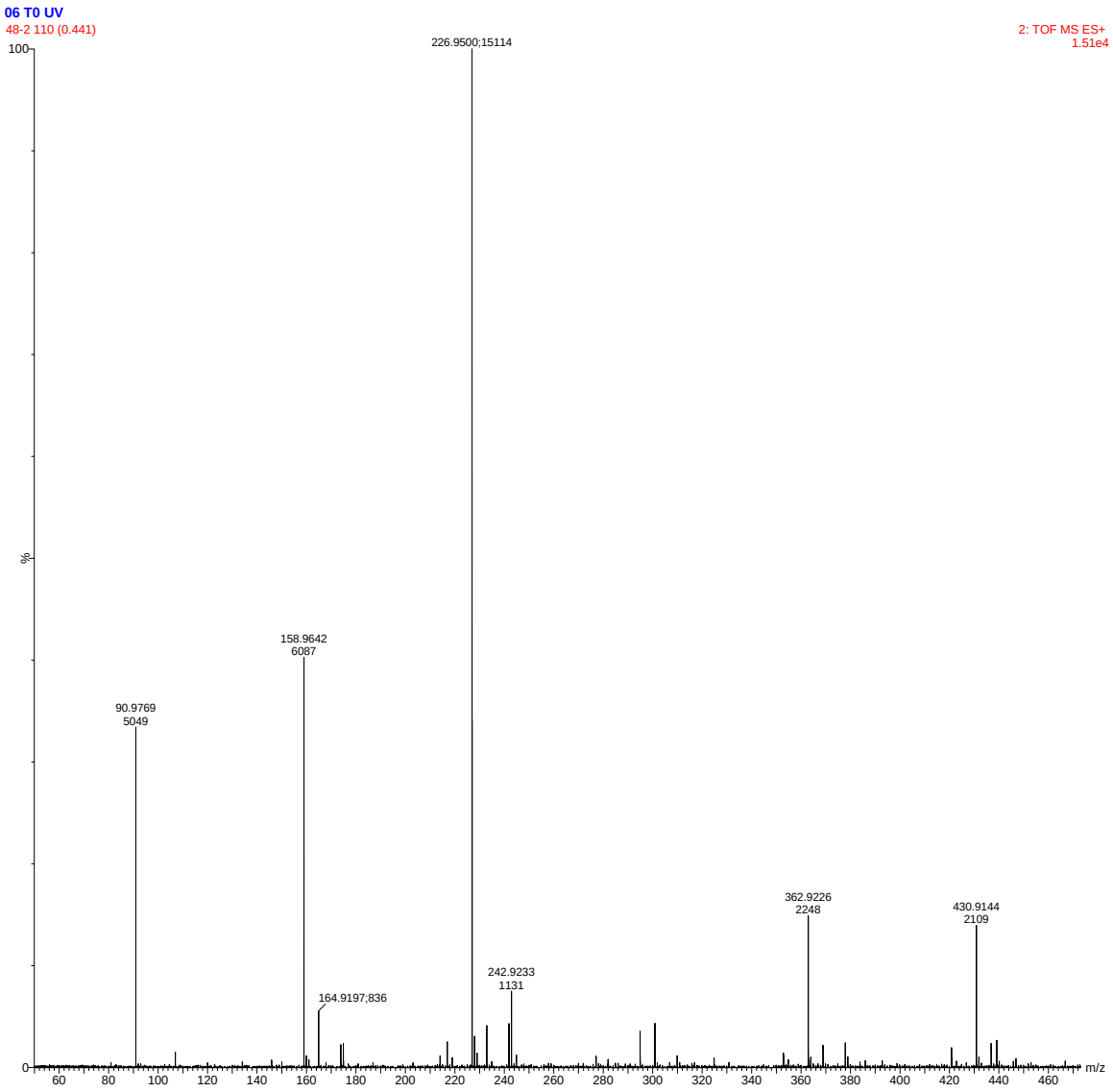

Figure 3.12. Fragmentation spectrum of compound 4 in *Microcystis aeruginosa* CPCC464 under high energy collision mode (positive mode). The separation chromatogram can be found in Appendix B (Figure B.8), with a RT of 0.45 min.

Comparison between the CPCC464 cultures before and after a 72-hours exposure to 150 ppb of atrazine (Figure 3.13) showed variation in another compound, Compound 5. Based on the separation chromatogram at RT 0.64 min (Figure B.12), major fragments were found with *m/z*=150.0580 Da, 262.0522 Da, 216.0438 Da, and 133.0316 Da (Figure 3.14), but those fragments were not sufficient for a successful identification of the compound. All fragments showed a decrease in signal intensity in cultures after 72 hours, in treatments and controls. However, the variation between replicates is high so the decrease was not significant ($p>0.07$) (Figure 3.15). Microcystins concentrations and ratios in the controls and treatment for the strains CPCC464 (Figure 3.16) and CPCC300 (Figure B.13) also did not change with exposure to atrazine.

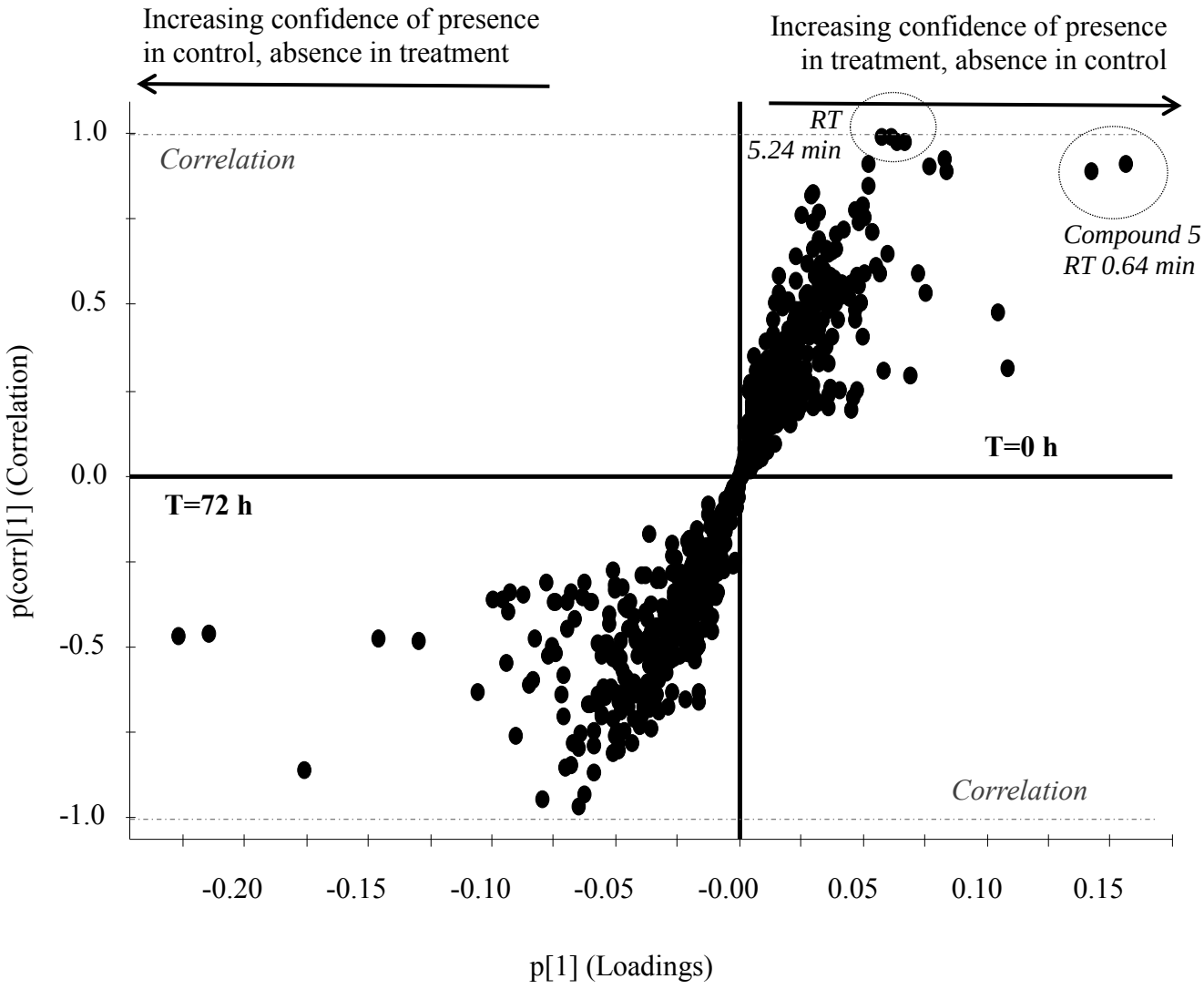

Figure 3.13. S-plot for the strain CPCC464 exposed to 150 ppb of atrazine. The signals of cultures exposed are present in the bottom left quadrant of the graph, while the cultures at start of experiment are in the top right quadrant.

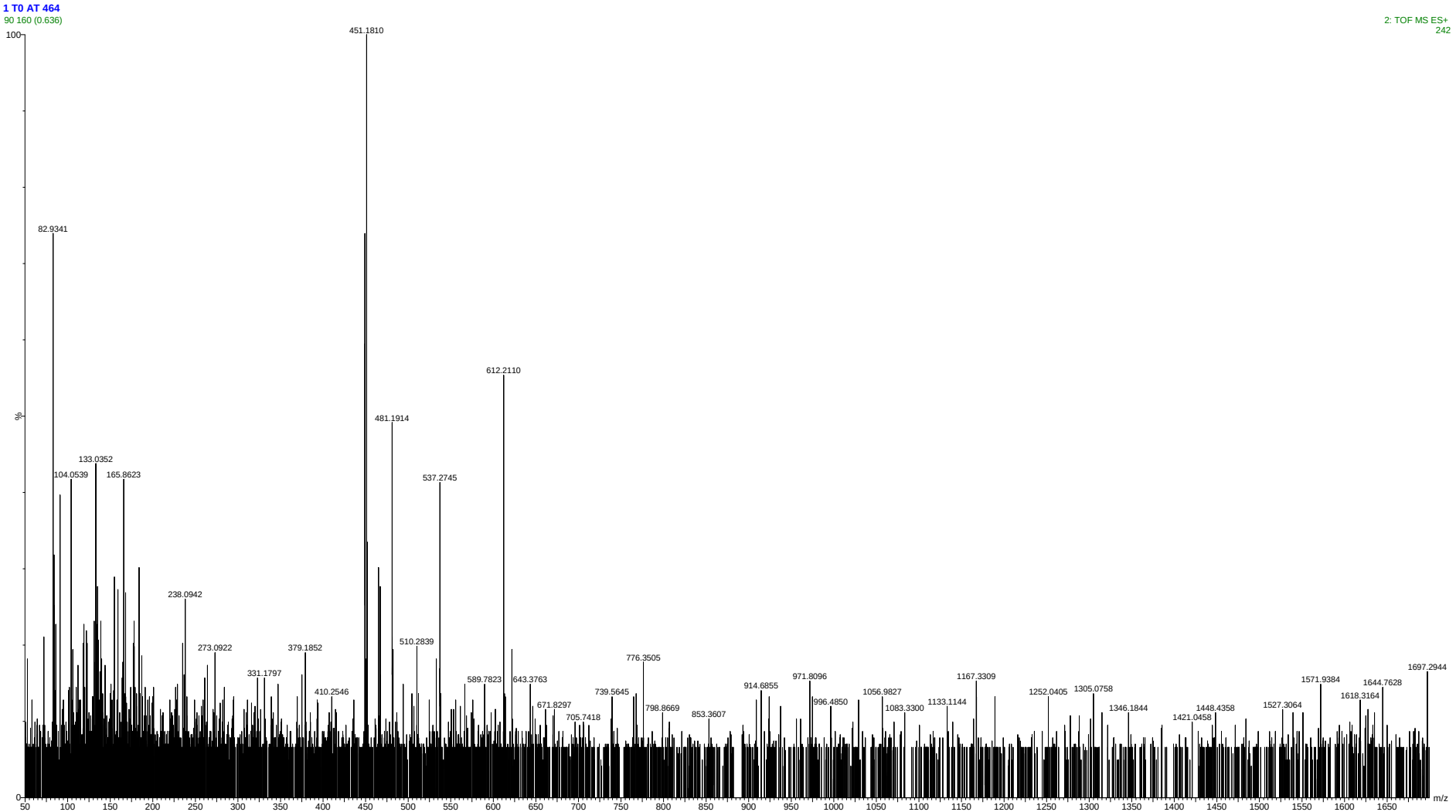

Figure 3.14. Fragmentation spectrum of compound 5 in in *Microcystis aeruginosa* CPCC464 under high energy collision mode (positive mode). The separation chromatogram can be found in Appendix B (Figure B.11), with a RT of 0.64 min.

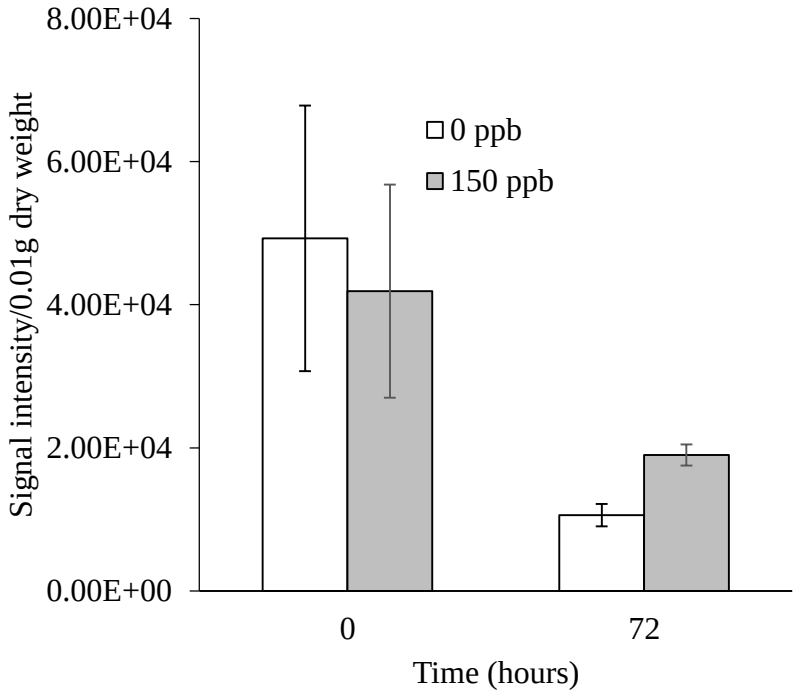

Figure 3.15. Unidentified compound 5 signal intensity variation in the MC-producing *Microcystis aeruginosa* strain CPCCC464 for the controls (n=3) and under a 150 ppb atrazine exposure for a 72-hours period (n=3). Error bars represent the standard deviation. A paired t-test showed no significant difference in the samples (p=0.07 for 0 ppb and p=0.13 for 150ppb).

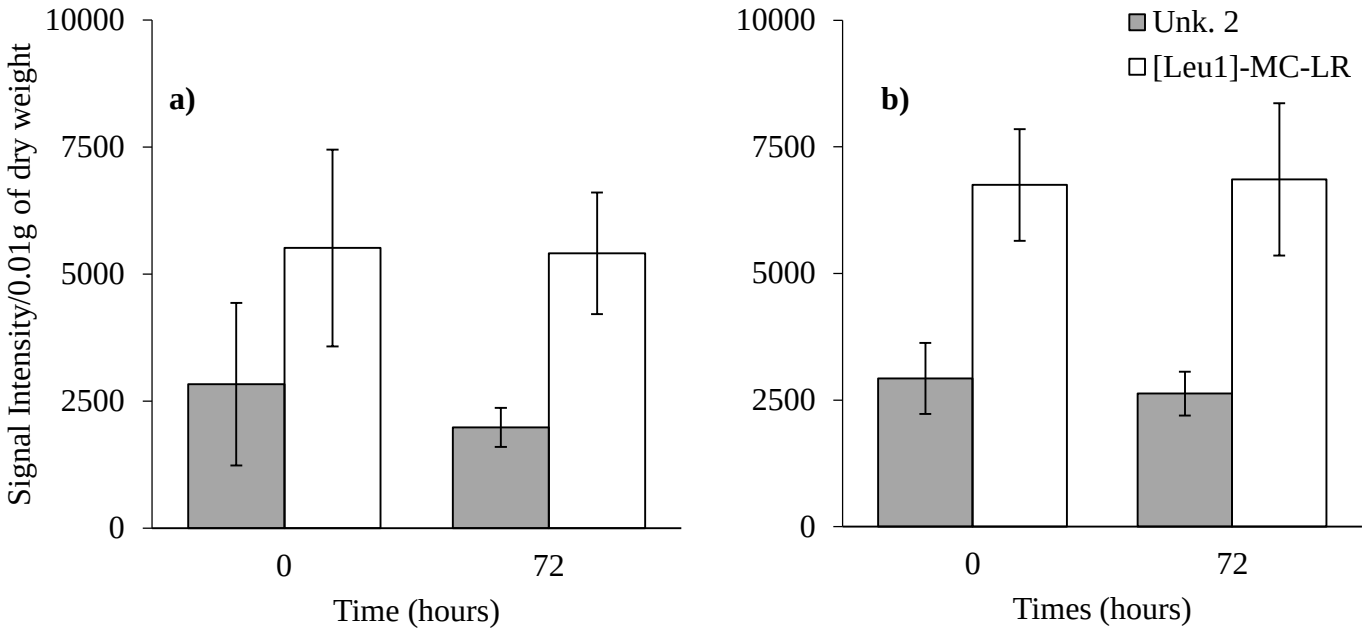

Figure 3.16. Microcystins concentration in *M. aeruginosa* CPCC464 **a)** in the controls (n=3); **b)** in cultures exposed to 150 ppb of atrazine (n=5) for a period of 72 hours. Errors bars represent the standard deviation of the average. A two way ANOVA showed no significant variation with time ($p=0.1$) or treatment ($p=0.06$) for both MC congeners.

3.4. Discussion

The objectives of this research were to assess the impact of oxidative stress on microcystin production in *Microcystis aeruginosa* as well as endpoints of chlorophyll a concentration and growth rate. I hypothesized that pure cultures exposed to different oxidative stress factors would affect the growth rates and the chlorophyll a concentrations negatively and increase the microcystin production if microcystin does protect against the stress.

UV radiation and atrazine, did not trigger the same response in the strains CPCC300, CPCC464 and PCC7806 for all the endpoints tested. In CPCC300, the concentrations for both MC-LR and [Asp^3]-MC-LR variants were slightly higher in the cultures exposed to UV than in the controls (Figure 3.5a), but the difference was not statistically significant. This tendency follows the idea of a protection against oxidative tress caused by UV radiation. However, this variation was not observed in the other microcystin producing strain exposed to the same conditions, PCC7806 (Figure 3.5b). The amounts of microcystin were the same between the treatments and the controls after the 30 minutes experiment. The same observation was made when comparing the response in CPCC300 and CPCC464 exposed to atrazine. As demonstrated in Chapter 2, strains of the same species have a different metabolomic profile. The difference observed between the two strains suggests CPCC300 metabolome contains less effective compounds than PCC7806 to protect against the stress caused by UV radiation. Various compounds are produced by cyanobacteria to protect against oxidative stress and could be involved in the process: enzymes (catalases, superoxide dismutases, peroxidases), vitamins (A, C, and E), pigments (carotenoids), etc. Targetting these compounds in a future extraction and purification process would be beneficial to further compare the metabolome of the different

strains. Furthermore, oxidative stress was not measured in the cells, despite tentatively doing so by the use of fluorescent probes.

Beside the microcystin content, UV radiation had an effect on another parameter. All treatment cultures showed signs of bleaching after the 30 minutes exposure. Some signs of this bleaching can be seen in the decrease of chlorophyll a concentrations per dry weight in CPCC300 and PCC7806 (Figure B.5), although this difference is not significant. A factor that could also have affected the cultures during the experiment is the temperature increase that affected PCC7806 and the mutant PCC7806*mcyB*- differently, although this variable was not independently tested. While it seems to enhance the microcystin producer, the mutant density decreased significantly (Figure 3.2). Knowing the only difference between the mutant and the wild type is the presence of microcystin (Chapter 2), its presence could have protected against the warming effect on the cultures. However, a similar decrease of density was observed in another microcystin producer, CPCC300 (Figure 3.1). This last strain seemed less tolerant to all environmental stresses than the two other strains.

While the highest level of atrazine clearly affected negatively the growth of CPCC300 (Figure 3.7), it looks like it enhanced the growth of CPCC464 (Figure 3.8). This is once again a sign of the variation in strains responses to environmental conditions. The resistance of CPCC464 to external stresses is more important than the resistance of CPCC300. With regards to the hypothesis of microcystin as a protection against oxidative stress, these results are not conclusive, as both cultures produce the toxin, in the same concentrations regardless of the treatment (Figures 3.16 and B.13). CPCC464 is known to produce more MC variants than CPCC300 (LeBlanc Renaud 2009), but those variants were not successfully detected in the strain (Chapter 2).

Both atrazine and UV had a sufficient effect on the cellular processes to trigger some response in the growth and chlorophyll a production in the cell. Beside microcystins, two unidentified compounds (compounds 4 and 5) were shown to disappear from the CPCC464 strain after exposure to 150 ppb of atrazine (Figure 3.10 and 3.13). The early RTs of 0.43 and 0.64 min suggest they are smaller polar peptides, but there was no successful identification of the compounds. The future identification of the compounds affected would determine if they are related to the microcystin production or related to another oxidative stress metabolic response.

Overall, the results of this experiment did not provide strong support for a unique role of microcystins in countering oxidative stress. Even within one species, *Microcystis aeruginosa*, strains varied in their responses to oxidative stress regardless of the presence of microcystins. Clearly there are other cellular mechanisms involved in resistance to oxidative stress that may vary from strain to strain and species to species and cyanobacteria appear well equipped to deal in a variety of ways with environmental stresses.

Chapter IV: Conclusion

The first objective of this research (Chapter 2) was to develop a new method for cyanobacterial extract analysis using an UPLC-QTOF tandem mass spectrometer. A good separation of individual microcystin congeners was obtained as shown by the separation of the standards. MC-LR and [Asp^3]-MC-LR congeners were identified in CPCC300 and PCC7806. Another microcystin, the [Leu^1]-MC-LR congener, was tentatively identified in CPCC299 and CPCC464, but was not confirmed as no standard was available. Three other molecules were tentatively identified as microcystins, but could not be more precisely linked to a specific variant (compounds 1 to 3 in CPCC299, compound 2 in CPCC464). With only a few standards commercially available and more than 246 variants discovered to date (Spoof & Catherine 2017), the identification of those microcystin congeners is still pending confirmation. Compounds would need to be concentrated from pure cultures to be analyzed via NMR spectra for further identification. More strains should be isolated from environmental samples as those available through culture collections and individual labs are likely quite limited in their metabolic diversity compared to the diversity in nature.

Microcystins were not the most abundant compounds found in the samples. Other groups, in particular, cyanopeptolins, aeruginosins and aerucyclamides were widely distributed in the selected strains of *Microcystis aeruginosa*. These compounds were tentatively identified with the Metlin database (as described in Chapter 2), as no standards for the specific variants were available. The method was useful to detect major groups of oligopeptides, but an optimized extraction protocol different for each class of compounds should be tested to ensure a good representation of each group in future research. However, in the interest of full metabolome analyses, compromises have to be made to ensure extraction of all metabolites. With their potential to be toxic to vertebrates (Chapter 1), the relative importance of these less studied

oligopeptides in common bloom-forming toxigenic genera such as *Microcystis* provides an additional reason to further investigate their production. With this first insight into the cyanobacterial metabolome, several metabolites of interest were identified and could be further investigated with respect to cellular responses to stress. Two unidentified compounds (Compounds 4 and 5) could be targeted for identification by NMR as they seemed to vary with exposure to atrazine and UV radiation.

The second objective (Chapter 2) was to assess the diversity of oligopetides within *Microcystis aeruginosa*, a common bloom-forming toxigenic species found world-wide (Bonilla & Pick 2017). There was a wide variation in the metabolome produced across strains of this one species grown under the same environmental conditions. This suggests that the choice of strain in studies needs to be carefully considered and comparisons need to be conducted within some common strains to compare results between experiments.

The results of Chapter 3 suggest that microcystins are not necessarily produced to counter oxidative stress. Growth rates were affected by the highest tested concentration of atrazine (150 ppb) in the two strains tested, but the microcystin concentrations did not change significantly with exposure. UV radiation did not affect the mutant and the wild type strain of *M. aeruginosa* differently. However, changes in the metabolome under those factors might indicate another response than toxin production. The cellular responses to oxidative stress in cells are likely complex and involve more than one specific mechanism or reaction. Cyanobacteria have many ways of protecting themselves against oxidative stress, including various metabolic pathways and small peptides. This is likely a result of their ancient evolutionary history in an environment with high UV. While a role for microcystins as protection against oxidative stress remains a good possibility based on the evidence presented in past studies (e.g. Zilliges *et al.* 2011; Chalifour &

Juneau 2011; Deblois *et al*. 2013;), many other mechanisms could have been implicated in the outcomes of these studies.

To further investigate the hypothesis of a protection against oxidative stress, microcystin expression could be measured through mRNA quantification following exposure to oxidative stress factors. The *mcy* gene cluster encodes the non-ribosomal complex for microcystin biosynthesis, but its regulation is not yet well understood (Nishizawa *et al*. 1999; Tillett *et al.* 2000; Kaplan *et al*. 2012). By measuring their transcription instead of intracellular concentrations, it is possible to determine if oxidative stress affects MCs production levels or the way they bind and unbind to proteins in the cells, which could affect their detection (Zilliges *et al.* 2011). Preliminary work done on this matter showed the complexity of mRNA extractions and purification in cyanobacteria cultures and a protocol optimization is required to pursue the research in this direction. One recent transcriptome analysis in cyanobacteria (Harke and Gobler, 2015) however showed good results of microcystin analysis through RNA quantification using a commercial kit, and gives new insights on the *mcy* gene cluster regulation by environmental factors (here, nutrients).

Optimization of a good protocol for ROS detection in cyanobacteria should also be included in future work, to insure the measured changes are caused by their production in the cell, even though the chosen factors (UV, atrazine) are well known to produce oxidative stress in cyanobacteria cells (Deblois *et al.* 2013, Soule *et al.* 2013).

References

Abou-Waly, H. et al., 1991. Dose-response relationship of Anabaena flos-aquae and Selenastrum capricornutum to atrazine and hexazinone using chlorophyll (a) content and 14C uptake. *Aquatic Toxicology*, 20(3), pp.195–204. Available at: http://www.scopus.com/inward/record.url?eid=2-s2.0-0025919534&partnerID=40&md5=7a7634f38757b982a16f0c41a031de1b.

Agha, R. & Quesada, A., 2014. Oligopeptides as biomarkers of cyanobacterial subpopulations. Toward an understanding of their biological role. *Toxins*, 6(6), pp.1929–1950.

Alfonso, M. & Kirilovsky, D., 2001. Redox Control of ntcA Gene Expression in Synechocystis sp . PCC 6803 . Nitrogen Availability and NtcA Protein 1. , 125(February), pp.969–981.

Andersen, R., 2005. *Algal Culturing Techniques*, Amsterdam: Elsevier Academic Press.

Anglada, L.V.D., Hilborn, E.D. & Backer, L.C., 2016. *Harmful Algal Blooms (HABs) and Public Health : Progress and Current Challenges*, Basel, Switzerland: MDPI.

Aranda-Rodriguez, R. et al., 2005. Pressurized liquid extraction of toxins from cyanobacterial cells. In *Environmental Toxicology*. pp. 390–396.

Bagchi, S.N., Das, P.K. & Ghosh, S.K., 2008. Screening and Evaluation of Protease Inhibitory Peptides in Microcystis spp. - Dominant Water Blooms. In T. Satyanarayana, ed. *Microorganisms in Environmental Management: Microbes and Environment*. pp. 175–190.

Beversdorf, L. et al., 2017. Variable Cyanobacterial Toxin and Metabolite Profiles across Six Eutrophic Lakes of Diffe ring Physiochemical Characteristics. *Toxins*, 9(2), p.62. Available at:

http://www.mdpi.com/2072-6651/9/2/62.

Beversdorf, L.J. et al., 2017. Variable Cyanobacterial Toxin and Metabolite Profiles across Six Eutrophic Lakes of Differing Physiochemical Characteristics.

Bister, B. et al., 2004. Cyanopeptolin 963A, a chymotrypsin inhibitor of Microcystis PCC 7806. *Journal of Natural Products*, 67(10), pp.1755–1757.

Bittencourt-Oliveira, M.D.C., 2003. Detection of potential microcystin-producing cyanobacteria in Brazilian reservoirs with a mcyB molecular marker. *Harmful Algae*, 2(1), pp.51–60.

Blot, N. et al., 2011. Light History Influences the Response of the Marine Cyanobacterium Synechococcus sp WH7803 to Oxidative Stress. *Plant physiology*, 156(4), pp.1934–1954.

Bonilla, S. & Pick, F.R., 2017. Freshwater bloom-forming cyanobacteria and anthropogenic change.

Briand, E. et al., 2016. Changes in secondary metabolic profiles of Microcystis aeruginosa strains in response to intraspecific interactions. *Environmental Microbiology*, 18(2), pp.384–400.

Briand, E. et al., 2012. Evidence of the Cost of the Production of Microcystins by Microcystis aeruginosa under Differing Light and Nitrate Environmental Conditions. *Plos One*, 7(1), pp.e29981–e29981.

Brooks, B.W. et al., 2016. Are harmful algal blooms becoming the greatest inland water quality threat to public health and aquatic ecosystems? *Environmental Toxicology and Chemistry*, 35(1), pp.6–13. Available at: http://www.ncbi.nlm.nih.gov/pubmed/26771345.

Chalifour, A. & Juneau, P., 2011. Temperature-dependent sensitivity of growth and

photosynthesis of Scenedesmus obliquus, Navicula pelliculosa and two strains of Microcystis aeruginosa to the herbicide atrazine. *Aquatic Toxicology*, 103(1–2), pp.9–17. Available at: http://www.scopus.com/inward/record.url?eid=2-s2.0-79952327938&partnerID=40&md5=c8428b3a3dbbde7b8445da75108c2969.

Chen, L. et al., 2016. A review of reproductive toxicity of microcystins. *Hazardous Materials*, 301, pp.381–399. Available at: http://dx.doi.org/10.1016/j.jhazmat.2015.08.041.

Chen, L. et al., 2012a. The combined effects of UV-B radiation and herbicides on photosynthesis, antioxidant enzymes and DNA damage in two bloom-forming cyanobacteria. *Ecotoxicology and environmental safety*, 80, pp.224–230. Available at: http://dx.doi.org/10.1016/j.ecoenv.2012.03.007.

Chen, L. et al., 2012b. The combined effects of UV-B radiation and herbicides on photosynthesis, antioxidant enzymes and DNA damage in two bloom-forming cyanobacteria. *Ecotoxicology and Environmental Safety*, 80, pp.224–230.

Chorus, I. & Bartram, J., 1999. *Toxic Cyanobacteria in Water: A guide to their public health consequences, monitoring and management*,

Cohen, S. a, 2012. Analytical techniques for the detection of α-amino-β-methylaminopropionic acid. *The Analyst*, 137(9), pp.1991–2005. Available at: http://www.ncbi.nlm.nih.gov/pubmed/22421821.

Cook, P.F. et al., 2015. Algal toxin impairs sea lion memory and hippocampal connectivity, with implications for strandings. *Science*, 403(6765), pp.80–84. Available at: http://www.sciencemag.org/cgi/doi/10.1126/science.aac5675.

Cox, P.A. et al., 2005. Diverse taxa of cyanobacteria produce Beta-N-methylamino-L-alanine, a neurotoxic amino acid. *PNAS*, 102(14), pp.5074–5078. Available at: http://www.jstor.org/stable/3375181.

Dawson, R.M., 1998. The toxicology of microcystins. *Toxicon*, 36(7), pp.953–962.

Deblois, C.P., Dufresne, K. & Juneau, P., 2013. Response to variable light intensity in photoacclimated algae and cyanobacteria exposed to atrazine. *Aquatic Toxicology*, 126, pp.77–84.

Deblois, C.P., Dufresne, K. & Juneau, P., 2013. Response to variable light intensity in photoacclimated algae and cyanobacteria exposed to atrazine. *Aquatic Toxicology*, 126, pp.77–84. Available at: http://www.scopus.com/inward/record.url?eid=2-s2.0-84868598713&partnerID=40&md5=cc86c80394a0dc4f515771a791f98bfd.

Dittmann, E. et al., 1997. Insertional mutagenesis of a peptide synthetase gene that is responsible for hepatotoxin production in the cyanobacterium Microcystis aeruginosa PCC 7806. *Molecular Microbiology*, 26(4), pp.779–787. Available at: http://www.scopus.com/inward/record.url?eid=2-s2.0-0030723581&partnerID=40&md5=7b183ba7a36bb5137a5f7d3903fb062d.

EPA, 2012. National Lakes Assessment 2012 Key Findings. *National Aquatic Resource Surveys*. Available at: https://www.epa.gov/national-aquatic-resource-surveys/national-lakes-assessment-2012-key-findings.

Fairchild, J.F., Ruessler, D.S. & Carlson, A.R., 1998. Comparative sensitivity of five species of macrophytes and six species of algae to atrazine, metribuzin, alachlor, and metolachlor. *Environmental Toxicology and Chemistry*, 17(9), pp.1830–1834.

Falconer, I.R., 2005. *Cyanobacterial Toxins of Drinking Water Supplies: Cylindrospermopsins and Microcystins*,

Faltermann, S. et al., 2014. Molecular effects of the cyanobacterial toxin cyanopeptolin (CP1020) occurring in algal blooms: Global transcriptome analysis in zebrafish embryos. *Aquatic Toxicology*, 149, pp.33–39. Available at: http://dx.doi.org/10.1016/j.aquatox.2014.01.018.

Fayad, P.B., Roy-lachapelle, A. & Duy, S.V., 2015. Toxicon On-line solid-phase extraction coupled to liquid chromatography tandem mass spectrometry for the analysis of cyanotoxins in algal blooms le Pr e. , 108, pp.167–175.

Gilliom, R.J. et al., 2006. *The Quality of our Nation's Waters - Pesticides in the Nation ' s Streams and Ground Water , 1992 – 2001* U. S. D. of the I.-U. G. Survey, ed.,

Graymore, M., Stagnitti, F. & Allinson, G., 2001. Impacts of atrazine in aquatic ecosystems. *Environment international*, 26(7–8), pp.483–495.

Gupta, N. et al., 2003. Comparative toxicity evaluation of cyanobacterial cyclic peptide toxin microcystin variants (LR, RR, YR) in mice. *Toxicology*, 188(2–3), pp.285–296.

Guyot, M., Doré, J.C. & Devillers, J., 2004. Typology of secondary cyanobacterial metabolites from minimum spanning tree analysis. *SAR and QSAR in environmental research*, 15(2), pp.101–114. Available at: http://www.ncbi.nlm.nih.gov/pubmed/15199946.

Ha, M.H., Contardo-Jara, V. & Pflugmacher, S., 2014. Uptake of the cyanobacterial neurotoxin, anatoxin-a, and alterations in oxidative stress in the submerged aquatic plant Ceratophyllum demersum. *Ecotoxicology and Environmental Safety*, 101(1), pp.205–212.

Harris, T.D. & Smith, V.H., 2016. Do persistent organic pollutants stimulate cyanobacterial blooms? *Inland Waters*, 6(2), pp.124–130. Available at: https://www.fba.org.uk/journals/index.php/IW/article/view/887%5Cnhttps://www.fba.org.uk/journals/index.php/IW/article/viewFile/887/531.

Hesse, K., Dittmann, E. & Börner, T., 2001. Consequences of impaired microcystin production for light-dependent growth and pigmentation of Microcystis aeruginosa PCC 7806. *FEMS Microbiology Ecology*, 37(1), pp.39–43. Available at: http://www.scopus.com/inward/record.url?eid=2-s2.0-0034868559&partnerID=40&md5=413110b9c6848ab1ec037f0b6143b067.

Hollister, J.W. & Kreakie, B.J., 2016. Associations between chlorophyll a and various microcystin-LR health advisory concentrations. *F1000Research*, 5(0), p.151. Available at: http://www.pubmedcentral.nih.gov/articlerender.fcgi?artid=4830210&tool=pmcentrez&rendertype=abstract.

Ishida, K. et al., 1999. Aeruginosins, protease inhibitors from the cyanobacterium Microcystis aeruginosa. *Tetrahedron*, 55(36), pp.10971–10988.

Ishida, K. et al., 2009a. Plasticity and evolution of aeruginosin biosynthesis in cyanobacteria. *Applied and Environmental Microbiology*, 75(7), pp.2017–2026. Available at: http://www.scopus.com/inward/record.url?eid=2-s2.0-63849226090&partnerID=40&md5=4e646777e074edf52edcd8375b4bd9c2.

Ishida, K. et al., 2009b. Plasticity and evolution of aeruginosin biosynthesis in cyanobacteria. *Applied and Environmental Microbiology*, 75(7), pp.2017–2026.

Ishitsuka, M.O. et al., 1990. Microviridin. A novel tricyclic depsipeptide from the toxic

cyanobacterium Microcystis viridis. *Journal of the American Chemical Society*, 112(22), pp.8180–8182. Available at: http://pubs.acs.org/doi/abs/10.1021/ja00178a060.

Jacoby, J.M. et al., 2000. Environmental factors associated with a toxic bloom of Microcystis aeruginosa. *Can. J. Fish. Aquat. Sci*, 57, pp.231–240.

Jang, M.H. et al., 2003. *Toxin production of cyanobacteria is increased by exposure to zooplankton*,

Jiang, H. & Qiu, B., 2011. Inhibition of photosynthesis by UV-B exposure and its repair in the bloom-forming cyanobacterium Microcystis aeruginosa. *Journal of Applied Phycology*, 23(4), pp.691–696.

Jiang, H. & Qiu, B., 2005. Photosynthetic adaptation of a bloom-forming cyanobacterium Microcystis aeruginosa (Cyanophyceae) to prolonged UV-B exposure. *Journal of Phycology*, 41(5), pp.983–992.

Jursinic, P.A. et al., 1991. Characteristics of 2 Atrazine-Binding Sites That Specifically Inhibit Photosystem-Ii Function. *Biochimica Et Biophysica Acta*, 1059(3), pp.312–322.

Jüttner, F. et al., 2010. β-Cyclocitral, a Grazer Defence Signal Unique to the Cyanobacterium Microcystis. *Journal of Chemical Ecology*, 36(12), pp.1387–1397.

Kaebernick, M. et al., 2000. Light and the transcriptional response of the microcystin biosynthesis gene cluster. *Applied and Environmental Microbiology*, 66(8), pp.3387–3392. Available at: http://www.scopus.com/inward/record.url?eid=2-s2.0-0033856746&partnerID=40&md5=645a96366df50f43382b0f3c13679a39.

Kaebernick, M. et al., 2000. Light and the Transcriptional Response of the Microcystin

Biosynthesis Gene Cluster Light and the Transcriptional Response of the Microcystin Biosynthesis Gene Cluster. , 66(8), pp.3387–3392.

Kaebernick, M. & Neilan, B.A., 2001. Ecological and molecular investigations of cyanotoxin production. *FEMS Microbiology Ecology*, 35(1), pp.1–9.

Kaplan, A. et al., 2012. The languages spoken in the water body (or the biological role of cyanobacterial toxins). *Frontiers in Microbiology*, 3(APR), p.138. Available at: http://www.scopus.com/inward/record.url?eid=2-s2.0-84873304817&partnerID=40&md5=c5d9a291871793239d601618f964263d.

Krienitz, L. et al., 2003. Contribution of hot spring cyanobacteria to the mysterious deaths of Lesser Flamingos at Lake Bogoria, Kenya. *FEMS Microbiology Ecology*, 43(2), pp.141–148.

Latifi, A., Ruiz, M. & Zhang, C.C., 2009. Oxidative stress in cyanobacteria. *FEMS Microbiology Reviews*, 33(2), pp.258–278.

LeBlanc Renaud, S., 2009. *Microcystin Production and the Dominance of Toxigenic Strains of Cyanobacterinn Lake and Culture Studies*. Canada: University of Ottawa.

Leikoski, N., Fewer, D.P. & Sivonen, K., 2009. Widespread occurrence and lateral transfer of the cyanobactin biosynthesis gene cluster in cyanobacteria. *Applied and Environmental Microbiology*, 75(3), pp.853–857.

Liu, C. et al., 2014. Effects of different light intensities on the toxicities of atrazine and paraquat to algae. *Huanjing Kexue Xuebao/Acta Scientiae Circumstantiae*, 34(5), pp.1339–1343. Available at: http://www.scopus.com/inward/record.url?eid=2-s2.0-

84901855026&partnerID=40&md5=b6e3c24874d42893c737f971019bdbdc.

Lürling, M. & Oosterhout, F. v., 2013. Controlling eutrophication by combined bloom precipitation and sediment phosphorus inactivation. *Water research*. Available at: http://www.scopus.com/inward/record.url?eid=2-s2.0-84883681654&partnerID=40&md5=2120aaf38009a8191c2eb7368abc2709.

Madronich, S. et al., 1998. Changes in biologically active ultraviolet radiation reaching the Earth's surface. *Journal of Photochemistry and Photobiology B: biology*, 46, pp.5–19.

Martin, C., Oberer, L., Buschdtt, M., Weckesser, J., et al., 1993. Cyanopeptolins, new depsipeptides from the cyanobacterium Microcystis sp. PCC 7806. *J. Antibiot.*, 46(10), pp.1550–1556. Available at: http://www.scopus.com/inward/record.url?eid=2-s2.0-0027482363&partnerID=40&md5=0e28c33fc91041713dcf0a46b73c2b30.

Martin, C., Oberer, L., Buschdtt, M. & Weckesser, J., 1993. Cyanopeptolins, new depsipeptides from the cyanobacterium Microcystis sp. PCC 7806. *J. Antibiot.*, 46(10), pp.1550–56.

Merel, S. et al., 2013. State of knowledge and concerns on cyanobacterial blooms and cyanotoxins. *Environment International*, 59, pp.303–327. Available at: http://dx.doi.org/10.1016/j.envint.2013.06.013.

Micallef, M.L. et al., 2015. Exploring cyanobacterial genomes for natural product biosynthesis pathways. *Marine Genomics*, 21, pp.1–12.

Michalak, A.M. et al., 2013. Record-setting algal bloom in Lake Erie caused by agricultural and meteorological trends consistent with expected future conditions. *Proceedings of the National Academy of Sciences of the United States of America*, 110(16), pp.6448–52.

Available at: http://www.pnas.org/cgi/content/long/110/16/6448.

Miller, M.A. et al., 2010. Evidence for a novel marine harmful algal bloom: Cyanotoxin (microcystin) transfer from land to sea otters. *PLoS ONE*, 5(9), pp.1–11.

Moon, Y.J.-J., Kim, S. Il & Chung, Y.-H.H., 2012. Sensing and Responding to UV-A in Cyanobacteria. *International Journal of Molecular Sciences*, 13(12), pp.16303–16332. Available at: http://www.scopus.com/inward/record.url?eid=2-s2.0-84871704245&partnerID=40&md5=144d96f4654f4b1b1daa406ad4987074.

Neilan, B.A. et al., 2013. Environmental conditions that influence toxin biosynthesis in cyanobacteria. *Environmental Microbiology*, 15(5), pp.1239–1253. Available at: http://www.scopus.com/inward/record.url?eid=2-s2.0-84876492505&partnerID=40&md5=90cf04b5e90b29731366e7a186f16274.

Niedermeyer, T.H.J., Schmieder, P. & Kurmayer, R., 2014. Isolation of Microcystins from the Cyanobacterium Planktothrix rubescens Strain No80. *Natural products and bioprospecting*, 4(1), pp.37–45.

Nishizawa, T. et al., 1999. Genetic analysis of the peptide synthetase genes for a cyclic heptapeptide microcystin in Microcystis spp. *Journal of biochemistry*, 126(3), pp.520–529.

Okino, T. et al., 1993. Microginin, an Angiotensin-Converting Enzyme Inhibitor from the Blue-Green Algae Microcystis Aeruginosa. *Tetrahedron Letters*, 34(3), pp.501–504.

Orr, P.T. & Jones, G.J., 1998. Relationship between microcystin production and cell division rates in nitrogen-limited Microcystis aeruginosa cultures. *Limnology and Oceanography*, 43(7), pp.1604–1614. Available at: http://www.scopus.com/inward/record.url?eid=2-s2.0-

0031771802&partnerID=40&md5=7c0f419471db72bf38e286402e10fd58.

Ortelli, D. et al., 2008. Fast screening and quantitation of microcystins in microalgae dietary supplement products and water by liquid chromatography coupled to time of flight mass spectrometry. , 7, pp.230–237.

Paerl, H.W. & Otten, T.G., 2013. Harmful Cyanobacterial Blooms: Causes, Consequences, and Controls. *Microbial ecology*, 65(4), pp.995–1010. Available at: http://www.scopus.com/inward/record.url?eid=2-s2.0-84876931018&partnerID=40&md5=ce4452b976b568a78d60b200b208ced5.

Park, H. et al., 2001. [D-Leu1] microcystin-LR, a new microcystin isolated from waterbloom in a Canadian prairie lake. *Toxicon*, 39, pp.855–862.

Pereira, D.A. & Giani, A., 2014. Cell density-dependent oligopeptide production in cyanobacterial strains. *FEMS Microbiology Ecology*, 88(1), pp.175–183.

Pick, F.R., 2016. Blooming algae: a Canadian perspective on the rise of toxic cyanobacteria. *Canadian Journal of Fisheries and Aquatic Sciences*, 10(October 2015), pp.1–10. Available at: http://www.nrcresearchpress.com/doi/abs/10.1139/cjfas-2015-0470#.VzVWAvkrLRY.

Portmann, C., Blom, J.F., Gademann, K., et al., 2008. Aerucyclamides A and B: Isolation and synthesis of toxic ribosomal heterocyclic peptides from the cyanobacterium Microcystis aeruginosa PCC 7806. *Journal of Natural Products*, 71(7), pp.1193–1196.

Portmann, C., Blom, J.F., Kaiser, M., et al., 2008. Isolation of aerucyclamides C and D and structure revision of microcyclamide 7806A: Heterocyclic ribosomal peptides from Microcystis aeruginosa PCC 7806 and their antiparasite evaluation. *Journal of Natural*

Products, 71(11), pp.1891–1896.

Pouria, S. et al., 1998. Fatal microcystin intoxication in haemodialysis unit in Caruaru, Brazil. *Lancet*, 352(9121), pp.21–26.

Puddick, J. et al., 2015. Further characterization of glycine-containing microcystins from the McMurdo dry valleys of Antarctica. *Toxins*, 7(2), pp.493–515.

Rastogi, R.P., Sinha, R.P., Incharoensakdi, A., et al., 2014. Microcystin production in Microcystis aeruginosa: effect of type of strain, environmental factors, nutrient concentrations, and N:P ratio on mcyA gene expression. *Aquatic Ecology*, 35(1), pp.1951–1978. Available at: http://www.mdpi.com/2072-6651/6/7/1951/.

Rastogi, R.P., Madamwar, D. & Incharoensakdi, A., 2015. Bloom dynamics of cyanobacteria and their toxins: Environmental health impacts and mitigation strategies. *Frontiers in Microbiology*, 6(NOV), pp.1–22.

Rastogi, R.P. & Sinha, R.P., 2009. Biotechnological and industrial significance of cyanobacterial secondary metabolites. *Biotechnology Advances*, 27(4), pp.521–539.

Rastogi, R.P., Sinha, R.P. & Incharoensakdi, A., 2014. The cyanotoxin-microcystins: current overview. *Reviews in Environmental Science and Bio/Technology*, 13(2), pp.215–249. Available at: http://link.springer.com/10.1007/s11157-014-9334-6.

Rath, J. & Adhikary, S.P., 2007. Response of the estuarine cyanobacterium Lyngbya aestuarii to UV-B radiation. *Journal of Applied Phycology*, 19(5), pp.529–536.

Regnault-Roger, C., 2014. *Produits de protection des plantes : Innovation et sécurité pour une agriculture durable*, Tec & Doc Lavoisier.

Renaud, S.L. et al., 2011. Effect of Light Intensity on the Relative Dominance of Toxigenic and Nontoxigenic Strains of Microcystis aeruginosa. *Applied and Environmental Microbiology*, 77(19), pp.7016–7022. Available at: http://aem.asm.org/cgi/doi/10.1128/AEM.05246-11.

Rohrlack, T. et al., 2008. Oligopeptide chemotypes of the toxic freshwater cyanobacterium Planktothrix can form sub-populations with dissimilar ecological traits. *Limnology and Oceanography*, 53(4), pp.1279–1293.

Rohrlack, T. et al., 1999. Role of microcystins in poisoning and food ingestion inhibition of Daphnia galeata caused by the cyanobacterium Microcystis aeruginosa. *Applied and Environmental Microbiology*, 65(2), pp.737–739. Available at: http://www.scopus.com/inward/record.url?eid=2-s2.0-0032976332&partnerID=40&md5=ccde50a7ce09f06dff4d18423ea2f88d.

Ross, C., Santiago-Vázquez, L. & Paul, V., 2006. Toxin release in response to oxidative stress and programmed cell death in the cyanobacterium Microcystis aeruginosa. *Aquatic Toxicology*, 78(1), pp.66–73. Available at: http://www.scopus.com/inward/record.url?eid=2-s2.0-33646369630&partnerID=40&md5=de6ed003dfabe6756779b0d3774f1135.

Rouhiainen, L. et al., 2004. Genes Coding for Hepatotoxic Heptapeptides (Microcystins) in the Cyanobacterium Anabaena Strain 90. *Applied and Environmental Microbiology*, 70(2), pp.686–692.

Roy-lachapelle, A. et al., 2014. Analytica Chimica Acta Total microcystins analysis in water using laser diode thermal desorption-atmospheric pressure chemical ionization-tandem mass spectrometry. *Analytica Chimica Acta*, 820, pp.76–83. Available at:

http://dx.doi.org/10.1016/j.aca.2014.02.021.

Roy-lachapelle, A., Solliec, M. & Sauvé, S., 2015. Determination of BMAA and three alkaloid cyanotoxins in lake water using dansyl chloride derivatization and high-resolution mass spectrometry.

Rutherford, A.W. & Krieger-Liszkay, A., 2001. Herbicide-induced oxidative stress in photosystem II. *Trends in Biochemical Sciences*, 26(11), pp.648–653.

Sano, T. et al., 2001. Isolation of new protein phosphatase inhibitors from two cyanobacteria species, Planktothrix spp. *Journal of Natural Products*, 64(8), pp.1052–1055.

Schatz, D. et al., 2005. Ecological implications of the emergence of non-toxic subcultures from toxic Microcystis strains. *Environmental Microbiology*, 7(6), pp.798–805.

Schatz, D. et al., 2007. Towards clarification of the biological role of microcystins, a family of cyanobacterial toxins. *Environmental microbiology*, 9(4), pp.965–970. Available at: http://www.scopus.com/inward/record.url?eid=2-s2.0-33947172645&partnerID=40&md5=b3bd910aab4c18adc7c0674a8258b8d4.

Schwarz, D. et al., 2013. Recent Applications of Metabolomics Toward Cyanobacteria. *Metabolites*, 3(1), pp.72–100. Available at: http://www.mdpi.com/2218-1989/3/1/72/.

Silverstein, R.M.; Webster, F.X.; Kiemle, D.J., 2007. *Identification spectrométrique de composés organiques* de Boeck.,

Sivonen, K. et al., 2010. Cyanobactins-ribosomal cyclic peptides produced by cyanobacteria. *Applied Microbiology and Biotechnology*, 86(5), pp.1213–1225.

Sivonen, K. & Jones, G., 1999. Cyanobacterial Toxins. In *Toxic Cyanobacteria in Water: A*

guide to their public health consequences, monitoring and management. pp. 55–124.

Soule, T. et al., 2013. The global response of nostoc punctiforme ATCC 29133 to UVA stress, assessed in a temporal DNA microarray study. *Photochemistry and Photobiology*, 89(2), pp.415–423.

Spoof, L. & Catherine, A., 2017. Appendix 3: Tables of Microcystins and Nodularins. *Handbook of Cyanobacterial Monitoring and Cyanotoxin Analysis*, pp.526–537. Available at: http://doi.wiley.com/10.1002/9781119068761.app3.

Stratton, G.W., 1984. Effects of the herbicide atrazine and its degradation products, alone and in combination, on phototrophic microorganisms. *Archives of Environmental Contamination and Toxicology*, 13(1), pp.35–42. Available at: http://www.scopus.com/inward/record.url?eid=2-s2.0-0021327392&partnerID=40&md5=198aec5048055726ad74424728c31f49.

Strid, ??ke, Chow, W.S. & Anderson, J.M., 1994. UV-B damage and protection at the molecular level in plants. *Photosynthesis Research*, 39(3), pp.475–489.

Stumpf, R.P. et al., 2012. Interannual variability of cyanobacterial blooms in Lake Erie. *PLoS ONE*, 7(8). Available at: http://www.scopus.com/inward/record.url?eid=2-s2.0-84864762325&partnerID=40&md5=f386a33a236a1986f984410800895af9.

Tao, Y. et al., 2013. Mechanisms of photosynthetic inactivation on growth suppression of Microcystis aeruginosa under UV-C stress. *Chemosphere*, 93(4), pp.637–644.

Taranu, Z.E. et al., 2015. Acceleration of cyanobacterial dominance in north temperate-subarctic lakes during the Anthropocene. *Ecology Letters*, 18(4), pp.375–384.

The American Chemical Society ACS, 2017. Chemical Abstract Service (CAS). Available at: http://www.cas.org/ [Accessed April 1, 2017].

Tillett, D. et al., 2000. Structural organization of microcystin biosynthesis in Microcystis aeruginosa PCC7806: An integrated peptide-polyketide synthetase system. *Chemistry and Biology*, 7(10), pp.753–764. Available at: http://www.scopus.com/inward/record.url?eid=2-s2.0-0033780306&partnerID=40&md5=5d26902a0af1be02bff2f04b38452713.

Tonk, L. et al., 2005. The microcystin composition of the cyanobacterium Planktothrix agardhii changes toward a more toxic variant with increasing light intensity. *Applied and Environmental Microbiology*, 71(9), pp.5177–5181. Available at: http://www.scopus.com/inward/record.url?eid=2-s2.0-25144454346&partnerID=40&md5=f93b6f29781c328f94793c594f06915e.

Utkilen, H. & Gjolme, N., 1995. Iron-stimulated toxin production in Microcystis aeruginosa. *Applied and Environmental Microbiology*, 61(2), pp.797–800.

van der Waal, D., 2010. *Out of Balance : Implications of climate change for the ecological stoichiometry of harmful cyanobacteria*,

Wang, J. et al., 2016. Effect of high-doses pyrogallol on oxidative damage, transcriptional responses and microcystins synthesis in Microcystis aeruginosa TY001 (Cyanobacteria). *Ecotoxicology and Environmental Safety*, 134, pp.273–279. Available at: http://dx.doi.org/10.1016/j.ecoenv.2016.09.010.

Wang, J. et al., 2013. Small water clusters stimulate microcystin biosynthesis in cyanobacterial Microcystis aeruginosa. *Journal of Applied Phycology*, 25(1), pp.329–336. Available at: http://www.scopus.com/inward/record.url?eid=2-s2.0-

84872487731&partnerID=40&md5=4d0d95254f110e06184c641b53bb26ba.

Wang, Y. et al., 2011. Physiological response of microcystis to solar UV radiation. *Shengtai Xuebao/ Acta Ecologica Sinica*, 31(21), pp.6532–6539. Available at: http://www.scopus.com/inward/record.url?eid=2-s2.0-82955197441&partnerID=40&md5=daef7f5848ad2132a86bca803c5a1693.

Weiz, A.R. et al., 2014. Harnessing the evolvability of tricyclic microviridins to dissect protease-inhibitor interactions. *Angewandte Chemie - International Edition*, 53(14), pp.3735–3738. Available at: http://www.scopus.com/inward/record.url?eid=2-s2.0-84897436581&partnerID=40&md5=64b5ea51d5eec31e0c96e65f6e982e51.

Welker, M. et al., 2006. Detection and identification of oligopeptides in Microcystis (cyanobacteria) colonies: Toward an understanding of metabolic diversity. *Peptides*, 27(9), pp.2090–2103.

Welker, M. et al., 2004. Diversity and distribution of Microcystis (cyanobacteria) oligopeptide chemotypes from natural communities studies by single-colony mass spectrometry. *Microbiology*, 150(6), pp.1785–1796.

Welker, M. & Von Döhren, H., 2006. Cyanobacterial peptides - Nature's own combinatorial biosynthesis. *FEMS Microbiology Reviews*, 30(4), pp.530–563.

WHO, 2003. Guidelines for safe recreational water environments : coastal and freshwaters. *Environments*, 1, pp.3505–3518.

Wiedner, C. et al., 2003. Effects of light on the microcystin content of Microcystis strain PCC 7806. *Applied and Environmental Microbiology*, 69(3), pp.1475–1481.

Wood, R., 2016. Acute animal and human poisonings from cyanotoxin exposure - A review of the literature. *Environment International*, 91, pp.276–282. Available at: http://dx.doi.org/10.1016/j.envint.2016.02.026.

Wu, H. et al., 2005. Effects of Solar UV Radiation on Morphology and Photosynthesis of Filamentous Cyanobacterium Arthrospira platensis Effects of Solar UV Radiation on Morphology and Photosynthesis of Filamentous Cyanobacterium Arthrospira platensis. , 71(OCTOBER), pp.5004–5013.

Yang, Z. et al., 2015. Effects of UV-B radiation on microcystin production of a toxic strain of Microcystis aeruginosa and its competitiveness against a non-toxic strain. *Journal of Hazardous Materials*, 283, pp.447–453. Available at: http://www.scopus.com/inward/record.url?eid=2-s2.0-84908388673&partnerID=40&md5=6d212b7ac4a836b6d458720f77939803.

Yang, Z. et al., 2014. UV-B radiation and phosphorus limitation interact to affect the growth, pigment content, and photosynthesis of the toxic cyanobacterium Microcystis aeruginosa. *Journal of Applied Phycology*, 26(4), pp.1669–1674. Available at: http://www.scopus.com/inward/record.url?eid=2-s2.0-84905232784&partnerID=40&md5=a076c5eea95b7ab9fed88504553a3337.

Young, F.M. et al., 2005. Immunogold localisation of microcystins in cryosectioned cells of Microcystis. *Journal of Structural Biology*, 151(2), pp.208–214.

Young, F.M. et al., 2008. Quantification and localization of microcystins in colonies of a laboratory strain of Microcystis (Cyanobacteria) using immunological methods. *European Journal of Phycology*, 43(2), pp.217–225.

Ziemert, N. et al., 2010. Exploiting the natural diversity of microviridin gene clusters for discovery of novel tricyclic depsipeptides. *Applied and Environmental Microbiology*, 76(11), pp.3568–3574. Available at: http://www.scopus.com/inward/record.url?eid=2-s2.0-77953045048&partnerID=40&md5=a2842542130df2fc968ffed33fc469a7.

Zilliges, Y. et al., 2011. The cyanobacterial hepatotoxin microcystin binds to proteins and increases the fitness of Microcystis under oxidative stress conditions. *PLoS ONE*, 6(3), pp.e17615–e17615. Available at: http://www.scopus.com/inward/record.url?eid=2-s2.0-79952802915&partnerID=40&md5=db574fe3c9a6760fe8289b1c5ab37a32.

Zurawell, R.W. et al., 2005a. Hepatotoxic cyanobacteria : A review of the biological importance of microcystins in freshwater environments. *Journal of Toxicology and Environmental Health, Part B*, 8, pp.1–37.

Zurawell, R.W. et al., 2005b. Hepatotoxic Cyanobacteria: A Review of the Biological Importance of Microcystins in Freshwater Environments. *Journal of Toxicology and Environmental Health, Part B*, 8(1), pp.1–37. Available at: http://www.tandfonline.com/doi/abs/10.1080/10937400590889412.

Appendix A:
Additional data for Chapter 2

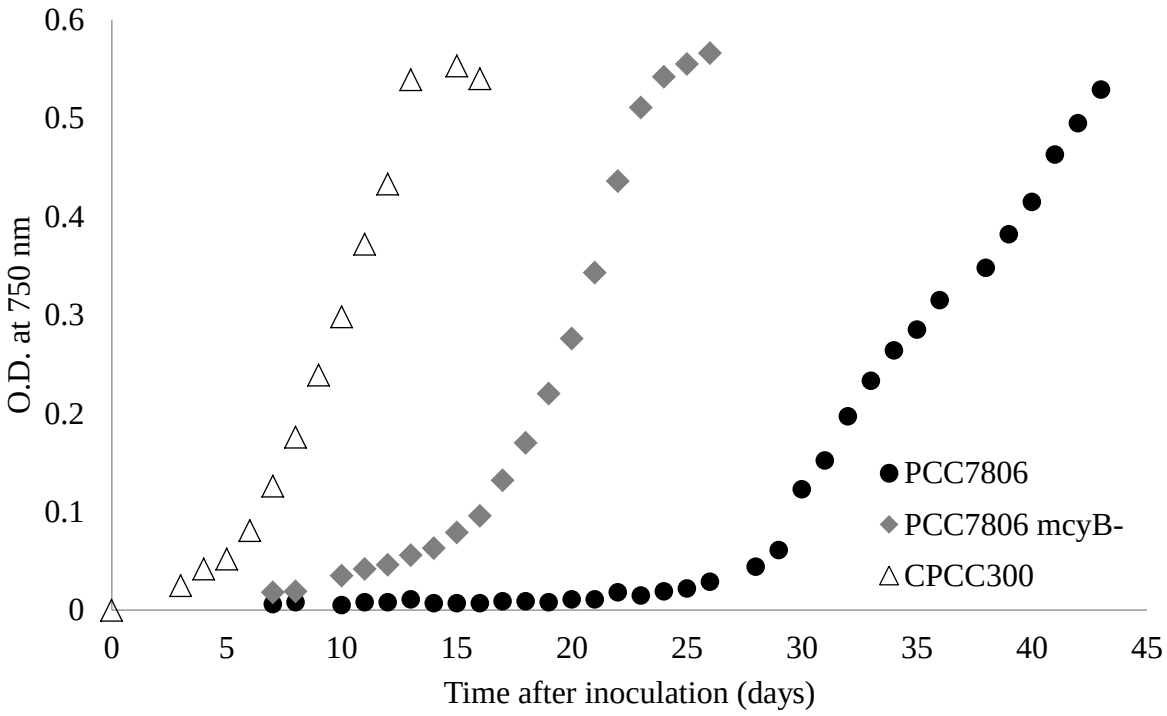

Figure A.1: Optical density at 750 nm for the strains CPCC300, PCC7806 (WT) and PCC7806*mcy*B. An initial lag phase of about 25 days is observed for the WT culture. A shorter lag phase of 10 days is observed for its mutant. Semi-continuous cultures were monitored and the exponential growth phase was underway when the optical density reached 0.4.

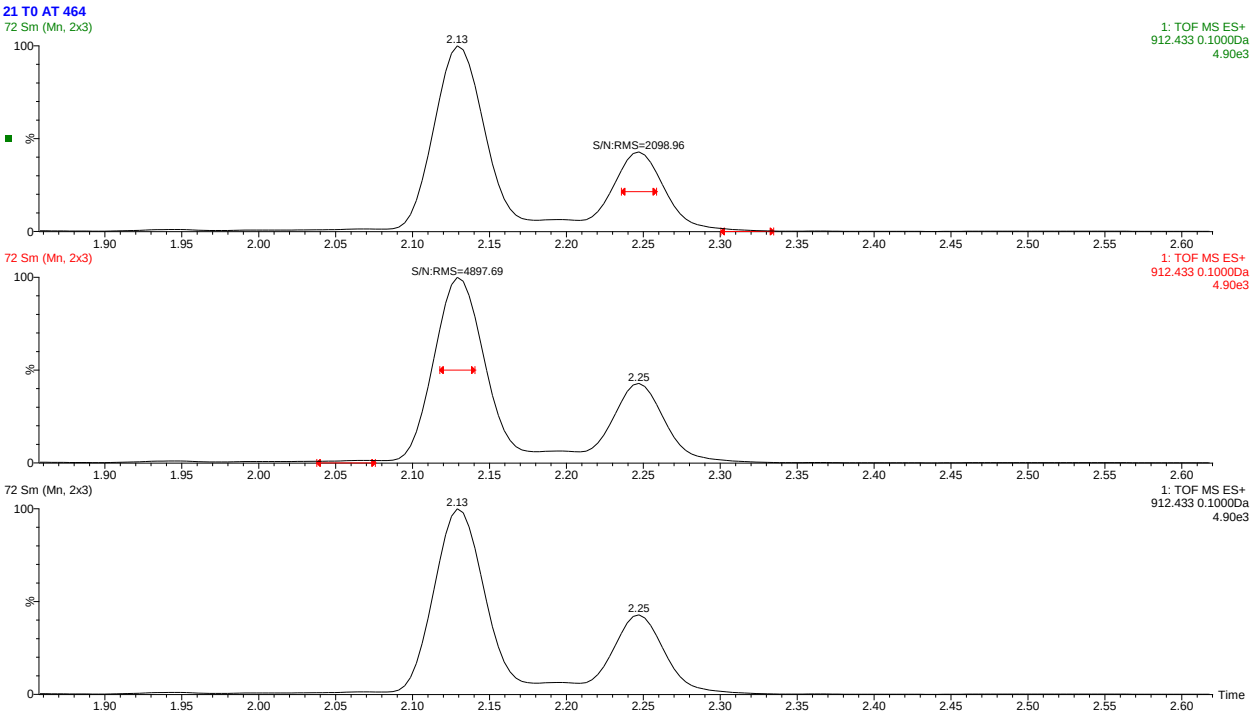

Figure A.2: S/N of the two signals corresponding to the masses and fragmentation of CPT911. Ratios above two were considered good signals to take into consideration for the study.

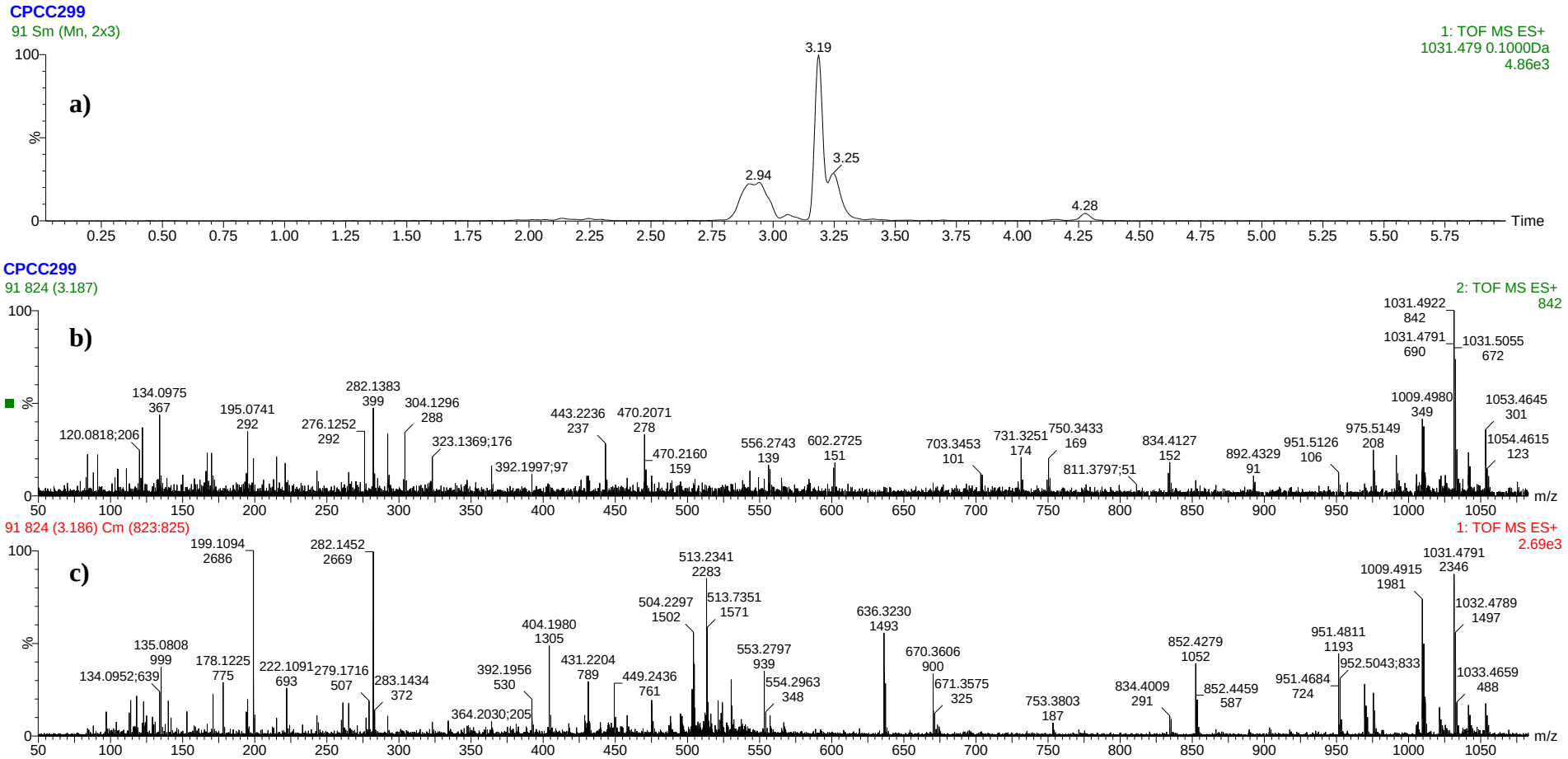

Figure A.3. Unidentified MC 1 separation chromatogram at RT 3.19 min **(a)**, and spectra under high energy **(b)** and low energy **(c)** collision in positive ionization mode. The *m/z* of 134.09 Da correspond to the mass of the Adda moiety present in all microcystins.

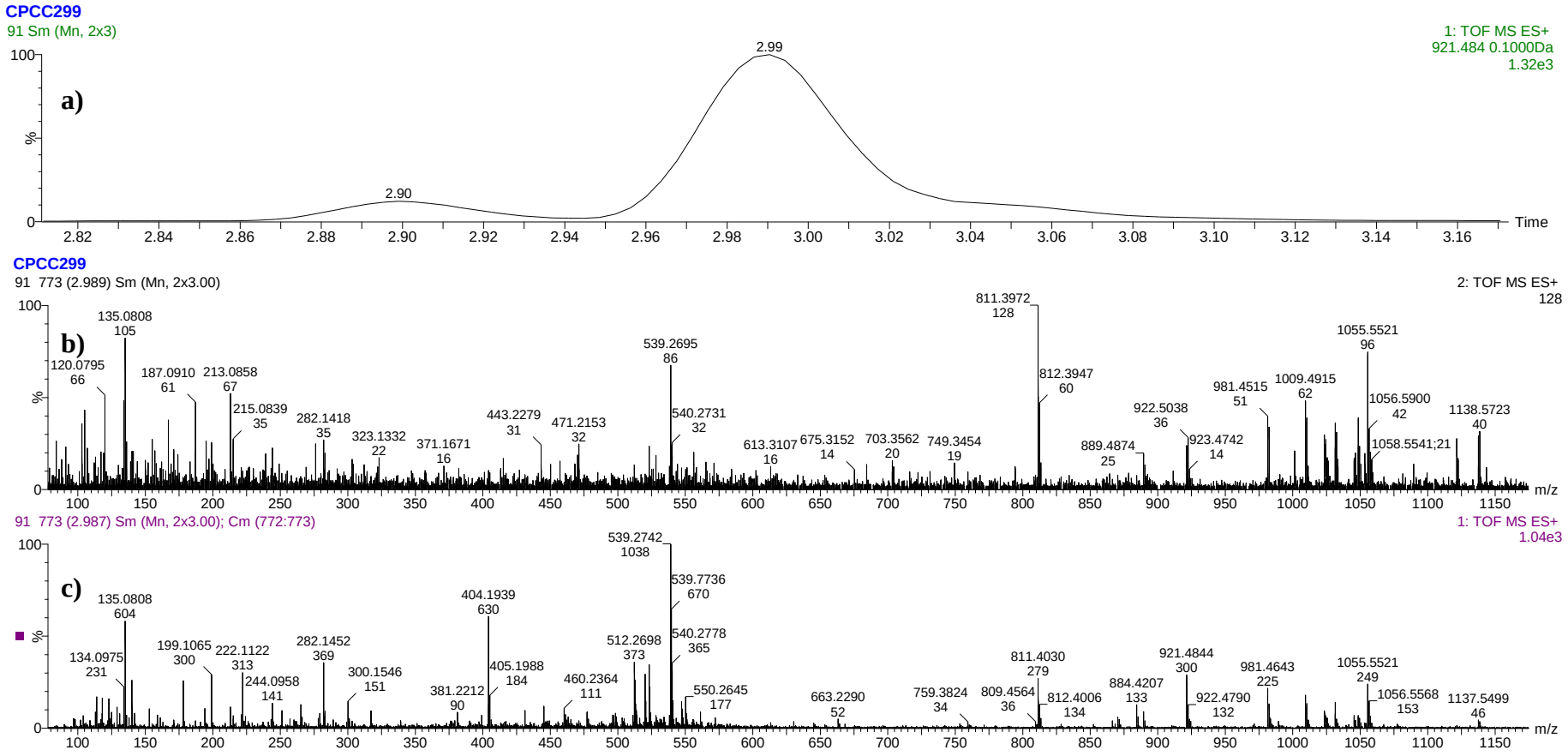

Figure A.4. Unidentified MC 2 separation chromatogram at RT 2.98 min **(a)**, and spectra under high energy **(b)** and low energy **(c)** collision in positive ionization mode. The *m/z* of 134.09 Da correspond to the mass of the Adda moiety present in all microcystins.

Table A.1: Major fragments of MC-LR detected in the standard solution at a RT of 2.84 min. *m/z* is presented as detected under positive ionization mode without mass correction.

Fragment Structure	Molecular Formula	*m/z* (Da)
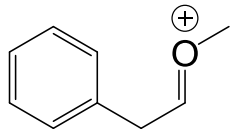	$C_9H_{11}O$ *(Adda moiety)*	135.08
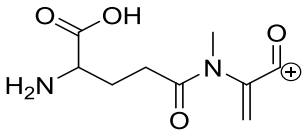	$C_9H_{13}N_2O_4$	213.09
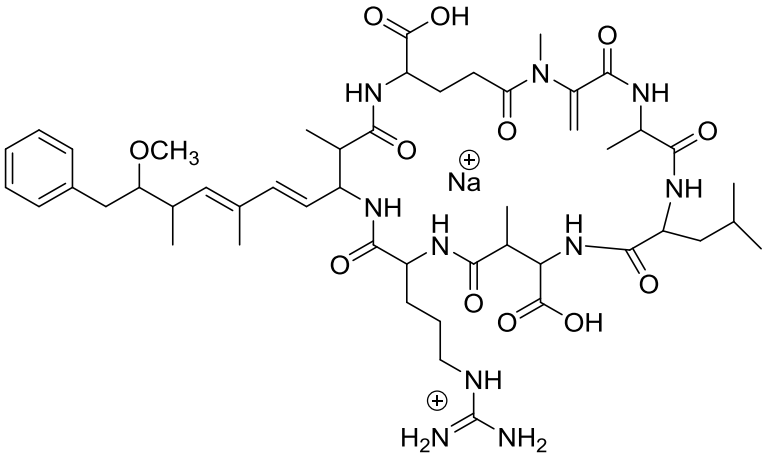	$C_{49}H_{75}N_{10}NaO_{12}$	509.25
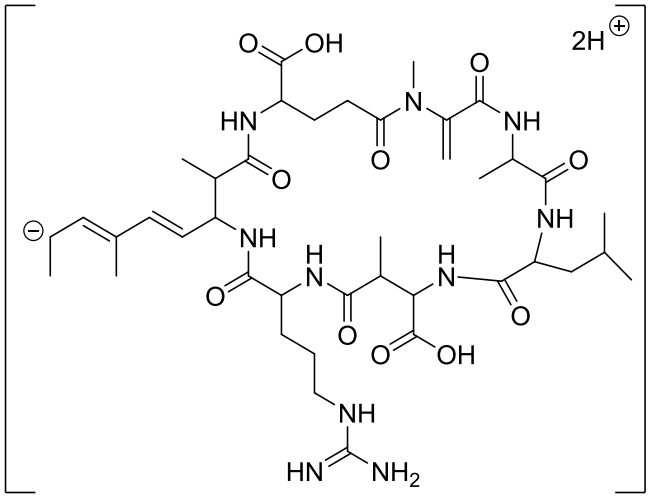	$C_{40}H_{63}N_{10}O_{11}$	861.50

Table A.2: Major fragments of cyanopeptolin CPT911 detected in the samples at RT 2.13 min and 2.25 min. *m/z* is presented as detected under positive ionization mode without mass correction.

Fragment Structure	Molecular Formula	RT (min)	*m/z*
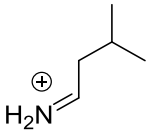	$C_5H_{12}N$	2.25	86.09
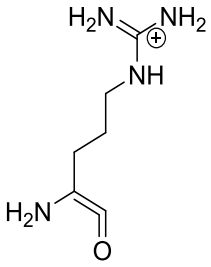	$C_6H_{13}N_4O$	2.13	157.09
		2.25	157.09

Table A.3: Compounds that have previously been observed in the strains of interest in this study, but for which no corresponding signal was found. Molecular weights are expressed in Daltons (Da). MC=microcystin, ARG=aeruginosin, CPT=cyanopeptolin.

Compounds	**Formula**	**MW (Da)**	**CPCC464**	**CPCC299**	**CPCC300**	**PCC7806**	**PCC7806 *mcyB*-**	**Reference**
[Dha^{7}]-MC-LR	$C_{48}H_{72}N_{10}O_{12}$	980.5331			X			(LeBlanc Renaud 2009)
Aerucyclamide A	$C_{24}H_{34}N_6O_4S_2$	534.2083				X	X	(Portmann, Blom, Gademann, et al. 2008)
Aerucyclamide B	$C_{24}H_{32}N_6O_4S_2$	532.1927				X	X	(Portmann, Blom, Gademann, et al. 2008)
Aerucyclamide C	$C_{24}H_{32}N_6O_5S$	516.2155				X	X	(Portmann, Blom, Kaiser, et al. 2008)
Aerucyclamide D	$C_{26}H_{30}N_6O_4S_3$	586.1491				X	X	(Portmann, Blom, Kaiser, et al. 2008)
ARG686	$C_{33}H_{50}N_3O_{10}Cl$	686.29				X	X	(Ishida et al. 2009b; Welker et al. 2006)
ARG684	*N/A*	684				X	X	(Briand et al. 2016)
BMAA[a]	$C_4H_{10}N_2O_2$	118.1344				X		Cox et al. 2005
CPT895	*N/A*	895				X	X	(Briand et al. 2016)
CPT963A	$C_{49}H_{69}N_7O_{13}$	964.111				X	X	(Bister et al. 2004)
CPTA	$C_{46}H_{72}N_{10}O_{12}$	956.5331				X	X	(Briand et al. 2016; Martin, Oberer, Buschdtt, Weckesser, et al. 1993)
CPTB	$C_{46}H_{72}N_8O_{12}$	928.5270				X	X	(Briand et al. 2016; Martin, Oberer, Buschdtt, Weckesser, et al. 1993)
CPTC	$C_{47}H_{74}N_8O_{12}$	942.5426				X	X	(Briand et al. 2016; Martin, Oberer, Buschdtt, Weckesser, et al. 1993)
CPTD	$C_{46}H_{72}N_{10}O_{12}$	956.5331				X		(Martin, Oberer, Buschdtt, Weckesser, et al. 1993)
MC-YR	$C_{52}H_2N_{10}O_{13}$	1045.1873	X					(LeBlanc Renaud 2009)
Microviridins	*(10 variants)*	1600-1900				X		(Micallef et al. 2015)

[a] *β-methylamino-L-alanine*

Appendix B:
Additional data for Chapter 3

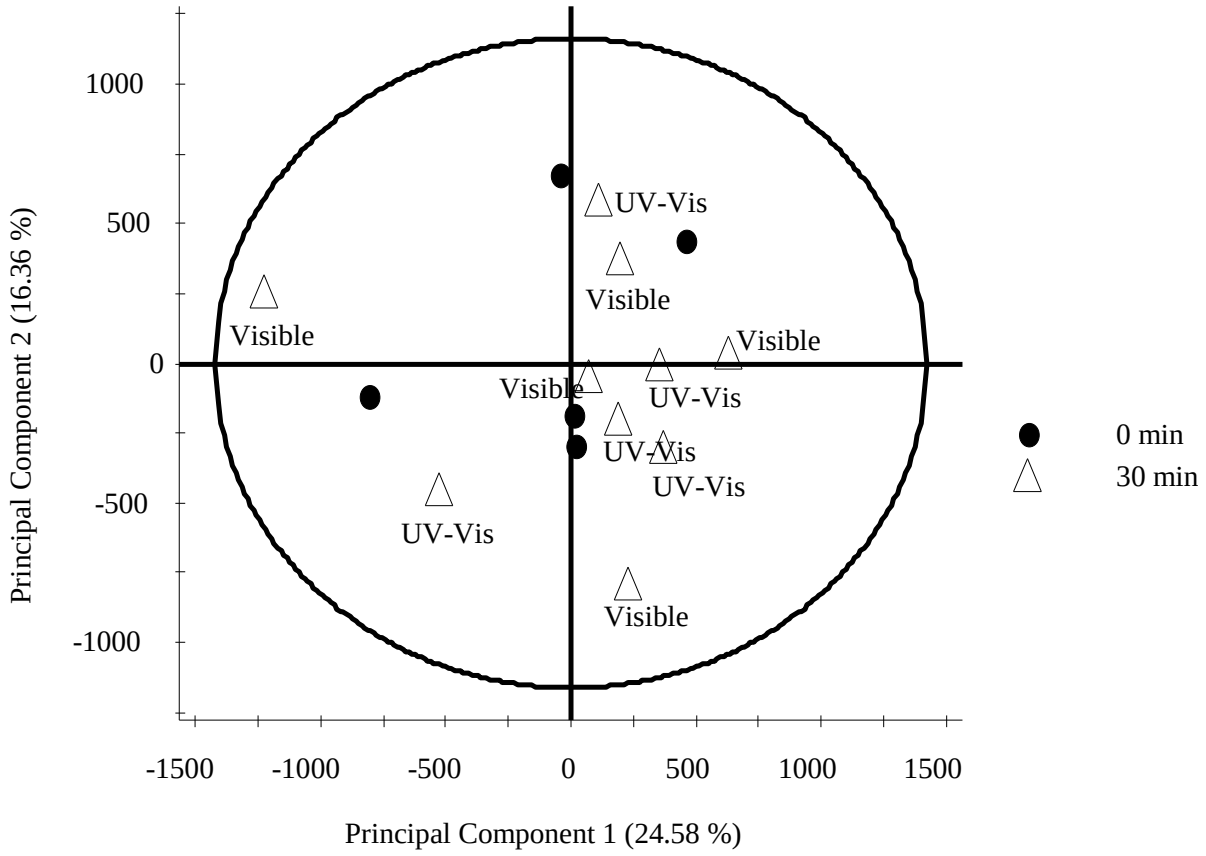

Figure B.1. PCA for the metabolome variation in samples of *M. aeruginosa* PCC7806 (MC-producing) exposed to UV and visible light, visible light only and controls at T=0 min.

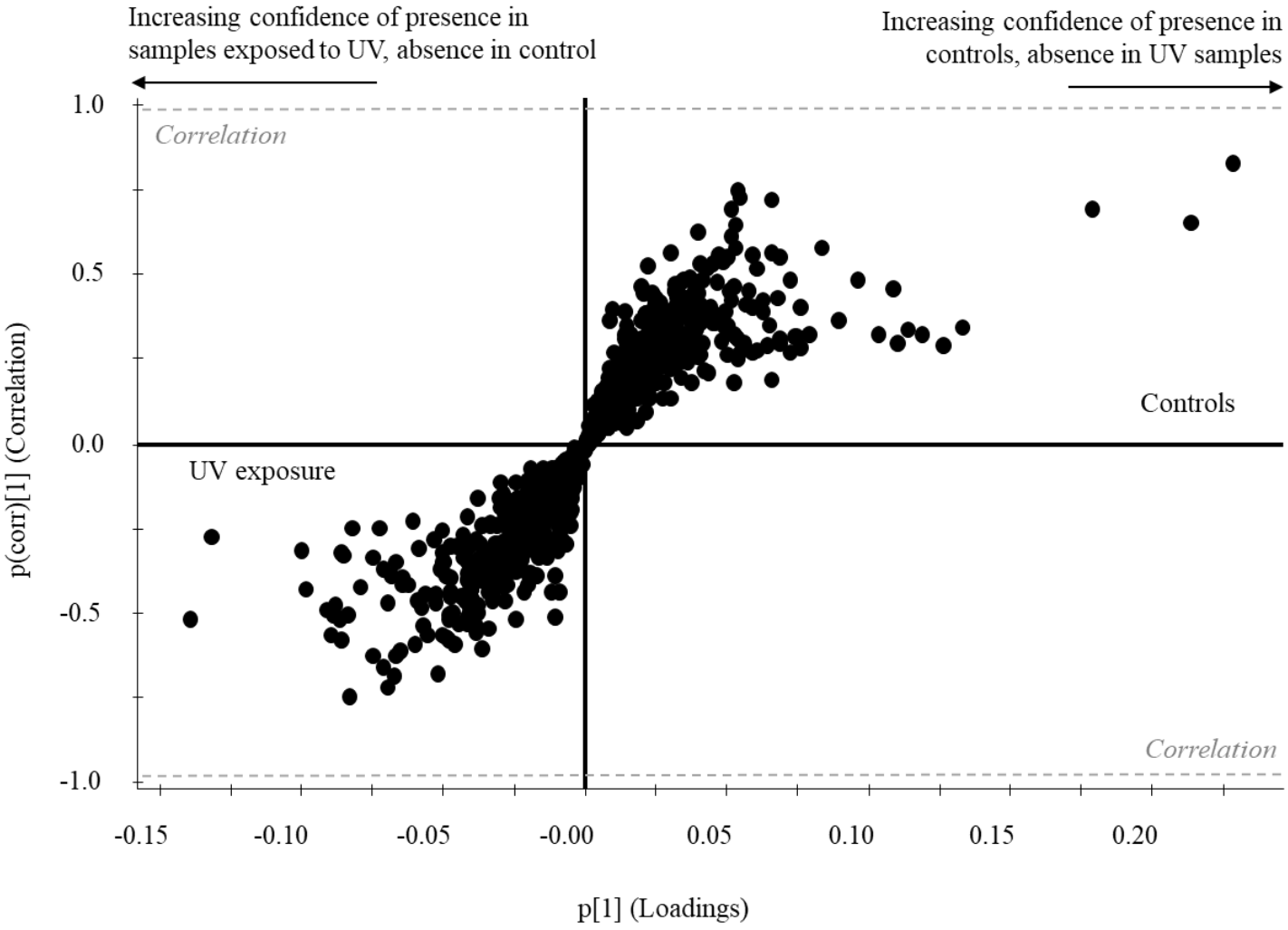

Figure B.2. S-plot for the metabolome variation in *M. aeruginosa* strain PCC7806 WT (MC-producing) exposed to 30 minutes of UV radiation. All treatments are plotted together as no difference were previously observed (Figure B.1). Each point represents a fragment at a specific RT.

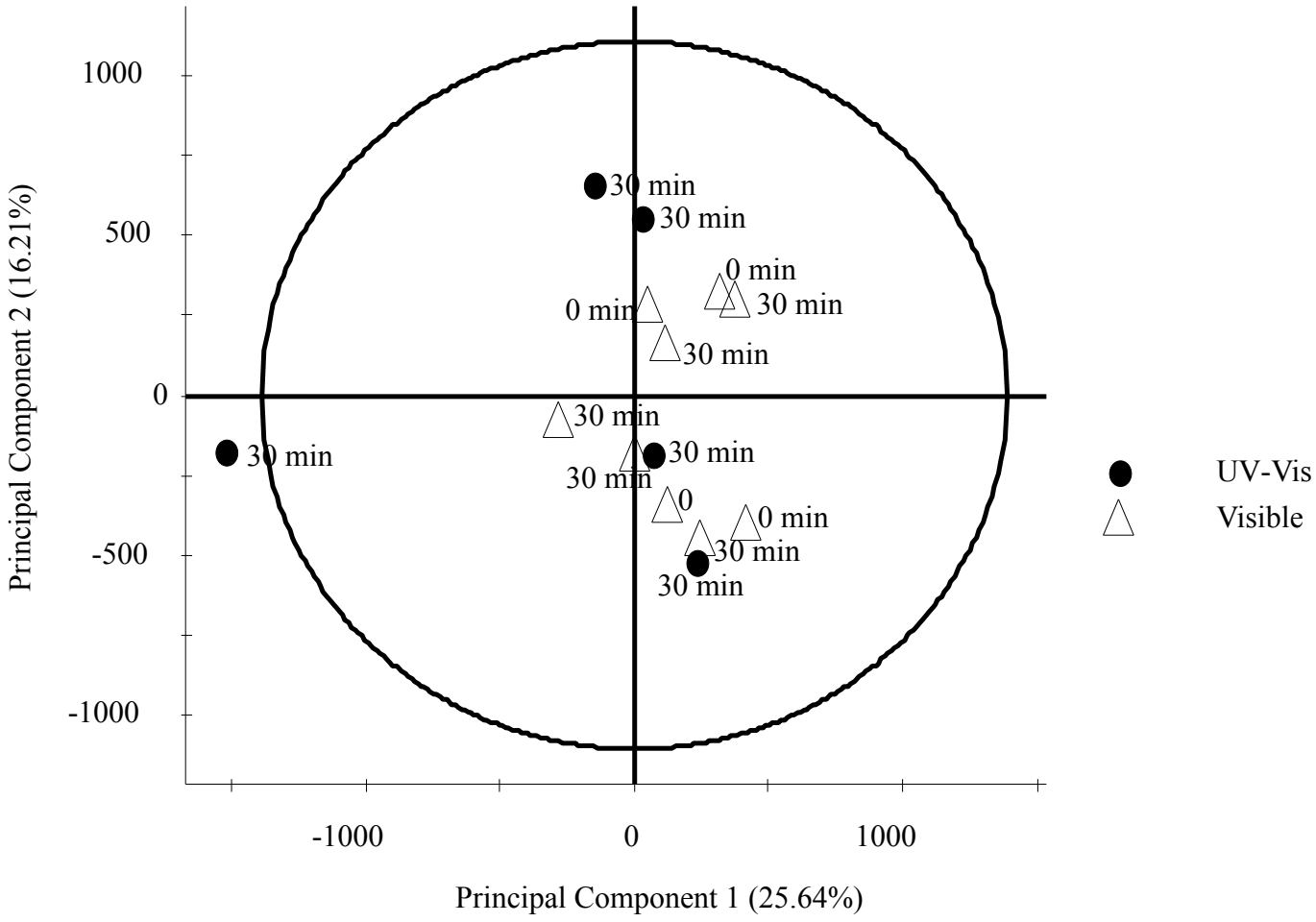

Figure B.3. PCA for the metabolome variation in samples of *M. aeruginosa* strain PCC7806 *mcy*B- (mutant for *mcy*) exposed to UV and visible light, visible light only and controls at 0 min.

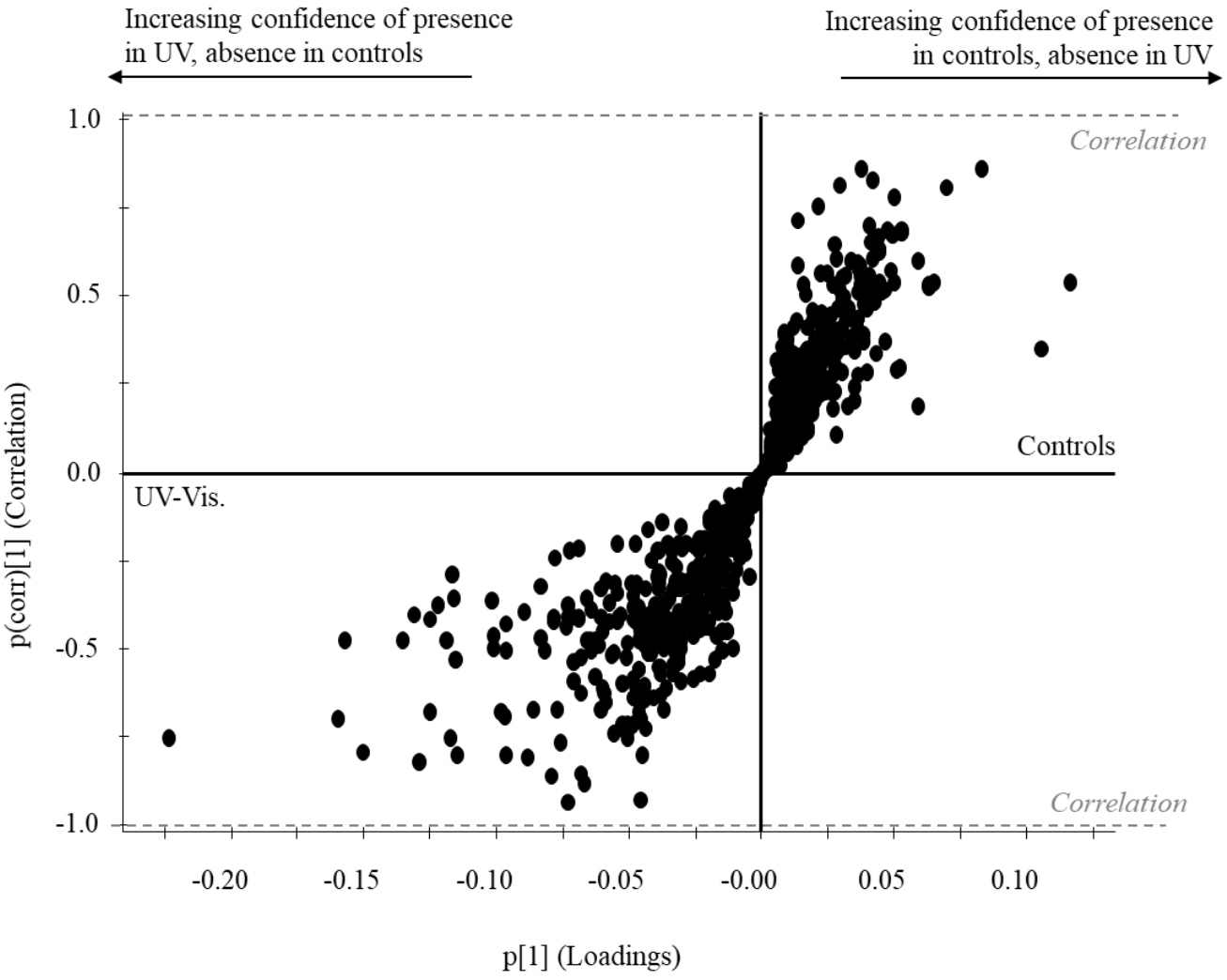

Figure B.4. S-plot for the metabolome variation in *M. aeruginosa* PCC7806*mcy*B- (mutant for *mcy*) exposed to 30 minutes of UV radiation. All treatments are plotted together as no difference were previously observed (Figure B.3). Each point represents a fragment at a specific RT.

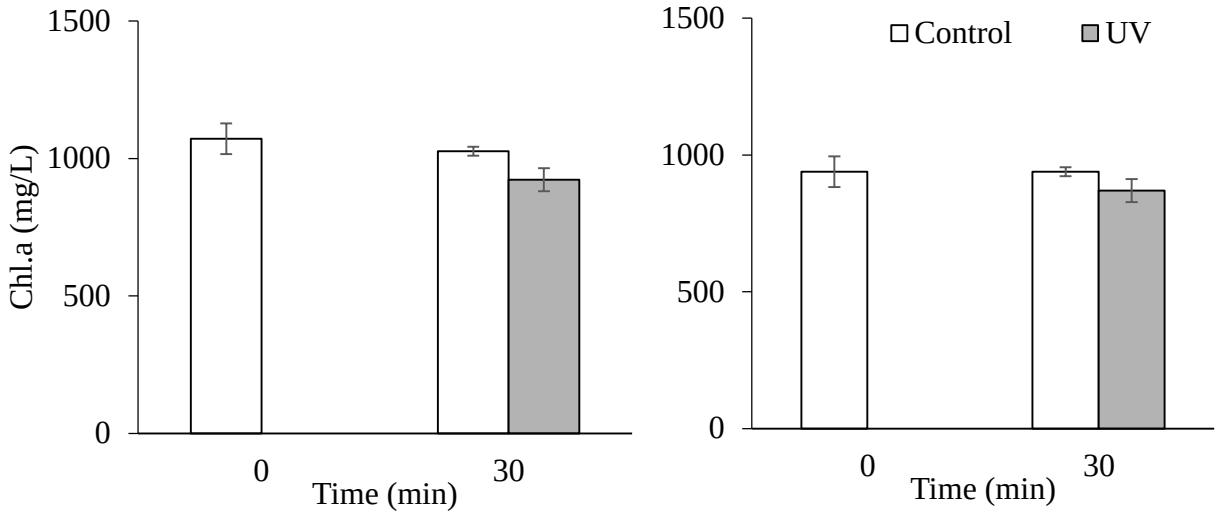

Figure B.5. Chl. a (mg/L) in **a)** PCC7806 (MC producer) and **b)** PCC7806*mcyB*- (mutant for *mcy*) over the 30 minutes experiment for UV exposure. Error bars represent the standard deviation of the average (n=3). Student's t-test showed no significant differences among treatments ($p>0.05$).

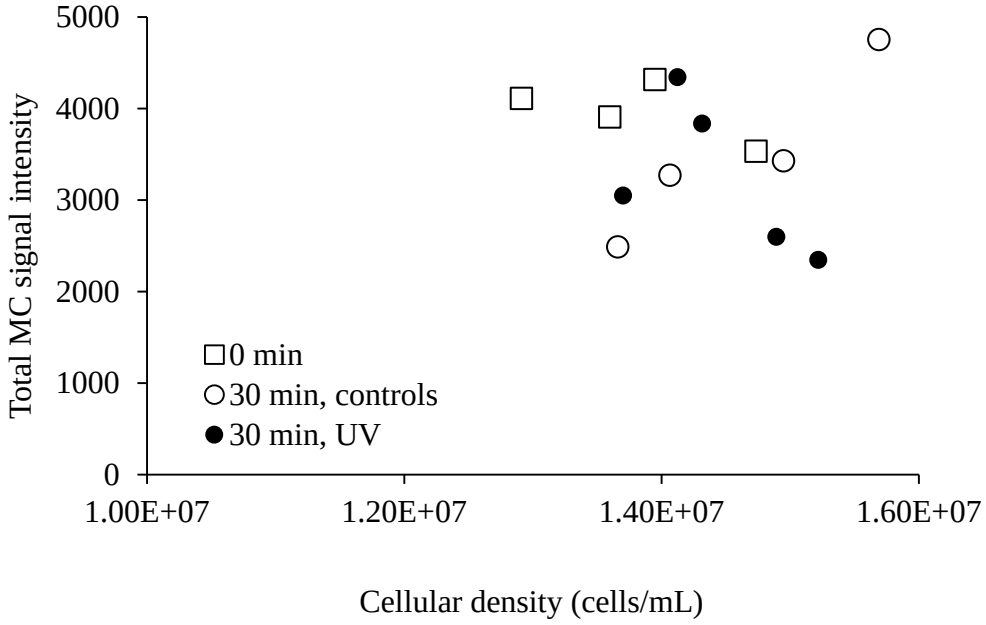

Figure B.6. Total microcystins signal intensity in the MC producer *Microcystis aeruginosa* PCC7806 (WT) in relation to the cellular density (cells/mL) in cultures before (n=4) and after UV treatments (n=5), as well as controls (n=4).

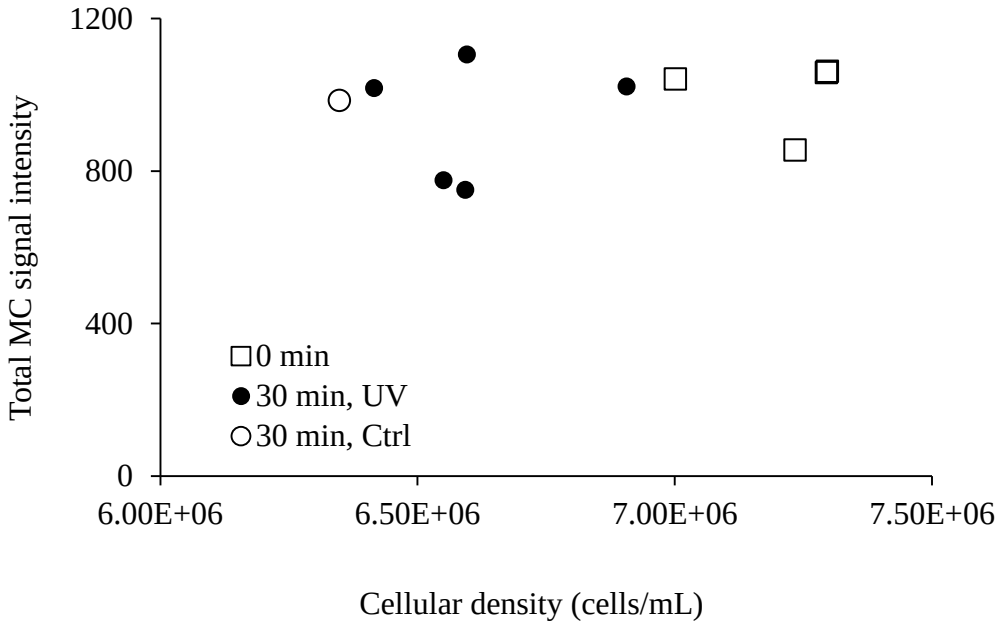

Figure B.7. Total microcystins signal intensity in the MC producer *Microcystis aeruginosa* CPCC300 in relation to the cellular density (cells/mL) in cultures before (n=4) and after UV treatments (n=5).

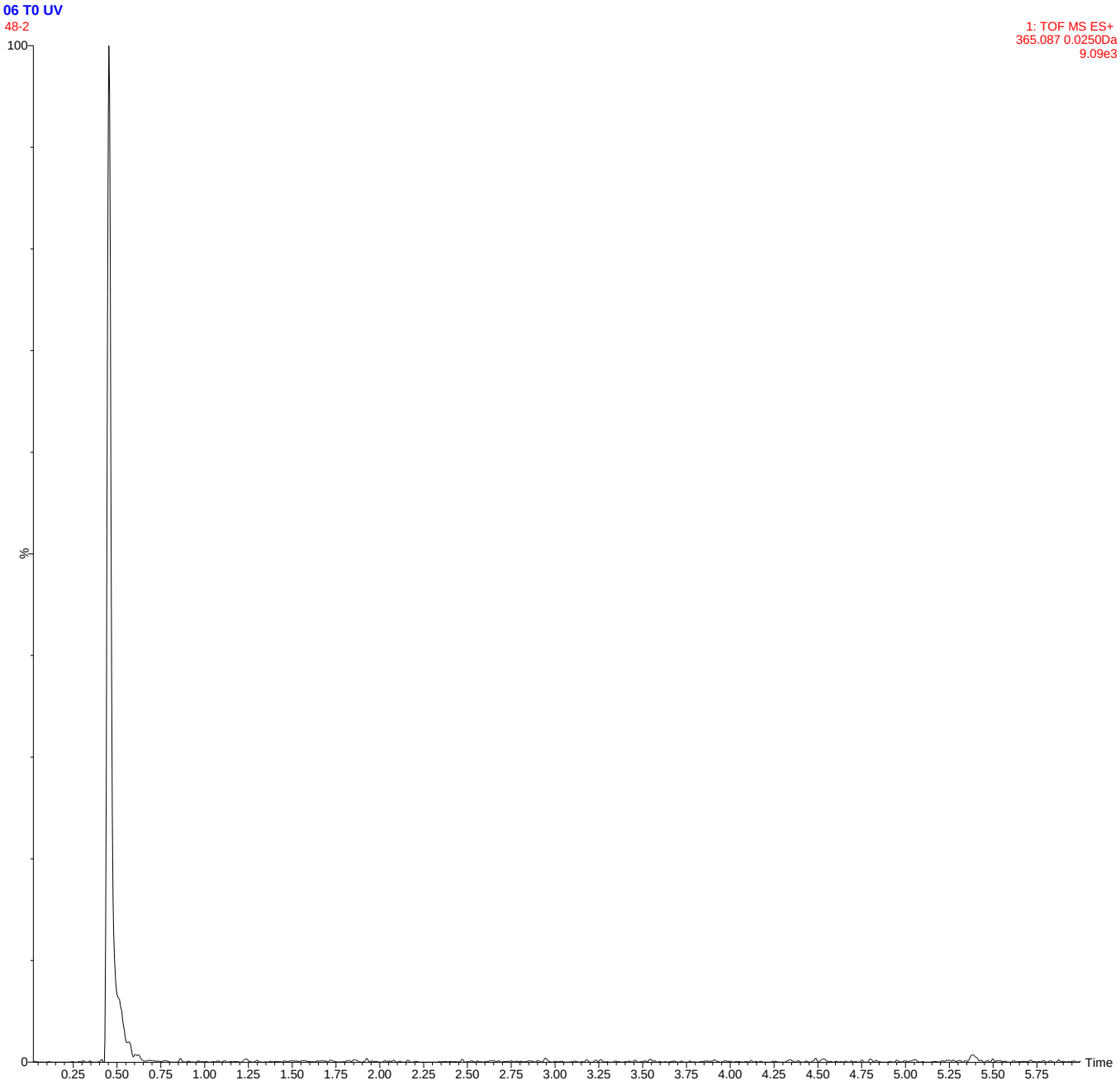

Figure B.8. Separation of unidentified compound 4 in the MC-producing *Microcystis aeruginosa* strain CPCC464 at RT 0.45min.

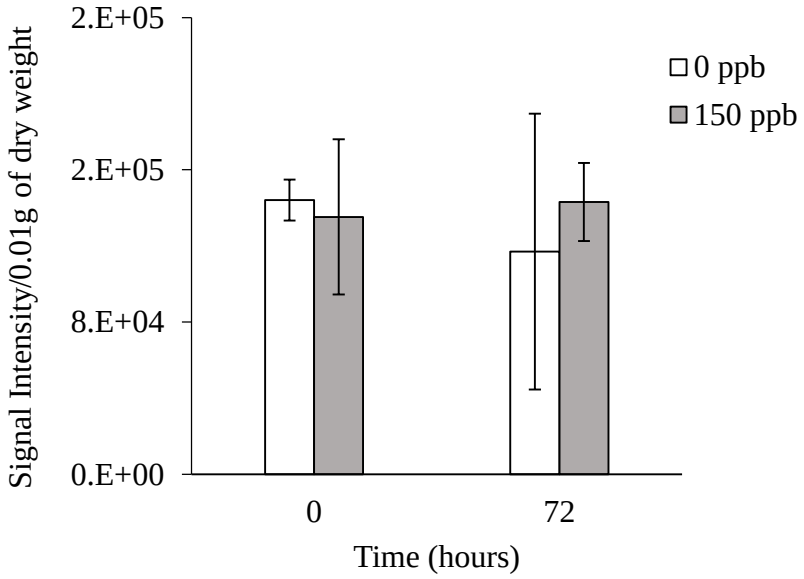

Figure B.9. Unidentified compound 4 signal intensity variation in *M. aeruginosa* strain CPCC300 for the controls and the 150 ppb treatment to atrazine at the beginning and at the end of the experiment. Error bars represent the standard deviation of the average (n=5). An unpaired t-test showed no difference between the controls and the 150ppb treatment after 72 hours exposure (p=0.47).

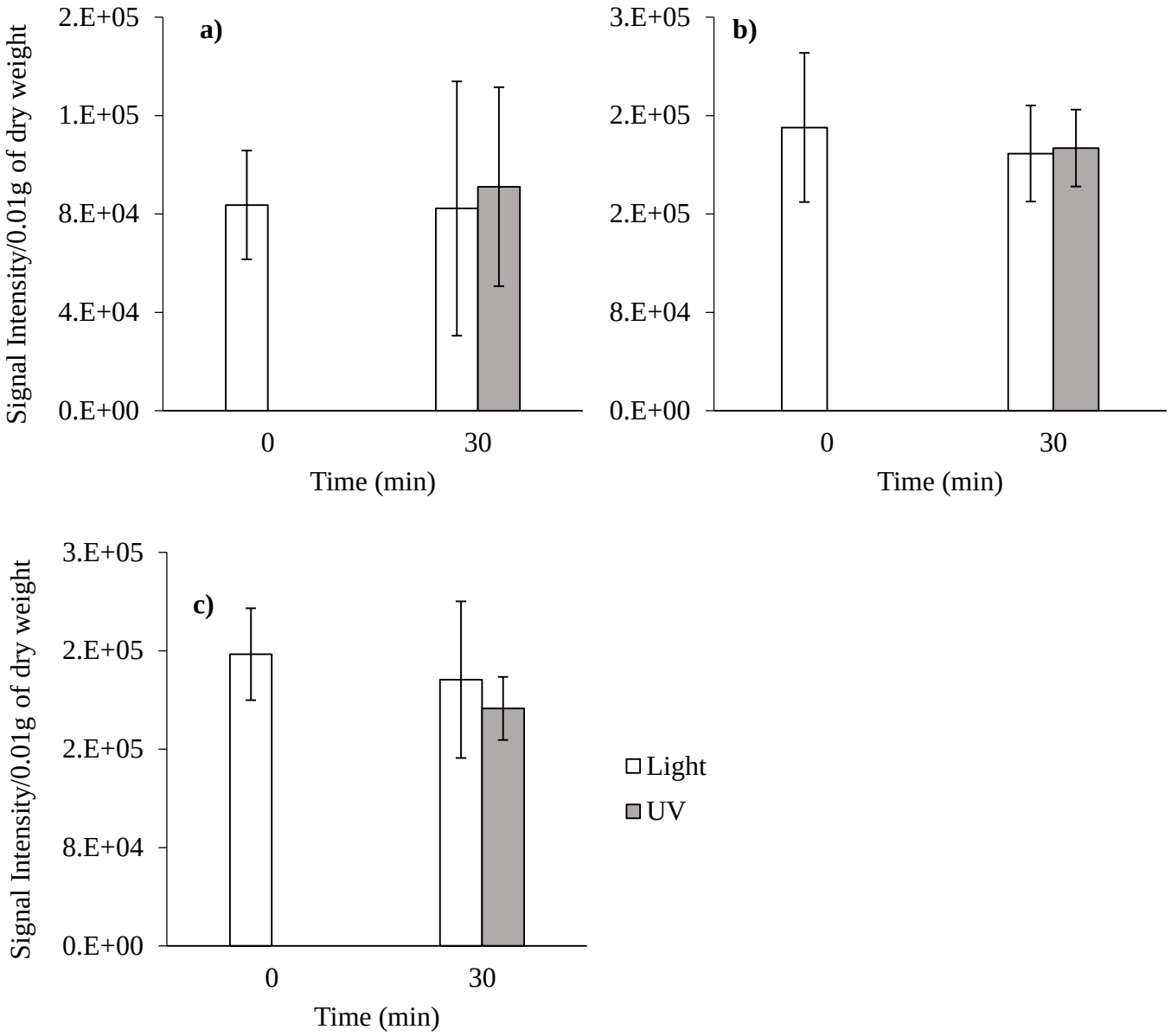

Figure B.10. Compound.4 signal intensity variation in *M. aeruginosa* strain a) CPCC300; b) PCC7806 (WT); c) PCC7806*mcyB*- for the controls and treatments before and after 30 minutes exposure to UV radiation. Error bars represent the standard deviation of the average (n=5). Note

the difference in scale. An unpaired t-test showed no variation between visible light and UV after 30 minutes (a. $p=0.8$; b. $p=0.8$; c. $p=0.5$).

Figure B.11. Separation of compound 5 in *Microcystis aeruginosa* CPCC464 at RT 0.64 min**.**

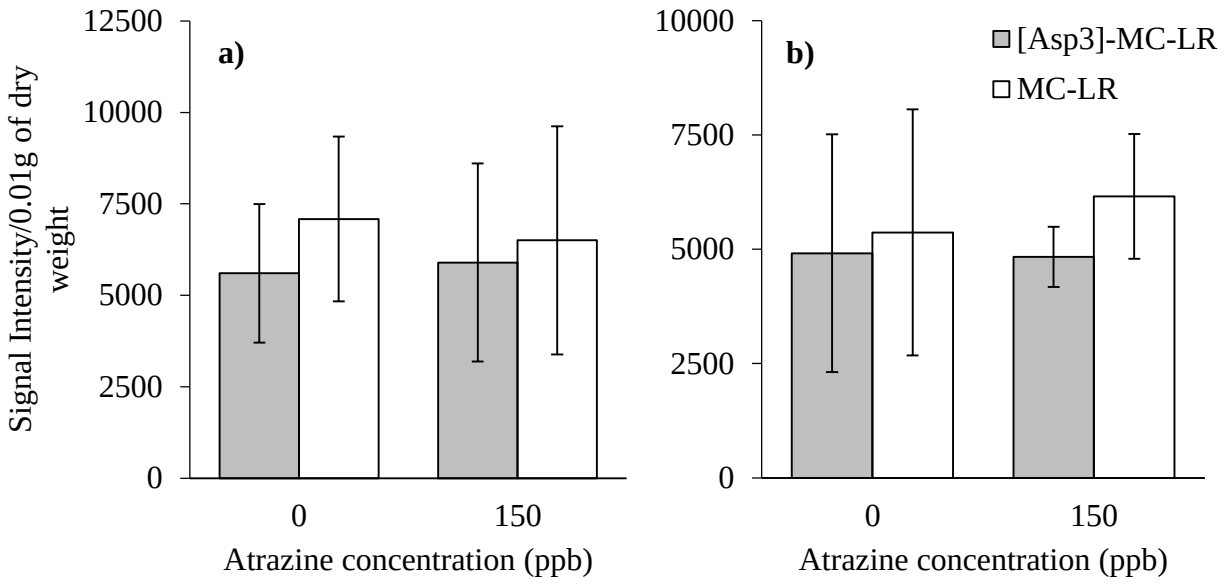

Figure B.12. Microcystins concentration in *M. aeruginosa* CPCC300 at **a)** T=0 of atrazine exposure (n=5); **b)** after 72 hours of exposure (n=4). Error bars represent the standard deviation of the average. Note the difference in scale. A two-way ANOVA showed no difference in treatment or time for both congeners ($p>0.4$).

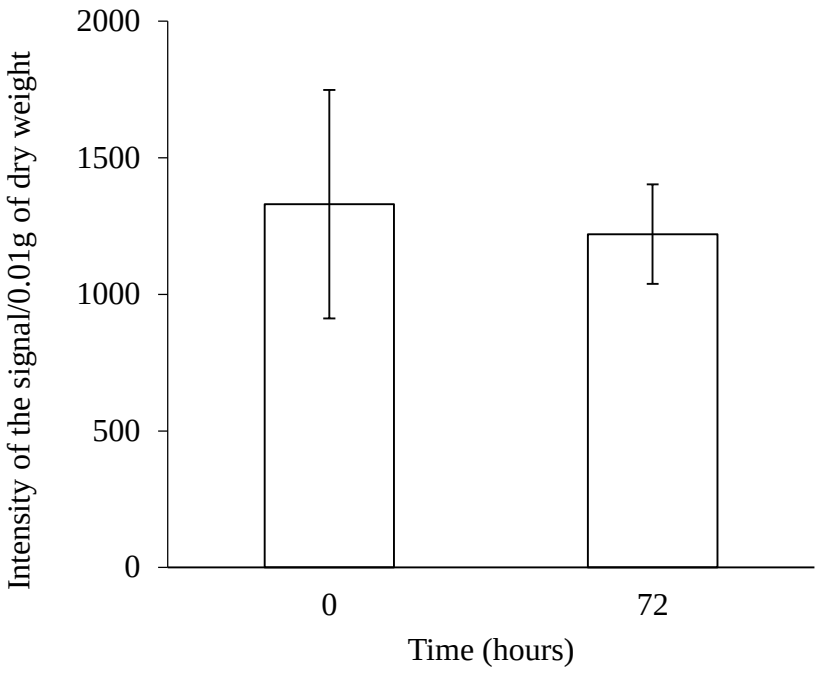

Figure B.13. Atrazine concentrations in CPCC300 at the beginning and the end of the experiment, after 72 hours. Subsamples at 0 min were taken right after the addition of 150 ppb of atrazine. The concentrations remained constant over the course of the experiment, assuring the cultures a constant exposure to oxidative stress. Error bars represent the standard deviation of three biological replicates. A paired t-test showed no variation in concentration over time ($p=0.9$).